Dissertation

submitted to the

Combined Faculty of Natural Sciences and Mathematics

of the Ruperto Carola University Heidelberg, Germany

for the degree of

Doctor of Natural Sciences

Presented by

Iakovos Bomponis (B.Sc.)

Born in Athens, Greece

Oral examination: 25.01.2021

Bacterial retrons encode phage-sensing toxin/antitoxin systems

Referees:

Dr. Mikhail Savitski

Prof. Dr. Michael Knop

Inspiration exists,
but it has to find you working.

-Pablo Picasso

Acknowledgements

This work was only possible due to the environment fostered by my mentor, Nassos Typas. Nassos gave me all the freedom I wanted in pursuing a highly risky project, that neither of us knew how it would turn out. This meant that, to find my way to something interesting, I had to do all sorts of dumb experiments. Nassos possesses a unique clarity of thinking that allows him to quickly weed out useful from useless directions, which was crucial in times when things didn't make much sense. Nevertheless, the best aspect of working with Nassos is not that he can solve problems. Rather, it is the genuine pleasure that comes from discussing wacky ideas with him (that were sometimes true), and his unending enthusiasm for solid science, which I will carry on with me.

I thank all the members of the Typas lab; they were my family away from home, and it has been a privilege and a pleasure to work alongside each and every one of them. Among them, I worked with a few special people in the same project. In order of appearance, I thank my friends: André Mateus, Karin Mitosch, Sarela Garcia-Santamarina, Joel Selkrig, Anna Sueki, and Matylda Zietek. It was (and is) so much fun working with you guys!

I thank our retron collaborators, Helene-Andrews Polymenis (Texas A&M University) and Johanna Elfenbein (University of Wisconsin-Madison). Without them, we would have never started working on retrons.

I also thank my thesis advisory and PhD defense committee members; Dr. Misha Savitski, Dr. Michael Knop, Dr. Orsolya Barabas, Dr. Abram Aertsen, and Dr. Axel Mogk, for selflessly spending time to improve the work reported here.

Finally, I thank my family and my girlfriend, the love of which made this work possible.

Abstract

Retrons are prokaryotic genetic systems containing reverse transcriptases (RTs) that produce multiple copies of small single-stranded DNA (msDNA). Despite our understanding of the complex msDNA biosynthesis, the physiological role of retrons has remained elusive. I established that the Retron-Sen2 in *Salmonella* Typhimurium (*S*Tm) encodes a toxin, which I have named RcaT (Retron cold-anaerobic Toxin). RcaT is activated when msDNA biosynthesis is perturbed and inhibits *S*Tm growth at ambient temperatures or during anaerobiosis. The RT and msDNA are both necessary to counteract RcaT, by forming an RT-msDNA complex that inactivates RcaT through direct protein-protein interactions. Thus, retrons constitute a novel family of tripartite toxin/antitoxin systems (TAs), where the RcaT toxin is inactivated by the RT-msDNA antitoxin.

Bacteria carry dozens of TAs in their chromosomes. Normally, the antitoxin is co-expressed and neutralizes its cognate toxin, but TAs can be activated to inhibit bacterial growth. Yet, when and how TAs are triggered remains an enigma, hindering our understanding of their physiological roles. I developed TIC/TAC (Toxin Inhibition/Activation Conjugation), a high-throughput reverse genetics approach, to systematically identify molecular blockers and triggers of TAs. By applying TIC/TAC to Retron-Sen2, I identified multiple blockers and triggers of phage origin. Diverse phage proteins trigger RcaT toxicity by directly interacting with the msDNA-part of the antitoxin. Phage proteins can circumvent activation by directly blocking the activity of RcaT. I propose that retron-TAs act as abortive-infection anti-phage defense systems and delineate the mechanistic principles behind the retron-phage arms-race.

Zusammenfassung

Retrons sind prokaryotische genetische Systeme, welche reverse Transkriptasen beinhalten, die mehrere Kopien kurzer einzelsträngiger DNA (msDNA) produzieren. Trotz unseres Verständnisses der komplexen msDNA Biosynthese bleibt die physiologische Relevanz von Retrons ungeklärt. Ich habe gezeigt, dass das Retron-Sen2 in Salmonella Typhimurium (STm) ein Enzym kodiert, welches ich RcaT (Retron cold-anaerobic Toxin) genannt habe. Wenn die msDNA Biosynthese gestört ist, wird RcaT aktiviert und inhibiert das Wachstum von STm bei kalten Temperaturen oder unter Anaerobiose. Die RT und msDNA sind beide notwendig um RcaT entgegenzuwirken, indem sie einen RT-msDNA Komplex formen, der RcaT durch direkte Protein-Protein-Interaktionen inaktiviert. Folglich bilden Retrons eine neue Gruppe von dreiteiligen Toxin/Antitoxin Systemen (TAs), in der das RcaT Toxin durch das RT-msDNA Antitoxin inaktiviert wird.

Bakterien codieren für Dutzende TAs. Normalerweise wird das Antitoxin co-exprimiert und neutralisiert das verwandte Toxin, allerdings können TAs aktiviert werden um das bakterielle Wachstum zu inhibieren. Wann und wie TAs aktiviert werden bleibt unklar, was unser Verständnis ihrer physiologischen Rolle begrenzt. Ich habe TIC/TAC (Toxin Inhibition/Activation Conjugation), einen high-troughput reverse genetics Ansatz, entwickelt, um systematisch molekulare Inhibitoren und Aktivatoren von TAs zu identifizieren. Durch die Verwendung von TIC/TAC mit Retron-Sen2 konnte ich multiple Inhibitoren und Aktivatoren identifizieren die ursprünglich von Phagen stammen. Diverse Phagenproteine können RcaT Toxizität direkt durch eine Interaktion mit der msDNA-Komponente des Antitoxins auslösen. Phagenproteine können die Aktivierung durch direktes Blockieren der RcaT-Aktivität umgehen. Ich stelle die These auf, dass Retron-TAs als Anti-Phagen Verteidigungssysteme wirken und beschreibe die mechanistischen Prinzipien die dem Retron-Phagen Wettrüsten zugrunde liegen.

Table of contents

Table of figures

Table of tables

1. Introduction

The aim of my thesis was to understand the biological function of bacterial retrons; a class of prokaryotic retroelements of unknown function. I introduce here prokaryotic retroelements, with a specific focus on retrons. I also introduce bacterial toxin/antitoxin systems, which I found to be intrinsically similar to retrons.

1.1. Diversity of prokaryotic systems containing reverse transcriptases.

RNA-dependent DNA polymerases, known as reverse transcriptases (RTs), were first discovered in vertebrate viruses (Baltimore, 1970; Temin and Mizutani, 1970). RNA viruses use their RTs to reverse transcribe their genome into DNA, which is later integrated in the host DNA. This was the first example of genetic information flowing retrogradely from RNA to DNA, giving rise to the latest update of the central dogma of molecular biology (Crick, 1970). Due to this RNA → DNA retrograde flow of information, viruses containing RTs are called retroviruses, and genetic elements containing RTs are referred to as retroelements.

RTs were subsequently found also in prokaryotes, as part of retroelements called retrons (Lampson *et al.*, 1989a; Lampson *et al.*, 1989b; Lim and Maas, 1989). Until bacterial retrons were discovered, RTs were thought to be a hallmark of eukaryotes and viruses (Temin, 1989). Owed to the genomic revolution, it is now clear that prokaryotic retroelements display an impressive evolutionary diversity (Zimmerly and Wu, 2015). Most retroelements (90%) can be separated into three major groups, a classification primarily based on their diverging RT protein sequences. Besides retrons (12% of retroelements), the remaining two groups are group II introns (75%), and diversity-generating retroelements (3%) (Zimmerly and Wu, 2015). The remaining 10% of RTs are sub-grouped in more than twenty smaller classes, depending on the analysis (Kojima and Kanehisa, 2008; Simon and Zimmerly, 2008; Toro and Nisa-Martínez, 2014). Thus, prokaryotic retroelements exhibit extensive sequence diversity, and can be classified into multiple groups.

1.1.1. Group II introns are selfish mobile retroelements

Retroelements of different classes share some properties, but have distinct functions. Group II introns (G2Is) were discovered in fungal mitochondrial DNA and plant

chloroplast DNA (Michel *et al.*, 1989), and subsequently in bacteria (Ferat and Michel, 1993). Bacterial G2Is are self-catalytic RNA ribozymes encoding an internal RT protein, and are able to splice themselves out of genomic loci *in vivo* and *in vitro* (Mills *et al.*, 1996). The splicing mechanism of G2Is is similar to the splicing of eukaryotic introns, which are in fact thought to have descended from bacterial G2Is (Cavalier-Smith, 1991; Sharp, 1991; Zimmerly and Semper, 2015). Besides self-splicing, G2Is are mobile retroelements, able to insert themselves into specific DNA target sites (retrohoming), or even in loci not identical to their targets, albeit with lower frequencies (Muñoz *et al.*, 2001; Toro *et al.*, 2007). Bacterial G2Is form an RT-ribozyme RNP complex, that is able to home in the DNA target site, get reverse transcribed, and integrate itself in the target locus (Figure 1A) (Belfort and Lambowitz, 2019).

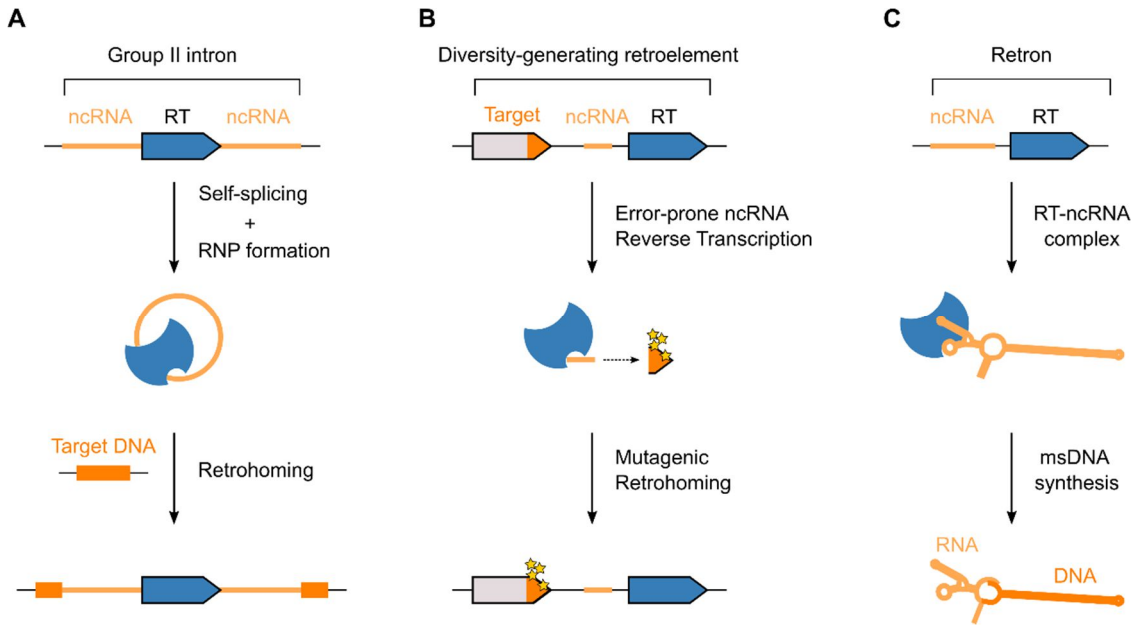

Figure 1. Diversity of reverse transcriptase functions across prokaryotic retroelements.

(A) Group II introns are mobile retroelements. A self-splicing non-coding RNA (ncRNA) encodes a protein containing a reverse transcriptase domain (RT). The RT binds the ncRNA (RNP complex), the ncRNA is reverse-transcribed by the RT, and inserted into a target DNA site (retrohoming). The mechanism depicted is overly simplified; for details I refer the reader to (McNeil *et al.*, 2016).

(B) Diversity-generating retroelements diversify C-termini of target genes. The RT along with an upstream ncRNA, is linked to a target gene. The RT reverse transcribes the ncRNA into cDNA (introducing mutations in adenines – golden stars), and the cDNA replaces the C-terminus of the target gene (mutagenic retrohoming). For more details, I refer the reader to (Wu *et al.*, 2018).

(C) Retrons produce msDNA by reverse transcription. The RT binds the highly structured ncRNA, and reverse transcribes a portion of it into cDNA. The final molecule is an RNA (light orange): DNA (deep orange) hybrid, called msDNA. The function (if any) of retrons and msDNA is unclear.

G2Is are presumed to be selfish retroelements due to their mobility, which also potentially explains their overabundance compared to other prokaryotic retroelements. Adding credence to this notion, G2Is seem to insert themselves preferentially in benign genetic loci without affecting host functions, or in mobile elements to presumably increase their passive mobility (Waldern *et al.*, 2020). Nevertheless, the group II intron LI.ltrB of a conjugative plasmid of *Lactococcus lactis* (Mills *et al.*, 1996) has been recently reported to inhibit plasmid conjugation (Qu *et al.*, 2018). This is because LI.ltrB is integrated in a relaxase gene, downregulating its expression, and thus reducing plasmid conjugation rates. This could imply a beneficial function for its bacterial host, in the form of inhibiting foreign genetic elements from being expressed. Notably, some group II intron RTs have coevolved with CRISPR-Cas1 systems, enabling spacer acquisition from phage RNA molecules, instead of DNA (Silas *et al.*, 2016). Thus, even if G2Is are currently considered as predominantly selfish mobile retroelements, they may allow the evolution of novel beneficial functions for their hosts indirectly.

1.1.2. Diversity-generating retroelements mutagenize genes *in vivo*.

Diversity-generating retroelements (DGRs) are the second class of prokaryotic retroelements, which confer fitness benefits to their hosts. DGRs contain RTs that mutate and ultimately diversify the C-terminal region of one target protein, that is usually surface exposed (Guo *et al.*, 2015). The DGR RT is >10,000 times more error prone in reverse transcribing adenines than the HIV-1 RT (~40% misincorporation) (Naorem *et al.*, 2017). In addition to the RT gene, DGRs encode a non-coding RNA (template repeat; TR), identical to the C-terminus of the target gene (variable repeat; VR). The DGR RT reverse transcribes the TR RNA in an error-prone fashion towards cDNA, which then replaces the VR through a unidirectional TR → VR retrohoming mechanism (Figure 1) (Doulatov *et al.*, 2004).

The first DGR was discovered in a *Bordetella*-infecting bacteriophage (phage), where the DGR diversifies a phage tail fiber protein (Liu *et al.*, 2002). This allows the phage progeny to adopt a wide spectrum of receptor-specificity against the everchanging *Bordetella* surface receptors (Doulatov *et al.*, 2004). Thus, the prototypical DGR helps phages to adapt to bacterial receptor surface changes. Yet, DGRs are predominantly found in bacterial chromosomes instead of phages (Wu *et al.*, 2018), where they also seem to diversify bacterial surface exposed proteins. The only two characterized

chromosomal DGRs, from *Legionella* and *Treponema* strains, diversify the surface exposed sections of lipoproteins (Le Coq and Ghosh, 2011; Arambula *et al.*, 2013). Both of these DGR-diversified surface exposed lipoproteins have no known function. Despite this, one can postulate that as in the bacterial-phage interaction, they are diversified to evade recognition of bacteria by their hosts. In both cases, sequence diversity in binding makes the difference between life and death. It is important to note that there is an impressive variety of uncharacterized DGRs left to explore, associated with very different target genes (Wu *et al.*, 2018). Thus, in contrast to group II introns, DGRs are not mobile and non-selfish, and seem to benefit their hosts by diversifying proteins involved in interspecies interactions.

1.1.3. Retrons are retroelements that produce peculiar DNA:RNA hybrids.

Retrons were the first RT-containing genetic elements discovered in bacteria. Retrons produce small extrachromosomal DNA, which were discovered before the retron RTs. This small DNA was serendipitously observed as a quickly-migrating satellite DNA band during electrophoresis of whole DNA extracts from *Myxococcus xanthus* (Yee *et al.*, 1984). The satellite DNA was named msDNA (multicopy single-stranded DNA), as it was produced at ~500 copies per cell, and was single-stranded DNA. It was later understood that these msDNAs were DNA:RNA hybrids, with the 5' end of msDNA being covalently joined with an RNA branch (Furuichi *et al.*, 1987a; Furuichi *et al.*, 1987b). Subsequently, it was shown that the RNA branch is derived from a longer precursor, that included the sequence of the DNA branch of msDNA. This suggested that the RNA precursor is the template to make msDNA, and the authors predicted that this required a reverse transcriptase (Dhundale *et al.*, 1987). Indeed, this later led to identifying the retron reverse transcriptases, which synthesize different msDNAs in diverse species (Lampson *et al.*, 1989a; Lampson *et al.*, 1989b; Lim and Maas, 1989). Retrons are operons containing a non-coding RNA (*msrmsd*) and an RT gene. The RT binds the ncRNA, and reverse transcribes a portion of it into DNA. The final product, msDNA, is usually a DNA:RNA hybrid molecule (Figure 1C).

1.1.3.1. Retrons are named after the species they reside in.

Retrons were traditionally named based on the species they are found in and the length of their msDNA (Lampson *et al.*, 1989b). For example, the prototypical retron (Yee *et al.*, 1984) was named Mx162 because it is found in *Myxococcus xanthus*, and its msDNA is 162 bases. This naming system is unwieldly, since it is not easy to calculate msDNA length from retron sequence alone. An improved nomenclature has been proposed (Simon *et al.*, 2019). The new retron nomenclature uses (1) the first letter of the genus, (2) the two first letters of the species, and, (3) an Arabic number denoting the chronological order by which retrons were discovered in a specific species. Using the new system, Mx162 would be renamed as Retron-Mxa1, because it is a retron isolated from *Myxococcus xanthus*. The Arabic numeral is 1, since Retron-Mxa1 was the first retron found in *Myxococcus xanthus*. I will use the (Simon *et al.*, 2019) naming system, while referring to the old nomenclature in brackets for clarity.

1.1.3.2. Retrons and msDNA have no known physiological roles.

It quickly became clear that retrons are not essential for bacterial survival, since deleting them produced no observable phenotypes under laboratory growth conditions. Additionally, the retron distribution pattern varied substantially even within bacterial species. Early experimental studies found retrons in 7 out of 113 *E. coli* clinical isolates (Sun *et al.*, 1989), in 9 out of 72 *E. coli* natural isolates (Herzer *et al.*, 1990), or in 10 out of 63 rhizobial bacterial strains (Rice *et al.*, 1993). On the other hand, retrons were identified in 27 out of 28 Myxococcal bacterial strains (Rice and Lampson, 1995). Notably, even when retrons were present in strains of the same species, the retrons and msDNA were highly divergent between strains. Combining (1) the absence of phenotypes from deleting retrons, (2) the patchy phylogenetic distribution pattern of retrons, and, (3) the notion that retroelements are usually selfish systems (e.g., group II introns), led to the hypothesis that retrons are also selfish mobile retroelements. This spurred investigations on retron mobility (Hsu *et al.*, 1990; Herzer *et al.*, 1992; Dodd and Egan, 1996; Lampson *et al.*, 2005; Inouye *et al.*, 2011), that did not provide evidence for retrons being able to retrotranspose. Thus, retrons are unlikely to be mobile retroelements.

An alternative hypothetical retron function was that msDNA production is used as a mutagen *in vivo*. This hypothesis came forth due to observing that overproducing the

msDNA from Retron-Eco1 [Ec86] and Retron-Eco4 [Ec83] was highly mutagenic (Maas *et al.*, 1994). Although msDNA are single-stranded DNA, and very little sequence homology exists between msDNA from different retrons, all msDNA contain extended hairpin regions forming double-stranded DNA (Figure 1C) (Lampson *et al.*, 2005). The authors noted that msDNA-Eco1 and -Eco4 contained mismatched base pairs in its hairpin DNA. These mismatched base pairs could sequester DNA repair enzymes from the cell, leading to increased mutation rates. Indeed, it was later shown that overproducing msDNA-Eco1 and -Eco4 sequestered the mismatch repair protein MutS, leaving the cell vulnerable to DNA damage (Maas *et al.*, 1996). Nevertheless, this is unlikely to be the physiological function of retrons. This is because (1) mutation rates were only increased upon overproducing msDNA, while remaining unaffected when retrons were deleted (Maas *et al.*, 1994), and, (2) not all retrons produce msDNA with mismatches, and these are not mutagenic (Mao *et al.*, 1996). Thus, despite substantial efforts, the physiological role of retrons remained elusive.

1.1.3.3. Some retrons encode additional ORFs of unknown function.

Although all retrons encode a reverse transcriptase and the RNA template to make msDNA (*msrmsd*), there have been reports that at least one third of retrons encode additional Open Reading Frames (ORFs) (Simon *et al.*, 2019). These ORFs usually do not have any or have limited domain similarity to known proteins, and they vary in sequence and location relative to the core retron genes (Figure 2). In all cases tested, these ORFs do not affect msDNA production from their respective retrons. For example, Retron-Sen2 [ST85] (Figure 2) has an additional ORF between the *msrmsd* and the RT gene (Ahmed and Shimamoto, 2003), that is not needed for synthesizing msDNA-Sen2 (Elfenbein *et al.*, 2015). Additionally, some retron reverse transcriptases are much larger in size than the average retron RTs. For instance, while most retron RTs are ~300 residues long, the RT of Retron-Eco2 [Ec67] is 587 residues long (Figure 2) (Hsu *et al.*, 1990). This suggests that some RTs contain extra domains, that might be analogous to the extra ORF of other retrons. Indeed, there have been reports of retron RTs containing variable domains (e.g., protease domain) (Zimmerly and Wu, 2015). Although these ORFs are genetically linked to retrons, it has not been shown that they are functionally linked. Thus, although all retrons contain *msrmsd* and an RT, some retrons seem to contain additional ORFs of unknown functions.

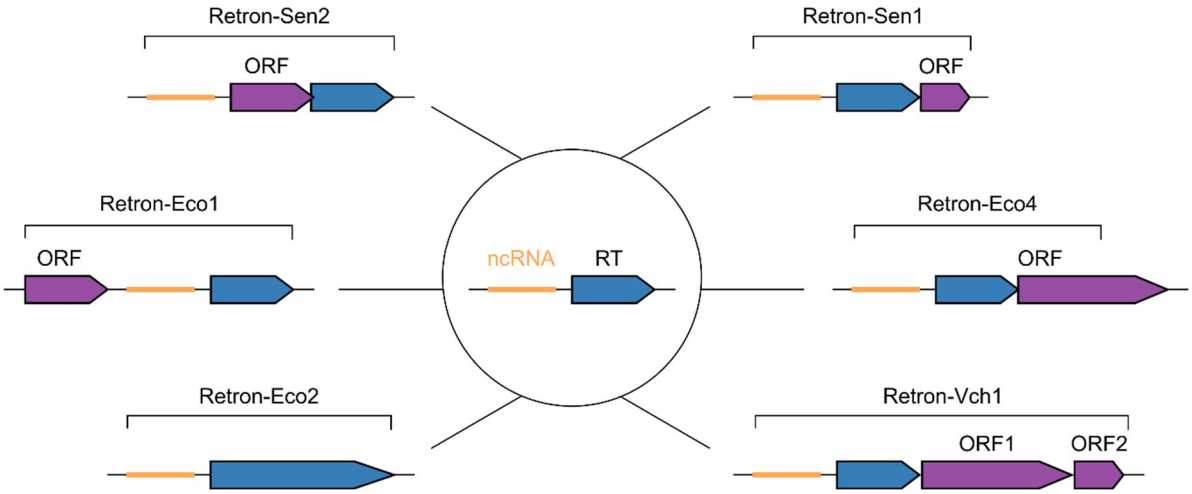

Figure 2. Retrons often contain additional ORFs of unknown function. Besides the reverse transcriptase gene (RT) and the non-coding RNA (ncRNA; *msrmsd*), some retrons encode linked additional ORFs of unknown function, in various locations relative to the core retron genes. Examples of retrons containing additional ORFs are shown. The additional ORFs are depicted in purple, and were first described in the following publications: Retron-Sen2 [ST85] (Ahmed and Shimamoto, 2003), Retron-Eco1 [Ec86] and Retron-Eco2 [Ec67] (Dodd and Egan, 1996), Retron-Sen2 [Se72] (Pilousova and Rychlik, 2011), Retron-Eco4 [Ec83] (Lim, 1992), and Retron-Vch1 [Vc95] (Inouye *et al.*, 2011).

1.1.3.4. Retrons produce msDNA through a complex reverse transcription pathway.

Retrons produce msDNA through a reverse transcription cascade involving multiple components with common and diverging features across retrons. I will describe the general msDNA synthesis pathway, while using the retron I studied as an example (Retron-Sen2 [ST85]) (Figure 3).

First, the RT and *msrmsd* are transcribed in a single transcriptional unit (Lampson *et al.*, 1989a). The msrmsd ncRNAs (msrmsd-RNA) are usually ~200 bp and vary widely in sequence between retrons (Lampson *et al.*, 2005), but their structural features are highly conserved. Specifically, all the msrmsd-RNAs have two sets of inverted repeats (IR). The first IR is formed between the start of *msr* and the end of *msd* and is usually 7-10 nucleotides long (Dhundale *et al.*, 1987). This first IR denotes the start and end of msrmsd-RNA (Figure 3B). The second IR is usually longer (10-20 nucleotides), sometimes contains mismatches, and is formed from sequences within *msd*. The second IR is the region that always gets reverse transcribed into cDNA from the retron RTs (Figure 3B).

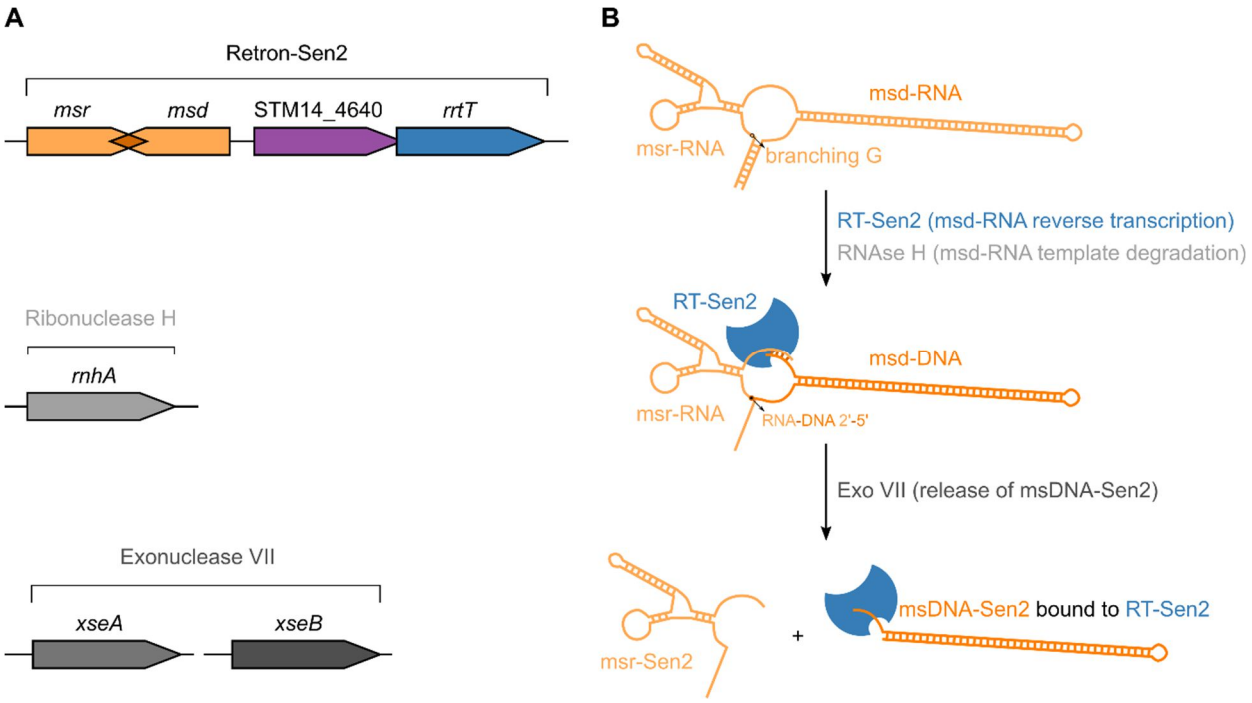

Figure 3. Biosynthesis of msDNA by retrons using Retron-Sen2 as an example.

(A) Genes involved in msDNA-Sen2 synthesis. Retron-Sen2 contains genes *msrmsd* (msrmsd-RNA), STM14_4640 (unknown function), and *rrtT* (RT-Sen2). Genes *rnhA* (ribonuclease H), and *xseA*/*xseB* (exonuclease VII) are not genetically linked with Retron-Sen2, but are involved in msDNA-Sen2 synthesis.

(B) msDNA-Sen2 synthesis pathway. The msrmsd-RNA is bound by RT-Sen2, which reverse transcribes the msd-RNA sequence into msd-DNA. Ribonuclease H (RNAse H) degrades the used msd-RNA template. The msr-RNA and msd-DNA are covalently linked through a 2'-5' phosphodiester bond (RNA-DNA 2'-5') formed by RT-Sen2. Although msDNA synthesis usually stops at the RNA: DNA hybrid stage, in some retrons like Retron-Sen2, four nucleotides are cleaved off from the 5' of msd-DNA by the action of exonuclease VII (Exo VII) (Jung *et al.*, 2015). This separates the RNA and the DNA branches of msDNA. The mature msDNA-Sen2 is an 81 nucleotides long single-stranded DNA, forming an elongated dsDNA hairpin, and RT-Sen2 presumably remains complexed with msDNA-Sen2 after its production, as inferred from other retrons (Lampson *et al.*, 1990; Jeong *et al.*, 1997).

The retron RT recognizes its cognate msrmsd-RNA in a highly specific manner. The C-terminal regions of retron RTs bind specifically to secondary structures of the msr-RNA (Shimamoto *et al.*, 1993; Inouye *et al.*, 2004). RTs from different retrons cannot bind and reverse transcribe non-cognate msrmsd-RNA, unless their msr regions are highly similar (Shimamoto *et al.*, 2013). Subsequently, retron RTs reverse transcribe the msd-RNA (template) into msd-DNA. Reverse transcription starts internally from an absolutely conserved guanosine residue of the msr-RNA (branching G; Figure 3B). Mutating the branching G towards other nucleotides abolishes msDNA production,

while not affecting msrmsd-RNA levels (Hsu *et al.*, 1989). Notably, the 2'-OH of the branching G is used to prime reverse transcription; thus, retron RTs create a unique 2'-5' phosphodiester bond between the msr-RNA and msd-DNA (Furuichi *et al.*, 1987a). Recently, a similar 2'-5' RNA-DNA phosphodiester bond was shown to form during the mutagenic retrohoming of diversity-generating retroelements (Handa *et al.*, 2018).

Besides the RT and msrmsd-RNA, ribonuclease H (RNAse H) is also needed for msDNA production. The evolution of reverse transcriptases are tightly intertwined with RNAse H (Moelling and Broecker, 2015). RNAse H degrades RNA strands in DNA:RNA hybrids, which are formed during reverse transcription. Viral reverse transcriptases contain RNAse H domains of their own, that assist in reverse transcription (Davies *et al.*, 1991). In contrast, Retron RTs do not have RNAse H domains, and utilize instead the bacterial RNAse H (gene *rnhA*; Figure 3A), which degrades the msd-RNA template after reverse transcription (Figure 3B). Mutating *rnhA* leads to producing lower quantities of irregularly shorter or longer msDNAs (Shimamoto *et al.*, 1995; Lima and Lim, 1995). Most retrons end their msDNA synthesis at that stage; with msd-DNA being linked to msr-RNA through a covalent 2'-5' bond and through four hydrogen bonds between their 3' ends (Figure 3B). Thus, retrons require the action of host RNAse H for proper msDNA production.

A minority of retrons produce msDNA that are modified after reverse transcription. Specifically, msDNAs-Eco4 [Ec83] and -Eco7 [Ec78] are produced without the msr-RNA being joined to the msd-DNA, and are called RNA-less msDNAs (Lima and Lim, 1997). These msDNAs are produced from DNA:RNA precursors, but their msd-DNA is cleaved close to the 2'-5' phosphodiester bond (between the fourth/fifth nucleotide of msd-DNA) (Kim *et al.*, 1997). The msDNAs-Sen2 [ST85], -Vch1 [Vc95], and -Vpa1 [Vp96] are also hypothesized to be RNA-less, based on their structural similarity to msDNAs-Eco4 and -Eco7 (Ahmed and Shimamoto, 2003). The cleaving in msDNAs-Eco4 and -Eco7 is carried out by a host deoxyribonuclease, exonuclease VII (Exo VII), encoded by the *xseA*/*xseB* genes (Figure 3A) (Jung *et al.*, 2015). Exo VII-mediated msd-DNA cleavage presumably separates the msd-DNA from the msr-RNA, producing mature msDNA (Figure 3B). Thus, some msDNA are pure single-stranded DNAs.

Finally, the retron RTs remain in a complex with their msDNA products. For example, RT-Eco2 [Ec67] (Figure 2) elutes as a very large complex (~600 kDa) after purification and gel filtration, while the protein itself is 65 kDa (Lampson *et al.*, 1990). This complex was shown to be predominantly composed of RT-Eco2 and its cognate msDNA, thus the RT is copurifying with its msDNA product. Another study focused on purifying RT-Eco4 [Ec83] (Figure 2), which also co-eluted with its cognate msDNA (Jeong *et al.*, 1997). Notably, although msDNA-Eco2 is an DNA:RNA hybrid, msDNA-Eco4 is an RNA-less msDNA. It is therefore likely that RT-msDNA interactions are mediated through protein-DNA interactions, rather than protein-RNA interactions. Thus, retron RTs remain bound to their msDNA products (Figure 3B).

1.1.3.5. Retrons enable *in vivo* directed mutagenesis in diverse species.

Retrons uniquely produce short ssDNA (msDNA) *in vivo* (Figure 3B). Genetic recombineering approaches frequently require external DNA oligo delivery, usually accomplished by electroporating PCR products in electrocompetent cells (Chassy *et al.*, 1988). After the exogenous DNA is in the cells, it recombines with homologous genomic-DNA regions, enabling site-directed mutagenesis (Datsenko and Wanner, 2000). Early reports have showed that retron RTs can reverse transcribe the msd-DNA hairpin irrespectively of its sequence (Mao *et al.*, 1995). Therefore, retrons can be used to produce any desired ssDNAs (msDNA) *in vivo*, in order to mutate homologous DNA-target regions. Indeed, overexpressing msDNA homologous against genomic target regions, enabled directed mutagenesis in bacteria (Farzadfard and Lu, 2014), initially with low efficiency. More recent reports exhibited retron-mediated directed mutagenesis with 100% efficiency in bacteria (Farzadfard *et al.*, 2020; Schubert *et al.*, 2020). Additionally, retron-mediated mutagenesis could be applied to eukaryotes, since retrons can produce msDNA in yeast (Miyata *et al.*, 1992) or in mammalian cell lines (Mirochnitchenko *et al.*, 1994). Thus, retrons present a viable alternative to CRISPR/Cas genome editing tools, with mutations requiring only expressing mutated msDNA homologous to target regions.

1.1.3.6. Retron-Sen2; first example of a retron-mediated phenotype in *Salmonella*.

Retrons were considered as selfish retroelements, largely due to the absence of phenotypes associated with deleting them. The first unambiguous retron phenotype was reported in *Salmonella enterica* ser. Typhimurium (*S*Tm), where Retron-Sen2

[ST85] was shown to affect the virulence of *S*Tm against calves (Elfenbein *et al.*, 2013). In this study, a single-gene deletion library of *S*Tm (Porwollik *et al.*, 2014) was screened for colonization efficiency against a calf-infection anaerobic model, that closely mimics the native calf intestine. Remarkably, deleting the *rrtT* gene (RT-Sen2, the reverse transcriptase of Retron-Sen2) strongly decreased the virulence of *S*Tm (Elfenbein *et al.*, 2013). In a follow up study, the same group showed that deleting either RT-Sen2 or the *msd* (i.e., abolishing msDNA) led to a severe growth defect of *S*Tm under anaerobic conditions (Elfenbein *et al.*, 2015). Thus, Retron-Sen2 was the first retron for which a phenotype was reported, with its presence being required for anaerobic growth of *S*Tm through an unidentified mechanism.

1.1.4. Abi-Type retroelements defend bacteria against phages.

Besides the three main prokaryotic retroelement classes, a small phylogenetically-related group of RTs (AbiK, AbiA, and Abi-P2) are anti-phage abortive infection systems (Zimmerly and Wu, 2015). Abortive infection (Abi) is an umbrella term describing bacterial anti-phage defenses triggered only after a phage successfully bypasses early bacterial defenses (such as restriction-modification or CRISPR/Cas systems) (Forde and Fitzgerald, 1999). Upon phage-mediated Abi triggering, the Abi systems inhibit phage proliferation by attacking the phage-infected bacteria themselves, and thus, spare the remaining bacterial population from phage attack. An impressive number of different Abi systems have been discovered in *Lactococcus lactis* (AbiA – AbiZ) (Chopin *et al.*, 2005), since *L. lactis* is used in dairy product fermentation; a phage-bacterial battleground of economic interest. AbiA and AbiK contain an RT domain in their N-terminus (Fortier *et al.*, 2005), but were initially found through their phage-resistance phenotype (Hill *et al.*, 1990; Emond *et al.*, 1997). Additionally, a phylogenetically similar anti-phage Abi-retroelement (Abi-P2) was found in a prophage of *Escherichia coli* (Odegrip *et al.*, 2006).

Although Abi-type retroelements have a clear antiviral function, their mechanism of action is largely unknown. Their RT domain is necessary for their function, since mutating it abolishes anti-phage activity (Fortier *et al.*, 2005). Nevertheless, AbiK also has a C-terminal domain, that is also essential for anti-phage activity, but displays no similarity to known domains (Fortier *et al.*, 2005). Additionally, AbiK does not seem to reverse transcribe specific RNAs to cDNA, but rather produces random strands of

DNA molecules, and covalently attaches them to itself (Wang *et al.*, 2011). Thus, although Abi-type retroelements are clearly related to RTs by sequence, more work is needed to understand how they confer anti-phage defense.

1.2. Toxin/antitoxin systems are diverse self-targeting growth inhibitors.

During my work, I discovered that Retron-Sen2 is a novel toxin/antitoxin system (TA). I will thus briefly introduce prokaryotic TA systems. The vast majority of toxin/antitoxin systems are formed by two genetically linked genes, a growth inhibitor (toxin) and an inhibitor of the toxin (antitoxin). Two hallmark phenotypes define TA systems: 1) antitoxin perturbations (e.g., deletion) activate its cognate toxin, which inhibits bacterial growth, and, (2) overexpressing the toxin inhibits growth, while co-expressing the toxin with its antitoxin alleviates the inhibition.

TA systems are wondrously diverse and abundant in bacteria. This diversity is reflected in the variable way that antitoxins (protein or RNA) inactivate their toxins (always proteins). TA systems are categorized in types based on how the antitoxin works. Four major types currently exist (Figure 4) (Page and Peti, 2016; Harms *et al.*, 2018), as well as three additional types with single TA representatives (Wang *et al.*, 2012; Aakre *et al.*, 2013; Marimon *et al.*, 2016), and even further subclassifications are proposed every year (Song and Wood, 2020). Type II TAs are the most abundant (Coray *et al.*, 2017), where the protein antitoxin directly binds and inactivates its cognate toxin by forming a tight complex (Tam and Kline, 1989). However, even within type II, there are (at least) twenty antitoxin subtypes based on sequence comparisons (Leplae *et al.*, 2011). In addition to antitoxins physically interacting with their toxins, some also need to phosphorylate (Yu *et al.*, 2020), or polyadenylate their cognate toxins (Yao *et al.*, 2020), or require a specialized SecB-like chaperone to keep them folded (Bordes *et al.*, 2011). On the other side of the coin, type II toxins also attack different bacterial targets. To name a few, toxins can target the DNA gyrase (Bernard and Couturier, 1992), directly ADP-ribosylate DNA (Jankevicius *et al.*, 2016), acetylate different charged tRNAs (Van Melderen *et al.*, 2018; Wilcox *et al.*, 2018), or phosphorylate tRNA synthetases (Nielsen *et al.*, 2019). Thus, even within the same type, TA systems exhibit a broad diversity in how antitoxins inhibit their toxins, and in how toxins inhibit bacterial growth.

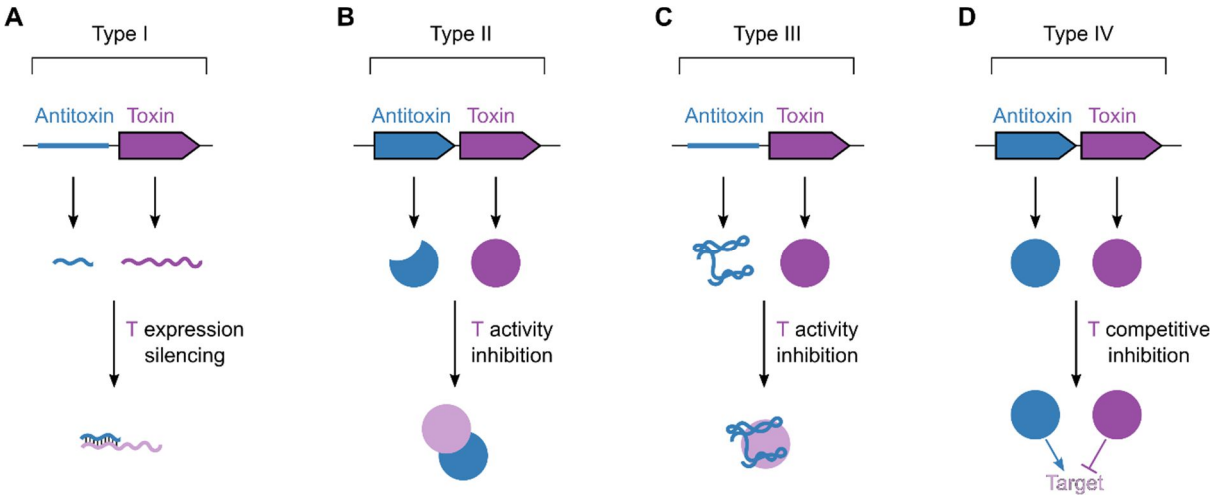

Figure 4. Major types of toxin/antitoxin (TA) systems based on antitoxin mode of action.

(A) Type I RNA-antitoxins silence toxin expression. The RNA-antitoxin is expressed, and inhibits toxin protein expression by directly base-pairing with the toxin mRNA.

(B) Type II protein-antitoxins inhibit toxin activity by direct binding. The protein-antitoxin directly binds and inhibits the toxin protein.

(C) Type III RNA-antitoxins inhibit toxin activity by direct binding. The RNA-antitoxin directly binds and inhibits the toxin protein.

(D) Type IV protein-antitoxins inhibit toxin activity by competing for the toxin target. The protein-antitoxin acts on the cellular target of the toxin, in an opposite fashion compared to the effect of the toxin.

1.2.1. TA systems addict bacteria to plasmids and defend against phages.

The majority of TAs still have unclear physiological roles in bacteria. The first TA systems were found to promote plasmid maintenance in bacteria (Ogura and Hiraga, 1983; Gerdes *et al.*, 1986; Lehnherr *et al.*, 1993). The property of TAs in enhancing plasmid maintenance is called “addiction” (Yarmolinsky, 1995), where TAs addict bacteria in keeping the plasmid that encodes them. Normally, the toxin expressed from a plasmid is nullified by forming a complex with its cognate antitoxin, and the cells grow. If the plasmid is lost (e.g., during bacterial division), the toxin is triggered, and inhibits the growth of plasmid free cells. The toxin is released due to the antitoxin being more labile than the toxin (Van Melderen *et al.*, 1994; Lehnherr and Yarmolinsky, 1995). Thus, plasmid-TAs confer a clear advantage to the plasmid that carries them, by inhibiting the growth of bacteria that lose said plasmid (Figure 5).

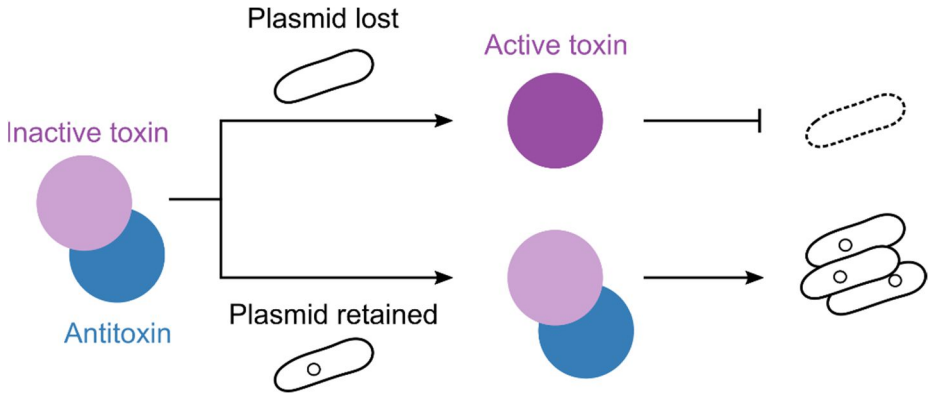

Figure 5. Plasmid addiction phenotype of toxin/antitoxin systems. Plasmids express toxin/antitoxin systems, where the toxin is kept inhibited by being bound by its antitoxin. When the plasmid is lost from a bacterium, cellular proteases preferentially degrade the antitoxin, triggering the toxin. The toxin inhibits the growth of plasmid-free segregant cells.

In the early times of bacterial genomics, it became clear that TA systems were also abundantly present in prokaryotic chromosomes (Pandey and Gerdes, 2005). For instance, *E. coli* K-12 encodes at least 35 distinct chromosomal-TAs (Harms *et al.*, 2018), while *Mycobacterium tuberculosis* H37Rv carries 88 type II chromosomal-TAs (Ramage *et al.*, 2009). In contrast to plasmid-based TAs, chromosomal-TAs do not seem to confer addictive phenotypes to genetic elements (Pedersen and Gerdes, 1999; Wilbaux *et al.*, 2007; LeRoux *et al.*, 2020). Therefore, in contrast to plasmid-encoded TAs, chromosomal-TAs do not seem to carry labile antitoxins. Thus, the function of chromosomal-TAs, and their triggering mechanism, has been the subject of an active debate for over 20 years, with multiple claims on hypothetical TA functions. Unfortunately, confirmation biases and artefacts have plagued the TA field, hindering progress in understanding the workings of chromosomal-TAs (Van Melderen and Wood, 2017; Goormaghtigh *et al.*, 2018b; Song and Wood, 2018; Goormaghtigh *et al.*, 2018a; Fraikin *et al.*, 2019).

A well-supported physiological role of TA systems is to defend against phages through abortive infection (Abi; 1.1.4). A handful of plasmid-TAs and chromosomal-TAs were shown to confer resistance against phage infections (Pecota and Wood, 1996; Fineran *et al.*, 2009; Blower *et al.*, 2012; Sberro *et al.*, 2013; Dy *et al.*, 2014; Dedrick *et al.*, 2017). Upon phage infection, bacterial toxins are triggered through unknown mechanisms, inhibiting the growth of the infected cells, which reduces phage

propagation, and thus spare the rest of the bacterial population (Figure 6). Notably, it has been shown in two cases that phages carry genes with the sole purpose of blocking toxins of TA systems. For instance, early reports identified an RNAse activity that decreases propagation of a mutant T4 Δ*dmd* phage in *E. coli* (Kai *et al.*, 1996). It was later understood that the mutant phage triggers an RNAse (RnlA) (Otsuka *et al.*, 2007), and that RnlA is in fact a toxin of a type II TA system (Koga *et al.*, 2011). Notably, the phage protein Dmd, was shown to directly bind the *E. coli* toxin RnlA and block its activity (Otsuka and Yonesaki, 2012). Analogously to Dmd, the *sanaTA* system confers defense only against a T7 Δ4.5 phage mutant, suggesting that phage gene 4.5 blocks the toxin of *sanaTA* (Sberro *et al.*, 2013) Thus, TA systems likely represent an arms-race battleground between bacteria and phages.

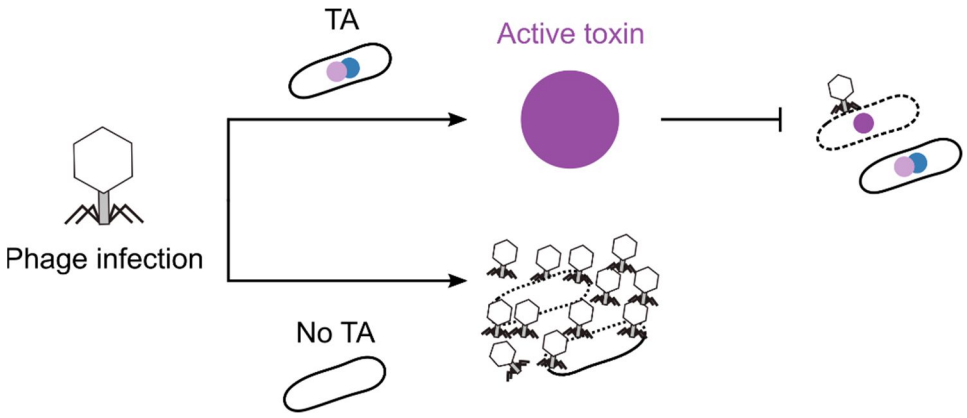

Figure 6. Toxin/antitoxin systems defend bacteria against phages. Upon phage infection, TA systems are triggered (by unknown mechanisms), and their active toxins inhibit the growth of the phage-infected cell, reducing phage propagation at the site of infection, and protecting the population. Without TA systems, phages propagate unobstructed.

1.3. Aim of my thesis.

The overall aim of my work was to find the biological function of retrons, by utilizing a Retron-Sen2 dependent phenotype identified in *Salmonella* (Pfalz, 2017).

The specific questions that I tried answering were:

1) **How is Retron-Sen2 affecting *Salmonella* growth in specific conditions?**
   The answer is that Retron-Sen2 encodes and inhibits a toxin protein (Chapter 2).

2) **What is the mechanism through which Retron-Sen2 inhibits its toxin?**
   The answer is that Retron-Sen2 is a novel toxin/antitoxin system (TA), where the RT-msDNA antitoxin directly inhibits the retron-encoded toxin by protein interactions (Chapters 2+3).

   - Answering these two questions led to a submitted manuscript:

   Bobonis, J., Mateus, A., Pfalz, B., Garcia-Santamarina, S., Galardini, M., Kobayashi, C., Stein, F., Savitski, MM., Elfenbein, JR., Andrews-Polymenis, H. and Typas, A. Bacterial retrons encode tripartite toxin/antitoxin systems. Preprint at bioRxiv (2020).

3) **How and when is the retron-TA activated?**
   Phage proteins directly trigger or block Retron-Sen2 toxicity (Chapter 4).

   - Answering this question also led to a submitted manuscript:

   Bobonis, J., Mitosch, K., Mateus, A., Kritikos, G., Elfenbein, JR., Savitski, MM., Andrews-Polymenis, H. and Typas, A. Phage proteins block and trigger retron toxin/antitoxin systems. Preprint at bioRxiv (2020).

Both manuscripts have undergone the first round of peer review and have received positive comments in general. I am currently finalizing the revisions for both papers.

4) **How can one find the target of the retron-encoded toxin? (Chapter 5).**
   The answer is still unclear, but the investigation reported here suggests that the retron-encoded toxin might be a ribonuclease (see also Discussion; 6.1.4, 6.2.5).

2. Retrons encode toxin/antitoxin systems.

The function of retrons has remained elusive for thirty years since their discovery, largely due to the absence of phenotypes associated with them. Retron-mediated phenotypes could be used to understand under which conditions retrons affect bacterial physiology, and therefore to find their biological function. Notably, our lab identified a retron-associated growth phenotype in *Salmonella* (Pfalz, 2017).

In Chapter 2

- I used a retron-associated growth phenotype to discover that Retron-Sen2 in *Salmonella* is a toxin/antitoxin system (TA). Besides the *msrmsd* and the RT, Retron-Sen2 encodes a toxin protein, which requires the mature msDNA to be inhibited (2.1, 2.2, 2.3).
- The Retron-Sen2 operon is the minimal genetic system required for the TA system to be functional, which works heterologously if expressed in *Escherichia coli* (*E. coli*). I took advantage of the *E. coli* retron-TA phenotype to find novel host factors affecting msDNA biosynthesis (2.4, 2.5, 2.6).
- I also show that a distinct retron found in an *E. coli* natural isolate (named Retron-Eco9), also functions as a retron-TA system, in a similar manner to Retron-Sen2 (2.7).

Collaborator contributions per figure

Figure 7: **Birgit Pfalz** (EMBL, Heidelberg) conducted the *S*Tm chemical genetics screen and analyzed the data with **Marco Galardini** (TWINCORE, Hannover).

Figure 9, Figure 14B: I collaborated with **Sarela Garcia Santamarina** (EMBL, Heidelberg) for the anaerobic growth curve experiments.

Figure 12: **Rastislav Horos** (EMBL, Heidelberg) kindly taught me *in vivo* UV-crosslinking.

Figure 13A: **Marco Galardini** (TWINCORE, Hannover) analyzed the genomic sequencing data from the suppressor mutants.

Figure 19: **Morgane Wartel** (EMBL, Heidelberg) helped me in setting up high-throughput plasmid conjugation on plates.

Figure 22: **Nazgul Sakenova** (EMBL, Heidelberg) BLASTed the RcaT/RT sequences in the *E. coli* natural isolates, which led to identifying Retron-Eco9.

2.1. Large-scale screen finds new Retron-Sen2 phenotype in *Salmonella*.

High-throughput reverse genetics screens connect genotypes to phenotypes, providing cues for investigating gene function. An arrayed systematic single-gene deletion library of *Salmonella* enterica ser. Typhimurium str. 14028s (*S*Tm) (Porwollik *et al.*, 2014) was growth profiled in 175 stress conditions (Pfalz, 2017). The *S*Tm library contained two retron-associated mutant strains, deleted in *rrtT* and *xseA* genes. Deleting *rrtT* or *xseA* inhibited the growth of *S*Tm at room temperature (~23°C, Figure 7). The *rrtT* gene encodes the reverse transcriptase (RT-Sen2) of Retron-Sen2 (Ahmed and Shimamoto, 2003), which is required to produce msDNA-Sen2 (Figure 3) (Elfenbein *et al.*, 2015). On the other hand, *xseA* encodes the large subunit of exodeoxyribonuclease VII (Exo VII), that helps in maturation of the msDNA produced from Retrons-Eco4 and -Eco7 from *E. coli* (Figure 3)(Jung *et al.*, 2015). I hypothesized that Exo VII processes msDNA-Sen2, since msDNA-Sen2 is similarly structured to msDNAs-Eco4 and -Eco7 (Ahmed and Shimamoto, 2003). Thus, deleting genes involved in msDNA-Sen2 biosynthesis inhibits *S*Tm growth in colder temperatures, suggesting that msDNA-Sen2 is required for growth in this condition.

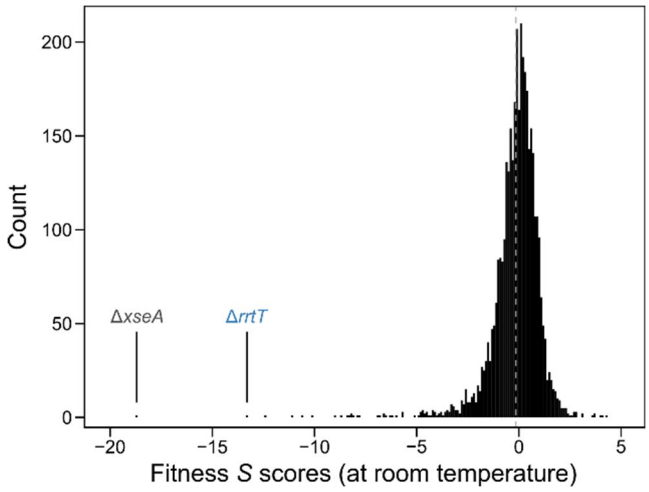

Figure 7. Strains Δ*rrtT* and Δ*xseA* are cold-sensitive. *S*Tm gene deletion strains (*n*=3781) were grown on LB plates at room temperature, and colony sizes were used to calculate fitness (*S* score, from *n*=8). Dashed vertical line denotes the mean *S* score for all strains. Negative *S* scores indicate diminished growth per strain per condition, compared to all other conditions.

2.1.1. msDNA production is required for growth in cold and anaerobiosis.

Retrons produce msDNA through a reverse transcription cascade, involving multiple gene products. I constructed clean deletion strains for every step of the cascade, and tested their growth in lower temperatures. Deleting any gene involved in msDNA-Sen2 biosynthesis produced varying degrees of cold-sensitivity (below 25°C), without impacting growth at 37°C (Figure 8). Deleting STM14_4640, the gene between *msrmsd* and *rrtT* (Figure 3) did not cause cold-sensitivity (Figure 8).

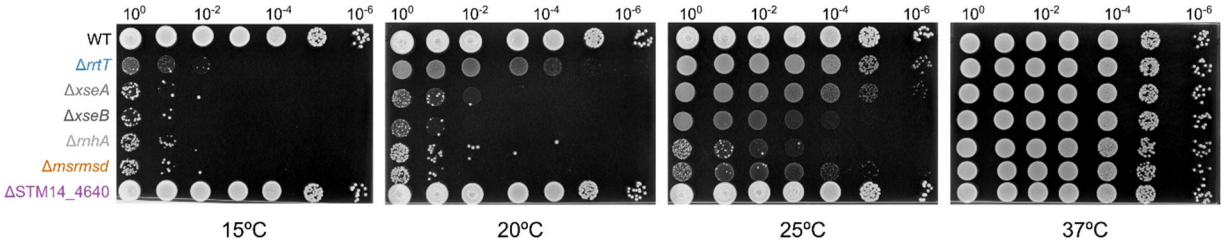

Figure 8. Inhibiting msDNA-Sen2 biosynthesis leads to cold-sensitivity. *S*Tm wildtype and Retron-Sen2 deletion strains were grown in LB/37°C for 6 hours, serially diluted, and spotted on LB plates. Plates were subsequently incubated either at 15, 20, 25, or 37°C. Representative results shown from four independent experiments.

The Retron-Sen2 was previously shown to regulate *S*Tm growth in anaerobic conditions (Elfenbein *et al.*, 2015). Confirming and extending previous results, all mutants except ΔSTM14_4640 grew less in anoxic conditions at 37°C (Figure 9). Thus, msDNA production is necessary for *S*Tm growth in cold and anaerobiosis.

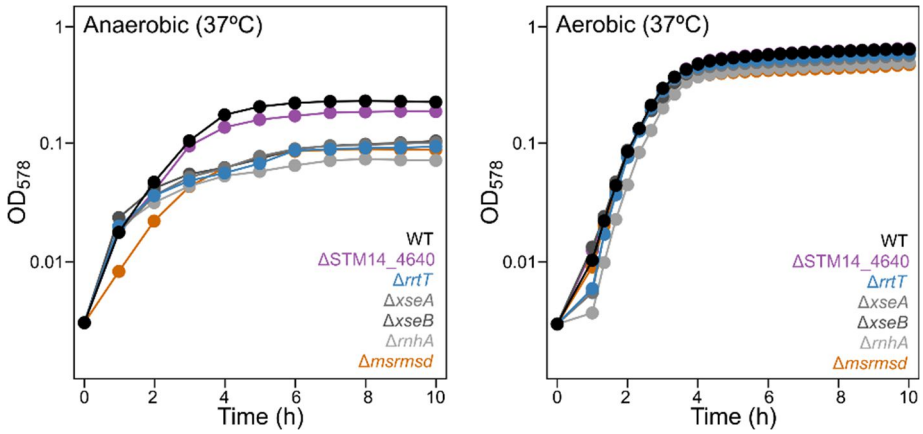

Figure 9. Retron-Sen2 mutants grow less in anoxic conditions. *S*Tm wildtype and retron-mutants were grown anaerobically or aerobically in LB medium/37°C, and growth curves were obtained by measuring OD_{578} in 96 well plates. Each data point is the average of OD_{578} measurements of n=11 wells (technical replicates), error bars denote standard deviation (not shown if smaller than symbols).

2.2. STm retron mutants exhibit defects in msDNA-Sen2 biosynthesis.

Deleting msDNA-Sen2 biosynthesis genes should impair its production. As for other retrons, the reverse transcriptase (encoded by *rrtT*) and the *msrmsd* are essential for producing the msDNA-Sen2 (Elfenbein *et al.*, 2015). Additionally, msDNA-Sen2 is (1) not produced in Δ*rnhA* (RNase H) strains, (2) produced as a longer form in Δ*xseAB* (Exo VII), and, (3) produced normally in ΔSTM14_4640 strains (Figure 10). My findings are consistent with reports on msDNA synthesis from other retrons (Shimamoto *et al.*, 1995; Jung *et al.*, 2015). Thus, the retron deletion mutants exhibiting cold- and anaerobic-sensitivity are indeed perturbed in msDNA-Sen2 synthesis.

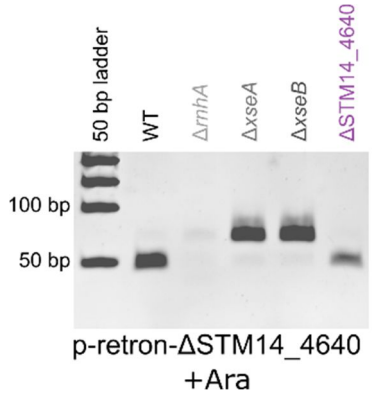

Figure 10. RNAse H and Exo VII aid msDNA-Sen2 synthesis. msDNA was isolated from *S*Tm wildtype or retron deletion strains overexpressing *msrmsd-rrtT* with Arabinose. Isolated msDNA was electrophoresed on a TBE-Polyacrylamide gel, and stained with ethidium bromide. A representative gel from three independent experiments is shown.

2.2.1. Exonuclease VII cleaves msDNA-Sen2 from its 5' end.

Exo VII was proposed to separate the RNA-part from the DNA-part of the msDNA, by cleaving nucleotides from the 5' side of the immature msDNA (Lima and Lim, 1997; Jung *et al.*, 2015). Since Exo VII has both 5' → 3' and 3' → 5' exonucleolytic capacities (Chase and Richardson, 1974), it could in principle cleave the msDNA from its 3' side. If that were the case, Exo VII would be an unlikely candidate for separating the RNA from the DNA, since these are joined at the 5' side of msDNA. To distinguish whether Exo VII cleaves nucleotides from the 5' or the 3' side of msDNA, I digested the mature and immature msDNA forms (purified from wildtype or Δ*xseA*, respectively) with the restriction enzyme Sau3AI. Different fragment size patterns translate to the side where Exo VII cleaves from (Figure 11A). The msDNA restriction analysis proved that Exo

VII cleaves the msDNA-Sen2 from its 5' side (Figure 11B). Thus, Exo VII-mediated cleavage is likely releasing the mature msDNA from its RNA: DNA preform (Figure 3).

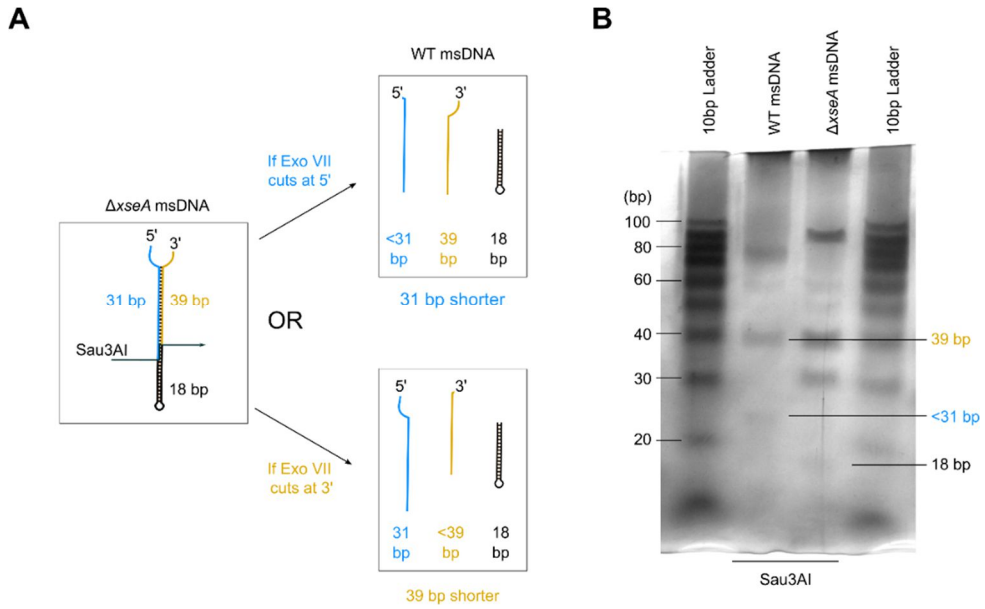

Figure 11. Exo VII cleaves off nucleotides from the 5' side of msDNA-Sen2.

(A) Schematic depiction of msDNA Sau3AI restriction analysis. Restriction enzyme Sau3AI cuts msDNA at a single site, separating it into three fragments. Depending where Exo VII cleaves nucleotides from (5' or 3' msDNA side), the WT msDNA fragment sizes change as depicted.

(B) Restriction analysis of msDNA-Sen2 with Sau3AI. msDNA were isolated from *S*Tm wildtype or Δ*xseA* strains, digested with Sau3AI overnight/37°C, and msDNA digests were electrophoresed on a denaturing TBE-Polyacrylamide gel. DNA is stained with silver.

2.2.2. The RNA-part of msDNA is affected by RNAse H, not by ExoVII.

Reverse transcription of msDNA requires the msrmsd-RNA template interacting with its cognate retron-RT (Inouye *et al.*, 1999). To assess the RT-msrmsd interaction state in the retron mutants, I UV-crosslinked the RT-msrmsd protein-RNA complexes (Holmqvist *et al.*, 2016; Horos *et al.*, 2019). If the RT binds msrmsd-RNA, a higher molecular weight RT-proteoform should be visible in an anti-RT immunoblot. Indeed, upon UV-crosslinking, an RNAse-sensitive higher molecular weight RT-form appears (Figure 12A). The identity of the RT-msrmsd complex was confirmed by deleting the *msrmsd* gene, which abolishes the higher molecular weight RT-form (Figure 12B). An even higher molecular weight RT-form appears upon deleting *rnhA*, corroborating that RNase H molds the mature msrmsd-RNA from a longer RNA precursor (Dhundale *et al.*, 1987). In contrast, deleting Exo VII does not perturb RT-msrmsd-RNA interactions, restricting the role of Exo VII in msDNA processing (Figure 12B).

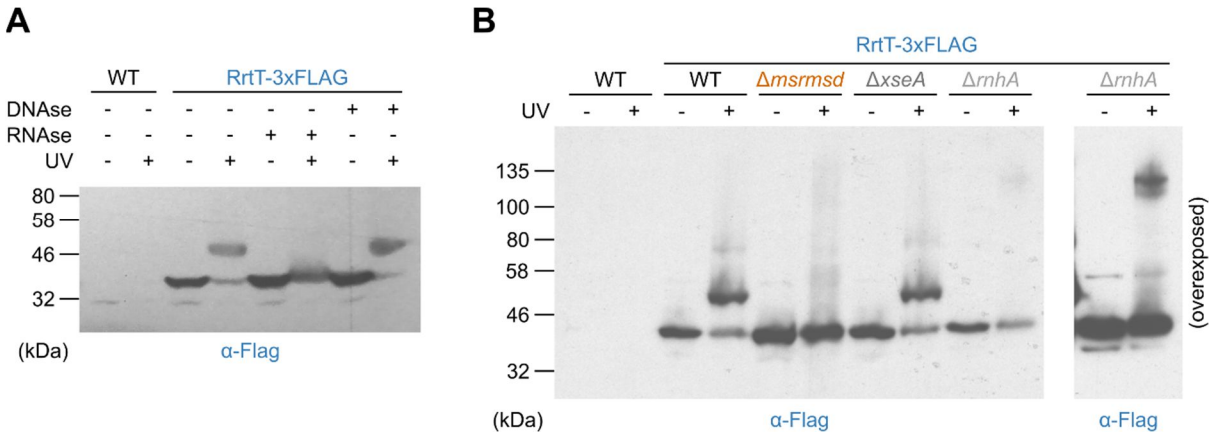

Figure 12. RT-msrmsd protein-RNA interactions in retron mutants.

(A) RT-Sen2 binds its cognate msrmsd-RNA. *S*Tm wildtype or *rrtT*-3xFlag strains were grown in LB/37°C until OD_{595} = 1, cells were UV-crosslinked, lysed, and subsequently treated with RNAse or DNAse. Proteins were separated with SDS-PAGE and immunoblotted.

(B) RNAse H, but not Exo VII, alters RT-msrmsd interactions. *S*Tm wildtype or retron deletion strains, and their *rrtT*-3xFlag counterparts, were treated as in panel **A**. The higher RT-msrmsd complex in Δ*rnhA* lanes is evident upon signal overexposure.

2.3. Retron-Sen2 encodes an msDNA-sensing toxin (*rcaT*).

Understanding why the msDNA is needed for *S*Tm growth in cold and anaerobiosis could open the door to understanding the biological function of retrons. Hence, I opted to understand why retron mutants are cold-sensitive, by isolating mutations that alleviate the phenotype. Conveniently, suppressor mutants would readily arise upon growing retron mutants in cold (e.g., see large colonies of Δ*msrmsd* strain at 15°C in Figure 8). To map the identity of the suppressing mutations, I collected 29 suppressors from strains Δ*rrtT*, Δ*xseA*, and Δ*msrmsd* (8, 8, and 13 respectively), and sequenced their genome. Every suppressor, but one, was mutated in STM14_4640, a gene of unknown function immediately upstream of *rrtT* (Figure 13A). The loss-of-function mutations in STM14_4640 ranged from frame shifts and early stop codons, to point mutations. All suppressors, but one, grew like wildtype at 15°C (Figure 13B). This suggested that, upon msDNA biosynthesis perturbations, the product of STM14_4640 inhibits growth in cold and anaerobic conditions. This configuration is reminiscent of TA systems, where toxins inhibit growth in the absence of the antitoxin. Thus, I named STM14_4640 as *rcaT* (*r*etron *c*old-*a*naerobic *T*oxin).

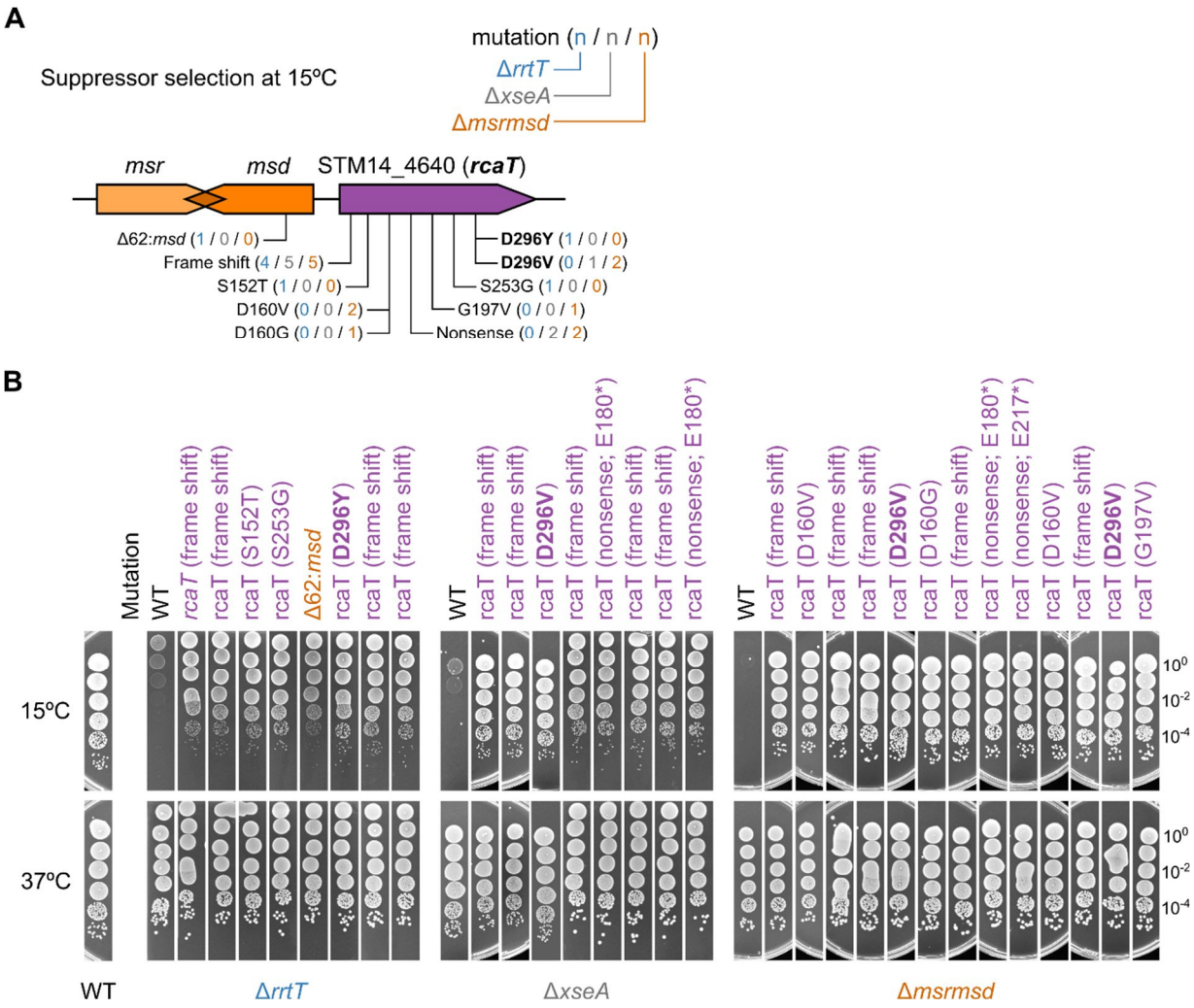

Figure 13. STM14_4640 (*rcaT*) causes the retron phenotypes.

(A) Suppressing mutations map in *rcaT*. Suppressor strains were isolated by incubating *S*Tm Δ*rrtT*, Δ*xseA*, and Δ*msrmsd* on LB plates at 15°C. The suppressors were genome sequenced, and alleviating mutations were mapped by comparing their genomes to wildtype *S*Tm.

(B) Suppressors are reverted to normal growth at 15°C. *S*Tm suppressor strains described in panel **A** were grown for 5-6 hours in LB/37°C, serially diluted, and spotted on LB plates. Plates were subsequently incubated at 15°C or 37°C. Identified suppressing mutations are indicated.

If *rcaT* is the source of the retron phenotypes, deleting it in retron mutants should revert both the cold- and anaerobic phenotypes to wildtype growth. Indeed, double retron-*rcaT* deletion mutants displayed fully restored growth in cold (Figure 14A) and anaerobic conditions (Figure 14B). This proved that all known retron phenotypes originate from RcaT, that acts as a toxin specifically activated upon msDNA perturbations.

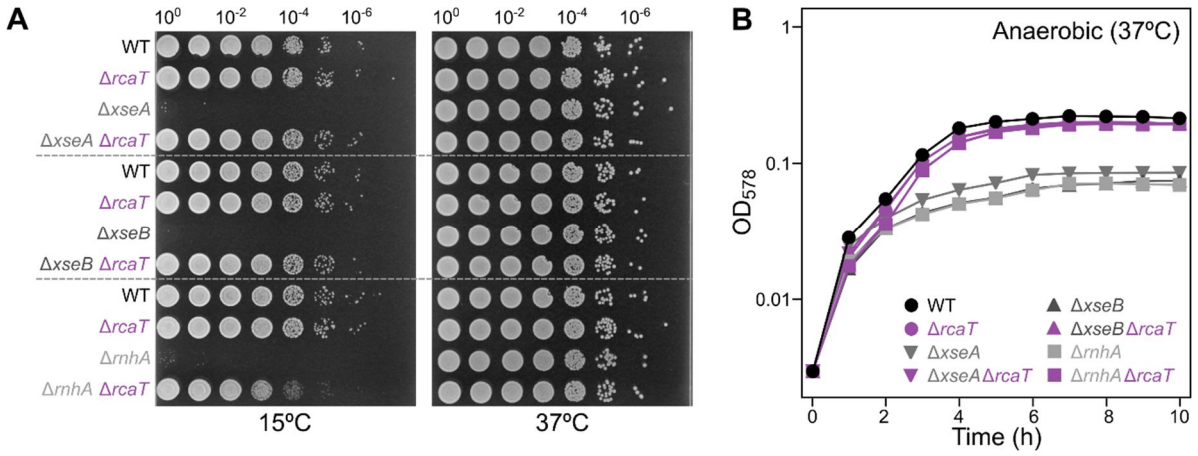

Figure 14. RcaT is the source of the retron phenotypes.

(A) Deleting *rcaT* in retron mutants alleviates their cold-sensitivity. The *rcaT* gene was deleted in *S*Tm wildtype and retron mutant strains (Δ*xseA*, Δ*xseB*, and Δ*rnhA*). Strains were grown for 5-6 hours in LB/37°C, serially diluted, and spotted on LB plates. Plates were subsequently incubated at 37°C or 15°C. Representative results from two independent experiments shown.

(B) Deleting *rcaT* in retron mutants alleviates the anaerobic phenotype. Growth curves of the same strains as in panel **A** were obtained by measuring OD_{578} in LB/37°C, under anaerobic conditions in a microtiter plate. Each point is the average OD_{578} of n = 11 (technical replicates), and error bars denote standard deviation (not shown if smaller than symbols).

2.3.1. Internal deletions in *msd* down-regulate RcaT levels.

The only alleviating mutation not mapping within *rcaT* was a deletion of 62 base pairs within the *msd* gene (Figure 13; mutant Δ62:*msd*). This mutant suggested a relationship between the msd-RNA (msDNA template) and RcaT toxicity. To explore this suppressor, I constructed a series of chromosomal scarless deletions within *msd* (Figure 15A). Deleting up to 71 base pairs of *msd* in the Δ*xseA* strain alleviated cold-sensitivity in varying degrees, but also produced cold-sensitivity in the WT strain (Figure 15B). On the other hand, deleting 79 bases produced a similar cold-sensitivity to Δ*msrmsd*. Since the *msd* deletions additionally produced cold-sensitivity in the WT, I wondered whether RcaT was active (i.e., the antitoxin is inactive), but down-regulated. Indeed, the RcaT levels were lower in *msd* deletion strains (Figure 15C). Thus, the *msd* deletions also alleviated the retron phenotype via RcaT, through an as of yet unclear regulatory crosstalk between msd-RNA and RcaT protein levels (it is possible that the activity of RcaT is also affected).

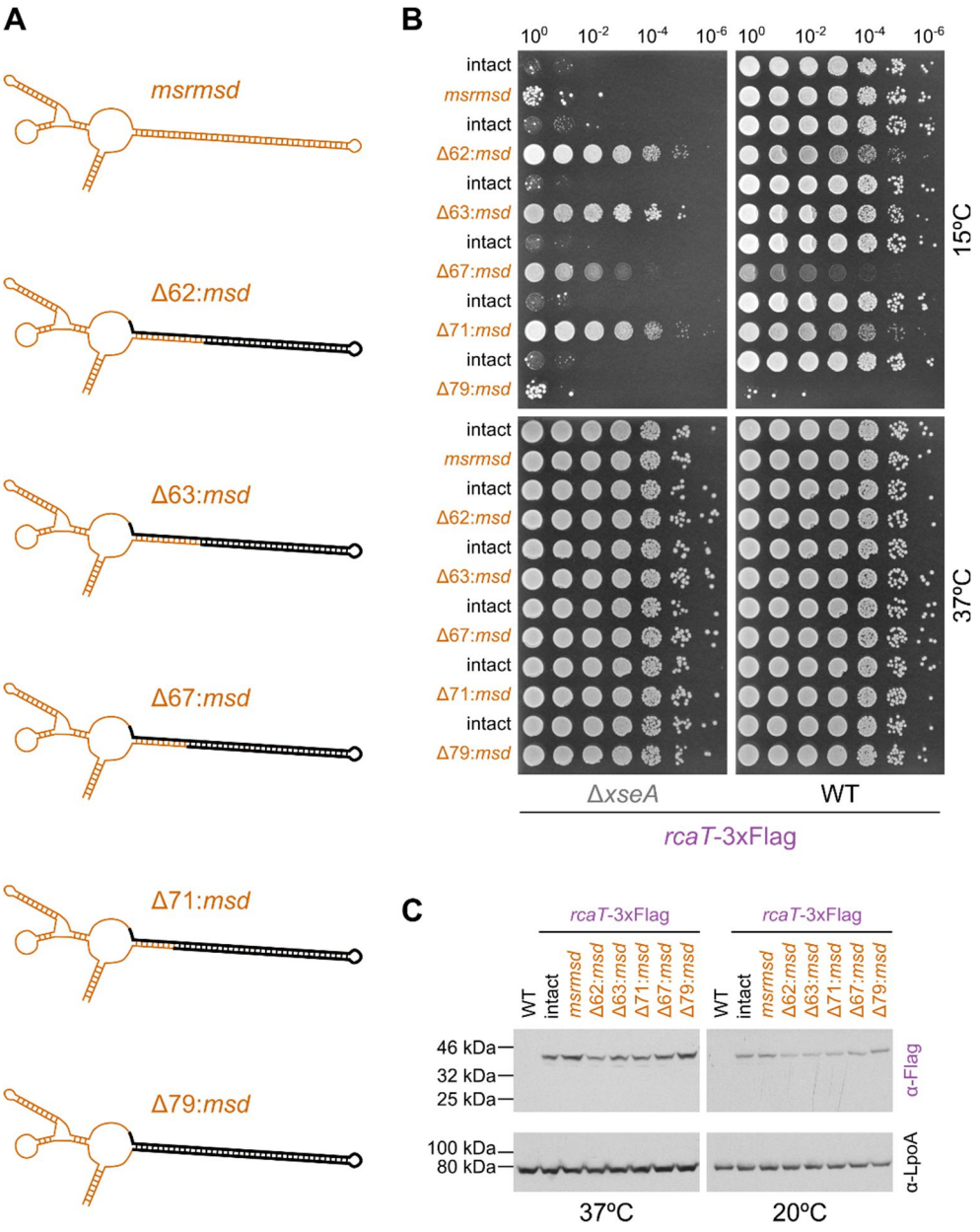

Figure 15. Internal deletions in *msd* downregulate RcaT protein levels.

(A) Constructed deletions in the *msd* region. The deleted bases in the msrmsd-RNA are shown in black.

(B) Deleting regions in *msd* simultaneously alleviates and incites cold-sensitivity. The black *msd* regions shown in panel **A** were deleted in *S*Tm *rcaT*-3xFlag wildtype and Δ*xseA* strains. Mutants were grown for 5-6 hours in LB/37°C, serially diluted, and spotted on LB plates. Plates were incubated either at 15°C or 37°C. Representative results from two independent experiments shown.

(C) Deleting regions in *msd* downregulates RcaT. The same strains as in panel **B** were grown in LB/37°C until OD_{595} = 1, or shifted for 5 hours at 20°C. Cells were lysed, and lysates were analyzed by SDS-PAGE and immunoblotting. LpoA protein levels were used as a loading control. Representative results from two independent experiments shown.

2.4. Overexpressing RcaT is toxic in *Escherichia coli*.

A hallmark of toxins of TA systems is damaging cells when overexpressed without their cognate antitoxin (Hall *et al.*, 2017). Following this archetype, overexpressing RcaT is toxic in *Escherichia coli* (*E. coli*) even at 37°C (Figure 16A), while a point mutant of RcaT alleviates the toxicity (Figure 16A; mutant D296V identified from experiments of Figure 13). Furthermore, RcaT toxicity in *E. coli* is aggravated in lower temperatures, presumably reflecting an inherent property of RcaT to be more active in cold (Figure 16B). Thus, RcaT behaves like a bona fide toxin when heterologously overexpressed in *E. coli*.

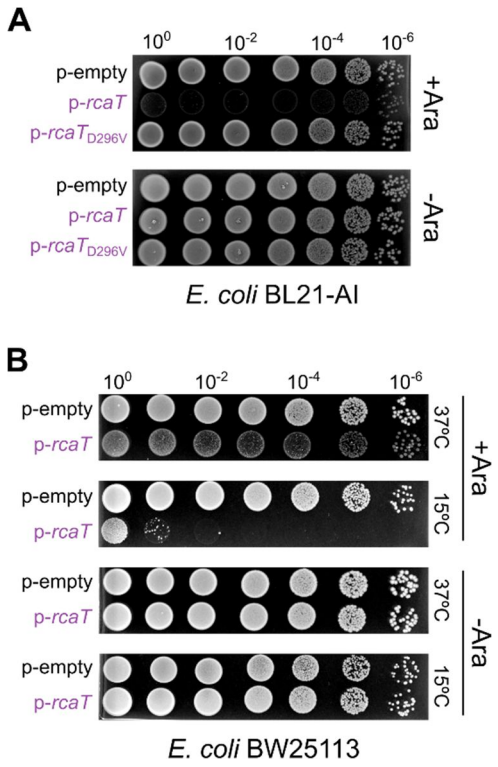

Figure 16. Overexpressing RcaT is toxic in *E. coli*.

(A) Expressing RcaT-WT, but not RcaT-D296V, is toxic in *E. coli* at 37°C. Arabinose inducible plasmids p-*rcaT*, p-*rcaT*-D296V, or the empty vector were transformed in *E. coli* BL21 arabinose-inducible (BL21 AI). Transformants were grown for 5-6 hours in kanamycin-LB/37°C, serially diluted, and spotted on kanamycin-LB plates with or without arabinose. Plates were incubated at 37°C. Representative results shown from two independent experiments.

(B) RcaT toxicity is aggravated when cells are grown in cold. *E. coli* BW25113 strains carrying plasmid p-*rcaT* or the empty vector were grown for 5-6 hours in kanamycin-LB/37°C, serially diluted, and spotted on kanamycin-LB plates with or without arabinose. Plates were incubated at 37°C or 15°C. Representative results from three independent experiments shown.

When their antitoxin is perturbed, toxins of TA systems only inhibit bacterial growth in their native hosts, but can kill cells when overexpressed (Hall *et al.*, 2017). Accordingly, although an *S*Tm Δ*msrmsd* retron mutant stops growing at 15°C (Figure 17A), cells retain almost complete viability (Figure 17B). In contrast, RcaT kills *E. coli* cells when overexpressed at 15°C (Figure 17C). Thus, like other toxins, RcaT is bacteriostatic at native levels and bactericidal when overexpressed.

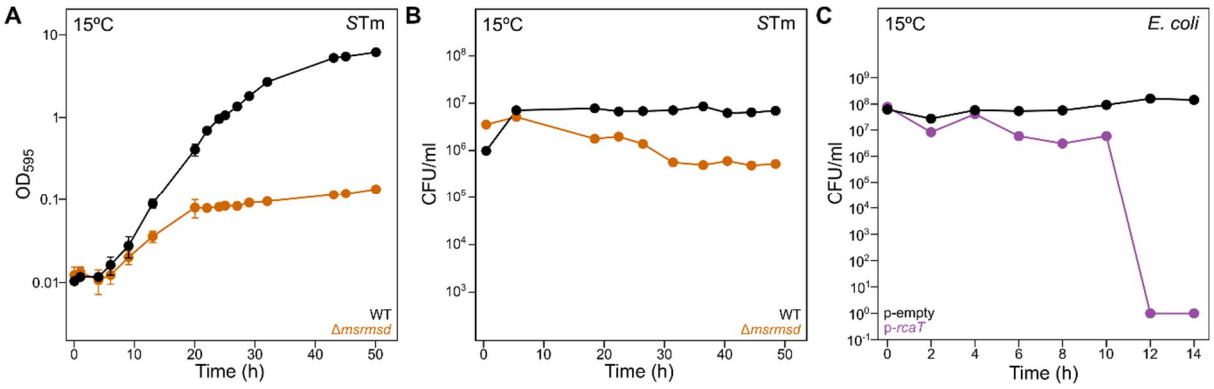

Figure 17. RcaT is bacteriostatic at native levels, but bactericidal when overexpressed.

(A) RcaT inhibits growth in *S*Tm at 15°C. *S*Tm wildtype and Δ*msrmsd* strains were grown in LB/15°C, and their growth was monitored by periodically measuring OD_{595}. Data points represent the average of three OD_{595} measurements (biological replicates). Error bars denote standard deviation (not shown if smaller than the symbols).

(B) RcaT is bacteriostatic in *S*Tm. Viability curves of the same strains as in panel **A** were obtained by periodically plating samples from them on LB plates to count colony forming units (CFU) per mL. Plates were incubated at 37°C. Data points represent one experiment.

(C) RcaT is bactericidal in *E. coli*. *E. coli* BW25113 strains carrying p-*rcaT* or an empty vector were grown in ampicillin-LB/37°C until OD_{595} = 0.4, cultures were transferred at 15°C and induced with arabinose. Viability curves were obtained by periodically plating culture samples on ampicillin-LB plates and counting colony forming units (CFU) per mL. Data points represent the average of two experiments (biological replicates). Error bars denote standard deviation (not shown if smaller than symbols).

2.5. Co-expressing RT-msDNA inhibits RcaT toxicity in *E. coli*.

Toxin inhibition requires co-expressing their cognate antitoxins. In line with this, although overexpressing RcaT is toxic, inducing the entire Retron-Sen2 (*msrmsd-rcaT-rrtT*) does not cause toxicity in *E. coli* (Figure 18A). Notably, co-expressing RcaT with only *msrmsd*, only *rrtT*, or *msrmsd*^{mut}*-rrtT* – where msrmsd-RNA is expressed, but cannot be reverse transcribed to msDNA (Hsu *et al.*, 1989) – was not sufficient to neutralize the RcaT toxicity (Figure 18A). This suggested that msDNA is necessary to

inhibit RcaT. Although co-expressing functional *msrmsd-rrtT* inhibited RcaT, it could be that unrecognized *cis* genetic elements in Retron-Sen2 affect this process. To exclude this possibility, I separated *rcaT* and *msrmsd-rrtT* in two different plasmids. Co-expressing *msrmsd-rrtT in trans* was also sufficient to inhibit RcaT (Figure 18B), therefore, *cis* genetic elements do not play a role in RcaT inhibition. In *S*Tm, msDNA synthesis requires RNAse H and Exo VII (Figure 10), which are also essential for antitoxin function (Figure 8). Similarly, although expressing Retron-Sen2 is not toxic in WT *E. coli*, retron induction in Δ*xseAB* or Δ*rnhA E. coli* strains is toxic (Figure 18C). Thus, also in *E. coli*, mature msDNA biogenesis is necessary for antitoxin activity.

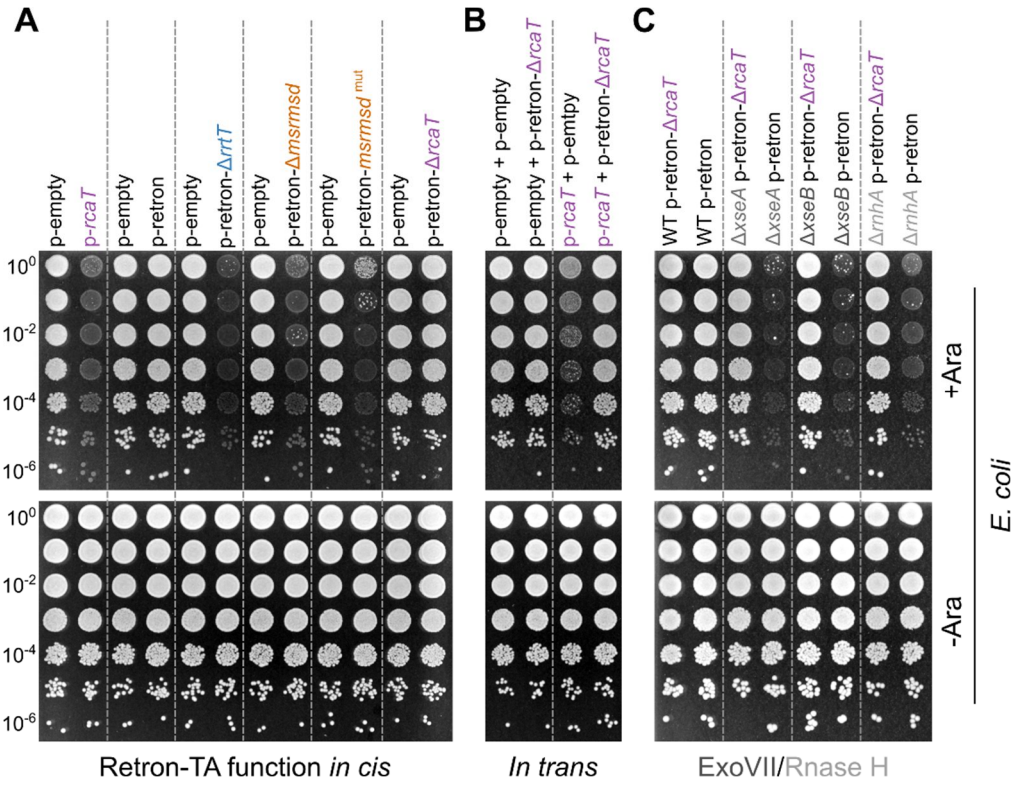

Figure 18. Retron-Sen2 acts like a toxin/antitoxin system in *E. coli*.

(A) Synthesis of msDNA is necessary for antitoxin activity. *E. coli* BW25113 carrying plasmids with retron components were grown for 5-6 hours in spectinomycin-LB/37°C, serially diluted, and spotted on spectinomycin-LB plates with or without arabinose. Plates were incubated at 37°C. Representative data shown from three independent experiments.

(B) *In trans* msDNA production inhibits RcaT. *E. coli* BW25113 carrying combinations of plasmids p-*rcaT*, p-retron-Δ*rcaT*, or an empty vector, were grown, serially diluted, and spotted as in panel **A**. Representative data from two independent experiments shown.

(C) RNase H and Exo VII are required to inhibit RcaT in *E. coli*. *E. coli* wildtype, Δ*rnhA*, Δ*xseA*, and Δ*xseB* strains carrying plasmids p-retron or p-retron-Δ*rcaT* were assayed as in panel **A**. Representative data shown from two independent experiments.

2.6. Conjugation screen in deletion library finds msDNA synthesis genes.

Retron RTs produce msDNA with the additional help of bacterial host genes (e.g., RNAse H, Exo VII). I devised an approach to identify potentially novel host genes involved in msDNA synthesis, in which I express Retron-Sen2 in the *E. coli* single-gene deletion library (Keio library; Baba *et al.*, 2006). Inducing Retron-Sen2 in strains deleted in msDNA-synthesis host genes would inhibit growth (e.g., Δ*rnhA*, Δ*xseA*, Δ*xseB*), due to RcaT activation (Figure 18C). Retron induction in the wildtype strain does not inhibit growth, since the RT-msDNA antitoxin inhibits RcaT (Figure 18A). Thus, by measuring the fitness of every strain upon Retron-Sen2 induction, it is possible to identify genes involved in msDNA biogenesis. Indeed, by conjugating and inducing the p-retron plasmid in the Keio library, I readily identified all previously known msDNA-biosynthesis host factors (*rnhA*, *xseAB*), and some potentially novel ones (*dnaQ*, *nfo*, *racC*, *ybjQ*, and *ppa*) (Figure 19). Thus, expressing retron-TAs in gene deletion libraries can be used to identify novel msDNA-synthesis host factors.

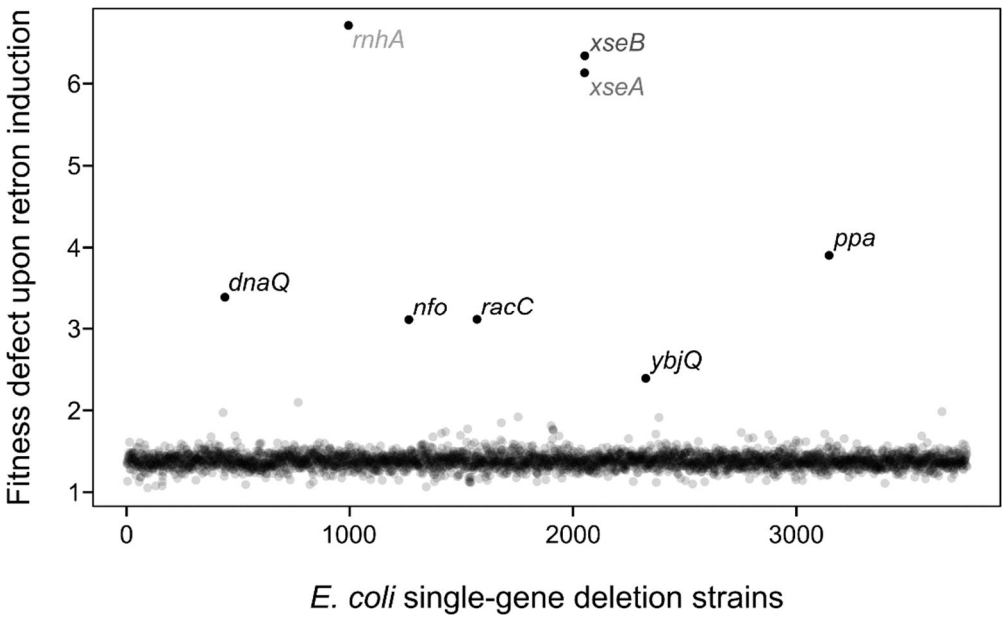

Figure 19. Host msDNA factors identification by inducing retrons in deletion libraries. Plasmid p-retron was conjugated into the single-gene *E. coli* library. Transconjugants were grown on spectinomycin-LB plates with or without arabinose. Fitness defect upon retron induction (y-axis) was calculated by dividing the (colony opacity of strain X in plates without arabinose) by the (colony opacity of strain X in arabinose plates). Data points represent the average of two ratios (biological replicates).

I validated the results for the novel host factors, by freshly transforming the p-retron plasmid in the corresponding *E. coli* gene deletion strains. The retron-sensitivity phenotypes observed in the screen held true, with different gene deletions exhibiting varying retron-toxicity degrees compared to the wildtype (Figure 20).

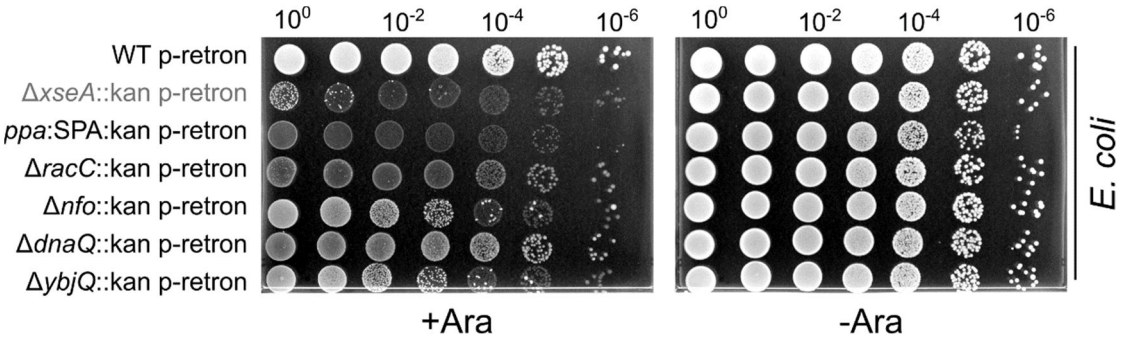

Figure 20. Validation of retron-sensitivity in *E. coli* host factor deletion strains. *E. coli* BW25113 wildtype or strains deleted in genes potentially involved in msDNA biosynthesis carrying plasmid p-retron were grown for 5-6 hours in spectinomycin-LB/37°C, serially diluted, and spotted on spectinomycin-LB plates with or without arabinose. Plates were incubated at 37°C. *E. coli ppa*-SPA strain is a SPA-tagged hypomorphic version of the essential *spa* gene (Butland *et al.*, 2005).

Multiple passages of library strains may result in secondary mutations that confound claims of genotype-phenotype causality. To exclude the effect of secondary mutations, I transduced the *E. coli* gene deletions of the potentially novel host factors (Figure 20) in a clean genetic background. Notably, only deletions of *racC* and *dnaQ* retained the retron-sensitivity phenotype after transduction (data not shown). This finding proved that retron-sensitivity in strains Δ*nfo*, Δ*ybjQ*, and *ppa* was due to secondary mutations, and these were not considered further. Thus, the retron-sensitivity phenotype was due to the mutated genes only in the Δ*racC* and Δ*dnaQ* strains.

Genes in the Keio library are replaced by a kanamycin resistance gene, that often results in upregulating gene(s) downstream of the insertion (Baba *et al.*, 2006). Collaterally upregulated genes can also confound claims of mutation causality. To account for this, I excised the kanamycin resistance cassette from the *racC* and *dnaQ* gene deletions, using the FLP-recombinase (Cherepanov and Wackernagel, 1995). The re-transduced *dnaQ* deletion strain grew inconsistently, in accordance with literature suggesting that *dnaQ* is nearly essential (Slater *et al.*, 1994) and was not considered further. Flipping-out the resistance cassette from the Δ*racC*::kan strain,

completely abolished the retron-sensitivity phenotype (Figure 21A). I hypothesized that upregulation of the gene downstream of *racC* (gene *recE*; Exonuclease VIII) was what actually caused the retron-sensitivity phenotype (Figure 21B). If that was the case, then co-expressing *recE* with Retron-Sen2 should cause toxicity. To test this, I co-induced the p-retron plasmid and a separate plasmid expressing *recE* (p1-*recE*) in wildtype *E. coli*. Indeed, co-expressing *recE* with the retron led to RcaT-dependent toxicity (Figure 21C). Thus, *recE* activates the RcaT toxin when overexpressed, presumably by affecting msDNA-biosynthesis.

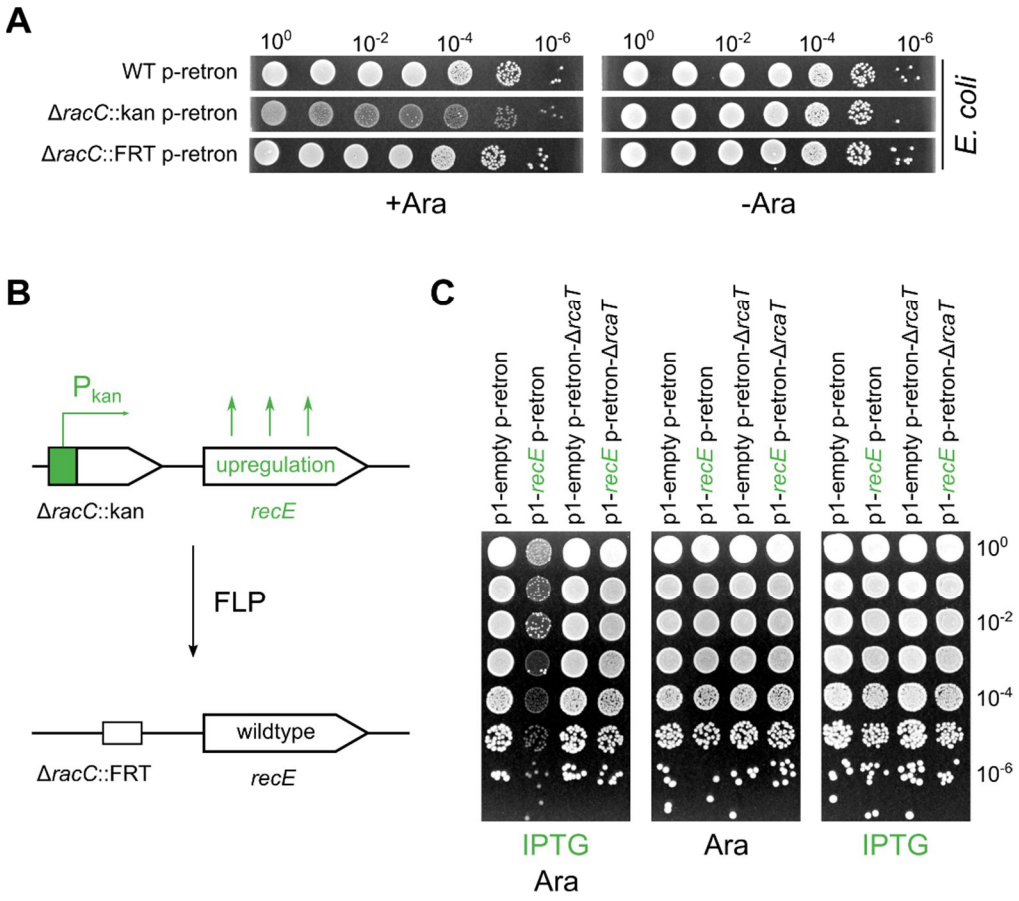

Figure 21. Collateral upregulation of RecE causes retron-sensitivity in *E. coli* Δ*racC*.

(A) Excising the kanamycin cassette abolishes Δ*racC* retron-sensitivity. *E. coli* BW25113 wildtype, Δ*racC*::kan, and Δ*racC*::FRT strains were grown for 5-6 hours in spectinomycin-LB/37°C, serially diluted, and spotted on spectinomycin-LB plates with or without arabinose. Plates were incubated at 37°C.

(B) Schematic depiction of kanamycin cassette in *racC* upregulating *recE*.

(C) RecE overexpression causes retron-sensitivity. *E. coli* BW25113 wildtype carrying combinations of p-retron, p1-*recE*, or empty vectors, were grown for 5-6 hours in antibiotics-LB, serially diluted, and spotted on antibiotics-LB plates with or without arabinose/IPTG. Plates were incubated at 37°C.

2.7. Retron-Eco9 of *E. coli* NILS 16 is also a retron-TA system.

Retron-Sen2 is widely conserved across *S*Tm isolates (Matiasovicova *et al.*, 2003), but only patchily conserved across other species. I wondered whether there are Retron-Sen2 homologues extant in *E. coli* strains. To explore this, I used the RcaT and RrtT protein sequences as pBLAST queries, and searched within a panel of 696 *E. coli* strains (Galardini *et al.*, 2017). *E. coli* strain NILS 16 (Bleibtreu *et al.*, 2014) carried a Retron-Sen2 homologue, which I named Retron-Eco9. Retron-Eco9 has the same operon structure as Retron-Sen2 (*msrmsd-rcaT-rrt*), and its genes display varying degrees of similarity to Retron-Sen2 genes (Figure 22A). Although their msDNA sequences are divergent in sequence, they share a common predicted structure (Figure 22B). Thus, Retron-Eco9 from *E. coli* NILS 16 is similar, yet distinct, to Retron-Sen2.

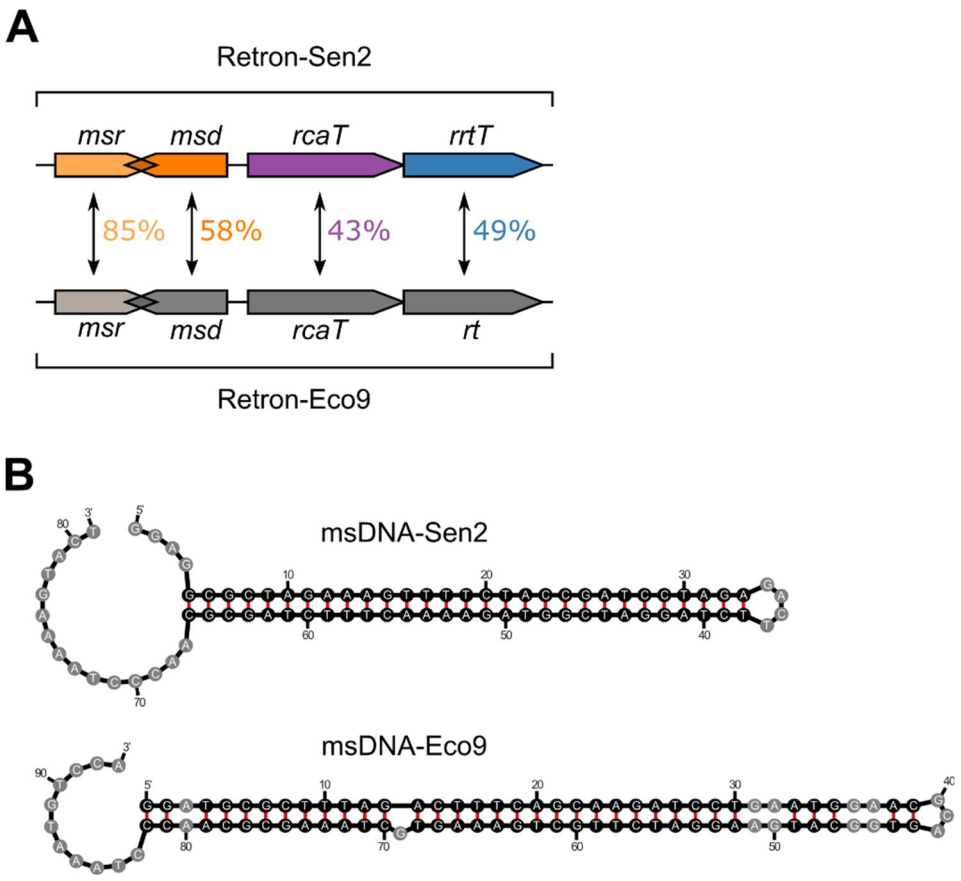

Figure 22. *E. coli* Retron-Eco9 is similar to Retron-Sen2 from *S*Tm.

(A) Retron-Eco9 has a similar operon structure to Retron-Sen2. Percentages between *msrmsd* regions express nucleotide identity, while between *rcaT-rt* regions denote amino acid identity between retrons. **(B)** msDNA-Eco9 has a similar structure to msDNA-Sen2. Structural models of msDNA-Sen2 and msDNA-Eco9 were built using Mfold (Zuker, 2003).

To assess whether retron-Eco9 is also a retron-TA system, I cloned *rcaT*-Eco9 and the entire Retron-Eco9, and expressed them in *E. coli* BW25113. Analogously to Retron-Sen2, expressing *rcaT*-Eco9 was toxic, while expressing retron-Eco9 was not (Figure 23). This suggested that RcaT-Eco9 is also inhibited by a retron-antitoxin.

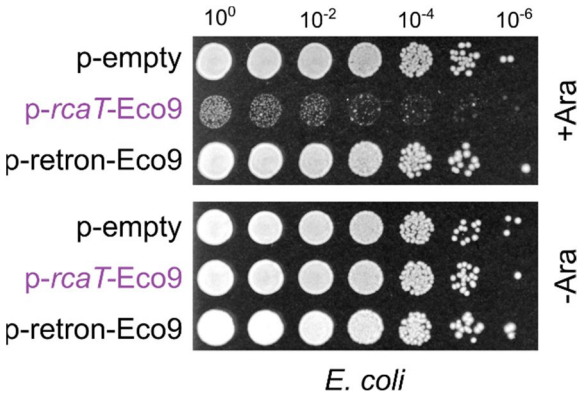

Figure 23. Retron-Eco9 acts like a retron-TA system. *E. coli* BW25113 strains carrying plasmids p-*rcaT*-Eco9, p-retron-Eco9, or an empty vector, were grown for 5-6 hours in chloramphenicol-LB, serially diluted, and spotted on chloramphenicol-LB plates with or without arabinose. Plates were incubated at 37°C. Representative data shown from three independent experiments.

To test whether msDNA synthesis is necessary for RcaT-Eco9 inhibition, I expressed Retron-Eco9 in *E. coli* Δ*xseA* and Δ*rnhA* mutants, where msDNA maturation/synthesis is abolished. Initially, I could not even transform the p-retron-Eco9 plasmid in these msDNA-synthesis mutants. Presumably, an internal promoter expressed Retron-Eco9 in substantial levels to inhibit the growth of Δ*xseAB*/Δ*rnhA* mutants. To circumvent this, I split the Retron-Eco9 in two plasmids, one carrying msrmsd (IPTG inducible), and the other RcaT-RT (arabinose inducible). Expressing the two plasmids together produced msrmsd-RcaT-RT-Eco9, which was benign for wildtype cells, but became toxic in the Δ*rnhA* mutant (Figure 24A). Surprisingly, IPTG-overexpression of msrmsd alleviated the RcaT toxicity in Δ*xseAB* mutants (Figure 24A). This result suggests that mature msDNA-Eco9 may be produced in the absence of Exo VII, alluding to the existence of redundant nucleases. Supporting this notion further, even without separately overexpressing msrmsd, trace amounts of mature msDNA-Sen2 (Figure 10) and msDNA-Eco9 (Figure 24B) are produced in Δ*xseA* strains. Generally, similar to msDNA-Sen2 synthesis, msDNA-Eco9 production is affected by Exo VII/RNase H mutations (Figure 24B). In summary, the Retron-Eco9 is a new retron-TA system in *E. coli*, functioning similarly to the Retron-Sen2 from *S*Tm.

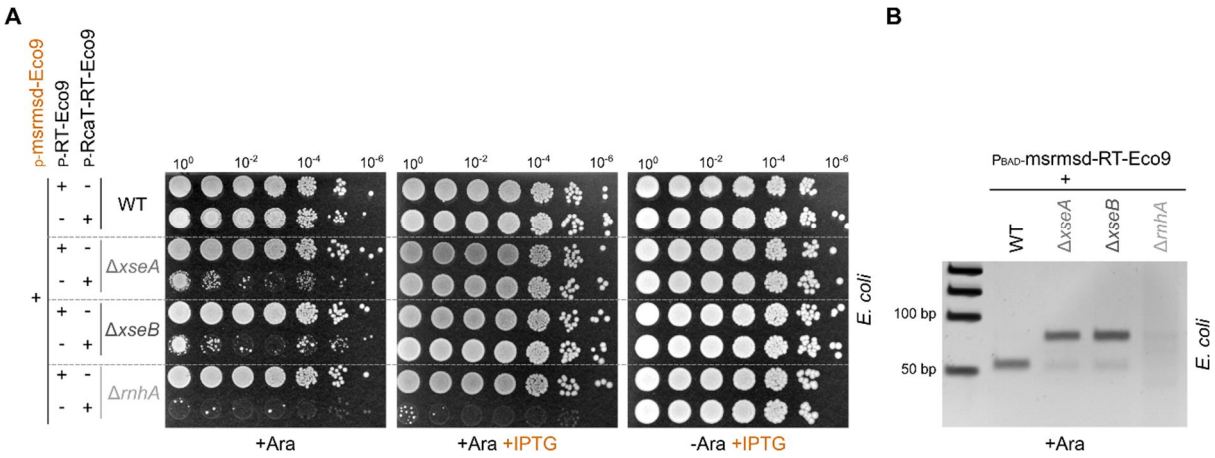

Figure 24. Retron-Eco9 is regulated similarly to Retron-Sen2.

(A) RNAse H and Exo VII are necessary to inhibit RcaT-Eco9. *E. coli* BW25113 wildtype, Δ*xseA*, Δ*xseB*, and Δ*rnhA* strains carrying combinations of plasmid p-msrmsd-Eco9, p-RT-Eco9, p-RcaT-RT-Eco9, or empty vectors were grown for 5-6 hours in LB with appropriate antibiotics, serially diluted, and spotted on antibiotics-LB plates with or without arabinose/IPTG. Plates were incubated at 37°C. Representative results of two independent experiments shown.

(B) RNAse H and Exo VII are necessary to produce msDNA-Eco9. msDNA were extracted from *E. coli* BW25113 wildtype, Δ*xseA*, Δ*xseB*, and Δ*rnhA* strains carrying plasmid p-msrmsd-RT-Eco9. msDNA extracts were electrophoresed on a TBE-Polyacrylamide gel, and DNA were stained with ethidium bromide.

2.8. Chapter 2 summary.

- Retron-Sen2 encodes a toxin (RcaT), which is activated upon msDNA-biosynthesis perturbations.
- Activated RcaT inhibits *S*Tm growth in cold and anaerobic conditions.
- Overexpressing RcaT is toxic in *E. coli*, and overexpressing RT-msDNA alleviates the RcaT toxicity.
- Overexpressing RecE activates Retron-Sen2, presumably by interfering with msDNA-biosynthesis.
- Retron-Eco9 from *E. coli* is homologous to Retron-Sen2, which also functions as a retron-TA system.

3. RT-msDNA inhibits RcaT by protein interactions.

Having established that Retron-Sen2 functions as a toxin/antitoxin (TA) system, I wished to mechanistically understand how RcaT is inhibited. Toxins of TA systems are kept inactivated by their cognate antitoxins in diverse ways (Figure 4). Usually, TA systems are bipartite, but Retron-Sen2 contains three components (msrmsd, RcaT, RT). Thus, although msDNA production is necessary to inhibit RcaT *in vivo* (Chapter 2), it is not clear which component confers the antitoxin activity.

In Chapter 3

- I showed that RcaT levels are not affected by the antitoxin (3.1).
- RT-RcaT interact through protein-protein interactions, independently of the presence of msDNA (3.2). On the other hand, RT binds its own msDNA (3.3).
- Both interactions (RT-RcaT, RT-msDNA) are required for antitoxin activity against RcaT (3.4).

Collaborator contributions per figure

Figure 26, Figure 27, Figure 29: I collaborated with **André Mateus** (EMBL, Heidelberg) for the immunoprecipitation experiments. **Frank Stein** (EMBL, Heidelberg) analyzed the results.
Figure 30: I collaborated with **Joel Selkrig** & **Anna Sueki** (EMBL, Heidelberg), as well as **Jacob Scheurich** & **Kim Remans** (EMBL, Heidelberg) to purify RT-Sen2.

3.1. RcaT is not inhibited via downregulation.

Antitoxins of TA systems display a wide mechanistic variety in how they inactivate their cognate toxins (Harms et al., 2018). For instance, RNA-antitoxins of type I TA systems keep their toxins in a latent state by preventing their expression (Figure 4A). To test if the retron-antitoxin downregulates RcaT, I Flag-tagged RcaT, and measured RcaT-3xFlag levels in *S*Tm wildtype and retron deletion strains. If the retron-antitoxin silences RcaT, its levels should be increased in retron deletion strains. RcaT was not significantly upregulated in retron deletion mutants irrespectively of growth temperatures (Figure 25A-B). The 3xFlag-tagged RcaT retained its functionality, as judged by a functional cold-sensitivity test in *S*Tm (Figure 25C). Thus, RcaT is not transcriptionally or translationally silenced by the retron antitoxin.

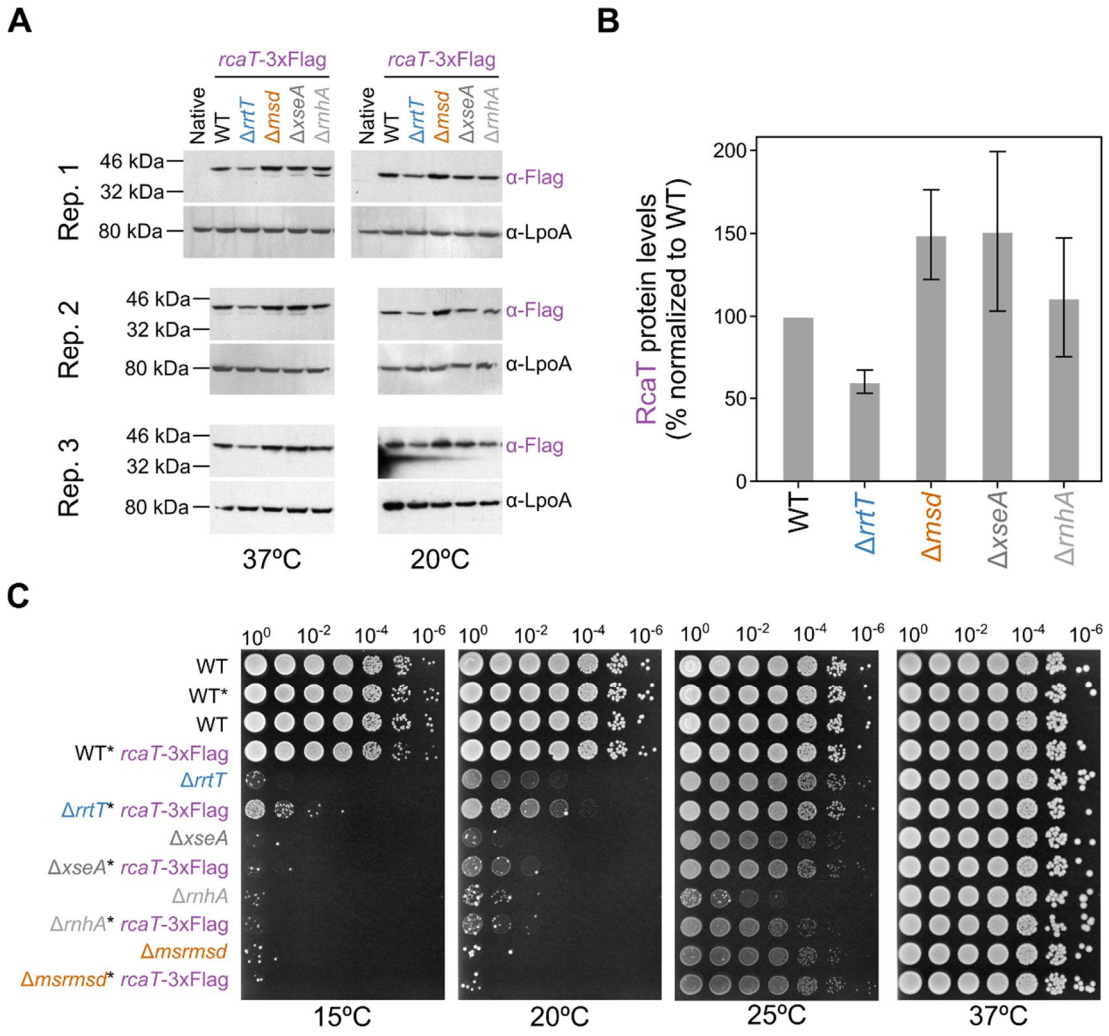

Figure 25. RcaT is not inhibited by downregulation.

(A) RcaT protein levels are unchanged in retron deletion strains. *S*Tm wildtype (native), and *rcaT*-3xFlag tagged wildtype (WT) and retron deletion strains, were grown in LB/37°C until OD_{595} = 0.5 (37°C samples), or transferred to a 20°C incubator for 5 hours (20°C samples). Next, samples were lysed, and proteins were analyzed by SDS-PAGE and immunoblotting. LpoA protein levels were used as a loading control.

(B) RcaT protein level quantification across *S*Tm strains. RcaT protein levels of immunoblots shown in panel **A** were quantified based on pixel density using ImageJ.

(C) C-terminal RcaT-3xFlag retains its toxicity. *S*Tm wildtype and retron deletion strains, along with their *rcaT*-3xFlag tagged versions, were grown in LB/37°C for 5-6 hours, serially diluted, and spotted on LB plates. Plates were incubated either at 15°C, 20°C, 25°C, or 37°C. * denotes the ΔSTM14_4645::cat mutation, used to co-transduce the scarlessly 3xFlag-tagged *rcaT*. Representative results of two independent experiments shown.

3.2. RT and RcaT reciprocally co-immunoprecipitate.

The protein antitoxins of type II, and the RNA antitoxins of type III TA systems, inhibit their cognate toxins by directly interacting with them (Figure 4B-C) (Tam and Kline, 1989; Short *et al.*, 2013). To test for potential protein interactions between the RT and RcaT, I chromosomally 3xFlag-tagged *rrtT* and *rcaT* in their C-terminus, and immunoprecipitated (IP) both proteins. If they interacted, RT should be co-IPed with RcaT, and vice versa. The IP samples were analyzed with mass spectrometry. Indeed, the RT and RcaT proteins co-IP with each other, suggesting that RT-RcaT physically interact (Figure 26). The RT-RcaT interaction occurs independently of temperature, since it was detected irrespectively of incubating cells at 37°C or 20°C (Figure 26). Thus, the toxin RcaT interacts with its cognate RT.

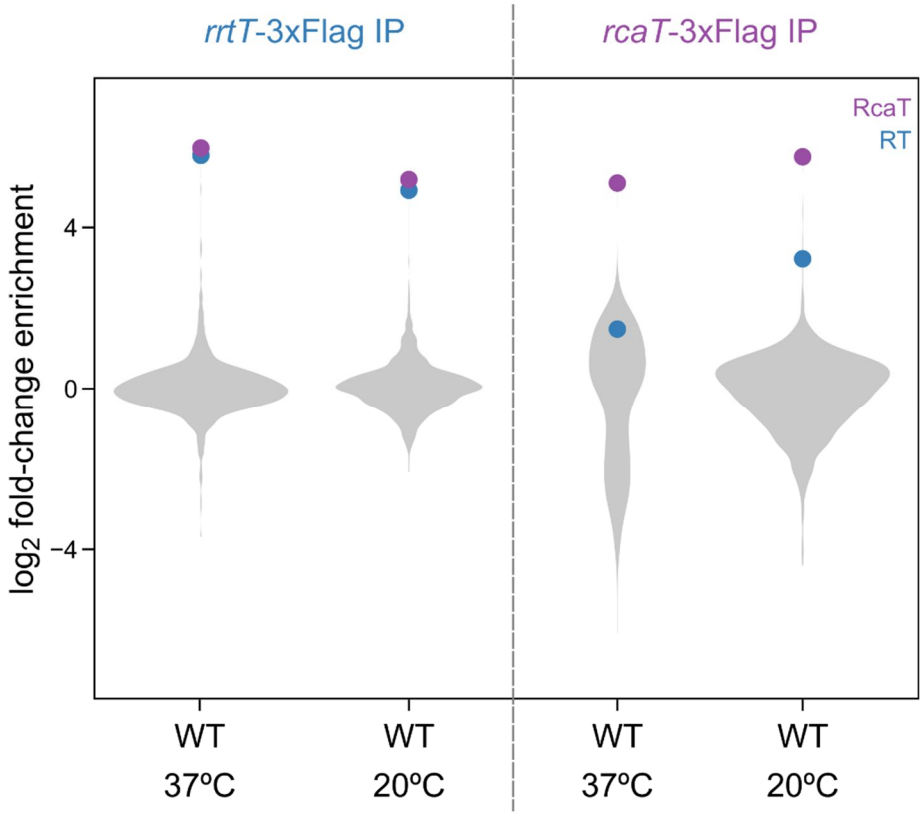

Figure 26. RcaT and RT co-immunoprecipitate with each other. RrtT-3xFlag and RcaT-3xFlag were immunoprecipitated (IP) from *S*Tm wildtype *rrtT*-3xFlag or *rcaT*-3xFlag strains, respectively. Prior to IP, cells were grown until OD_{595} = 1 in LB/37°C (37°C samples), and shifted to 20°C for 5 hours (20°C samples). Protein abundance in IP samples was compared with IP samples of wildtype untagged *S*Tm strain (y-axis). Data shown are the average from two biological replicates.

Since msDNA synthesis is required to inhibit RcaT (Figure 18A), I then asked if the RT-RcaT interaction was msDNA-dependent. For this, I transferred the 3xFlag-tagged *rrtT*/*rcaT* either in *S*Tm wildtype or msDNA maturation/synthesis mutant strains (Δ*xseA*, and Δ*msrmsd*/Δ*msd*). If msDNA mediated the RT-RcaT interaction, the two proteins should not co-IP in mutants where msDNA is not properly (Δ*xseA*) or not at all (Δ*msd*) produced. In contrast, the RT-RcaT interaction was detected in all backgrounds (Figure 27). Furthermore, the RT-RcaT interaction was not affected by the activity state of RcaT, since it was detected in retron deletion mutants incubated at 20°C (where RcaT is active). Thus, RT and RcaT interact irrespectively of msDNA, presumably through direct protein-protein interactions, which alone does not affect the toxicity of RcaT.

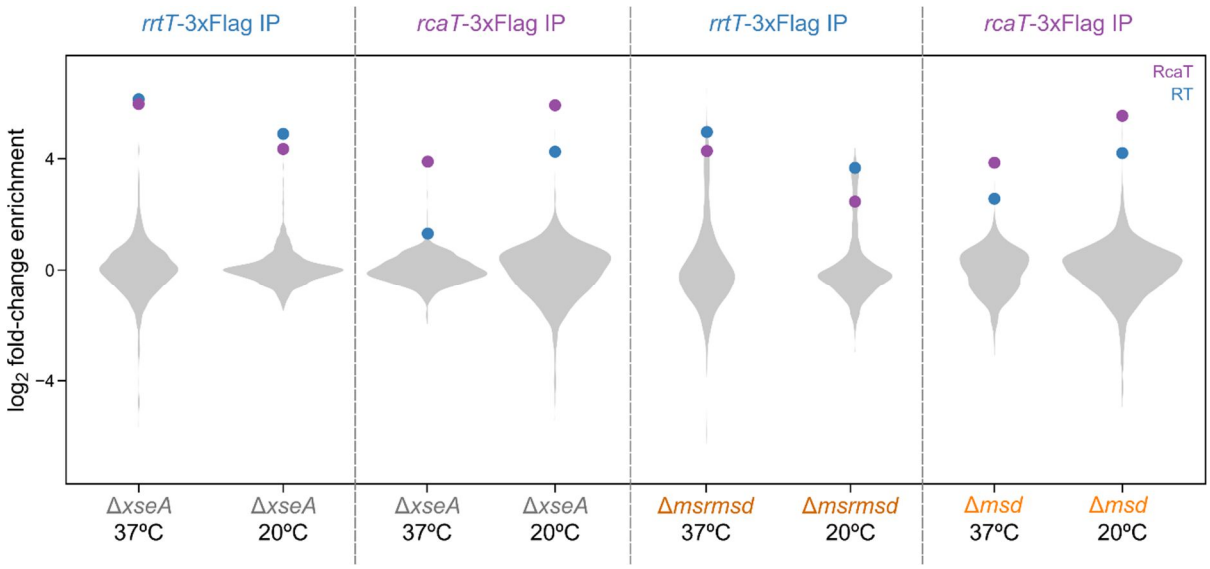

Figure 27. RT and RcaT interact independently of msDNA. RrtT-3xFlag and RcaT-3xFlag were immunoprecipitated (IP) from *S*Tm wildtype, Δ*xseA*, Δ*msrmsd*, and Δ*msd* strains, carrying 3xFlag-tagged versions of *rrtT* or *rcaT*, respectively. IPs were conducted as in **Figure 20**. Data shown are the average from two biological replicates.

Flag-tagging RT or RcaT might have interfered with their function and interactions. To exclude this I tested both chromosomally tagged rcaT-3xFlag and rrtT-3xFlag, which were functional in STm (Figure 25C and Figure 28).

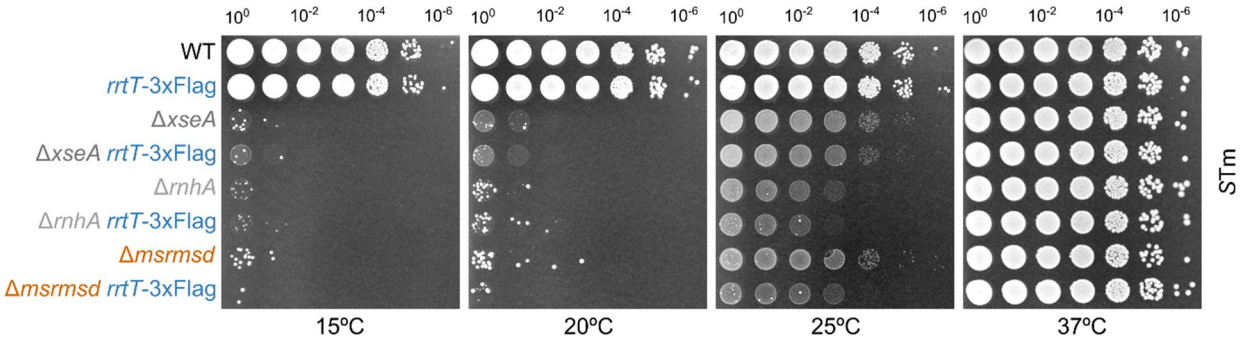

Figure 28. RT-3xFlag retains its antitoxin functionality. *rrtT*-3xFlag tagged *S*Tm wildtype and retron deletion strains, and their untagged counterparts, were grown for 5-6 hours in LB/37°C, serially diluted, and spotted on LB plates. Plates were subsequently incubated at 15°C, 20°C, 25°C, or 37°C. Representative results shown from two independent experiments.

The observed RT-RcaT co-immunoprecipitation could be an artefact of upregulation of RT or RcaT, due to 3xFlag-tagging of the other. I analyzed the proteome samples prior to IP (full proteome samples; FP), to assess whether the 3xFlag-tagging altered RcaT/RT protein levels. RcaT/RT protein levels remained unchanged compared to the wildtype strain in *rrtT*-3xFlag tagged strains (Figure 29A), but were reduced in *rcaT*-3xFlag tagged strains (Figure 29B; RcaT is not even detected in the *rcaT*-3xFlag FP samples). The RT/RcaT downregulation in *rcaT*-3xFlag strains potentially explains the lower level of RT-RcaT co-enrichment in IP samples, compared to *rrtT*-3xFlag strains (Figure 26). Thus, chromosomally tagging *rrtT*/*rcaT* did not affect the validity of the co-IP results.

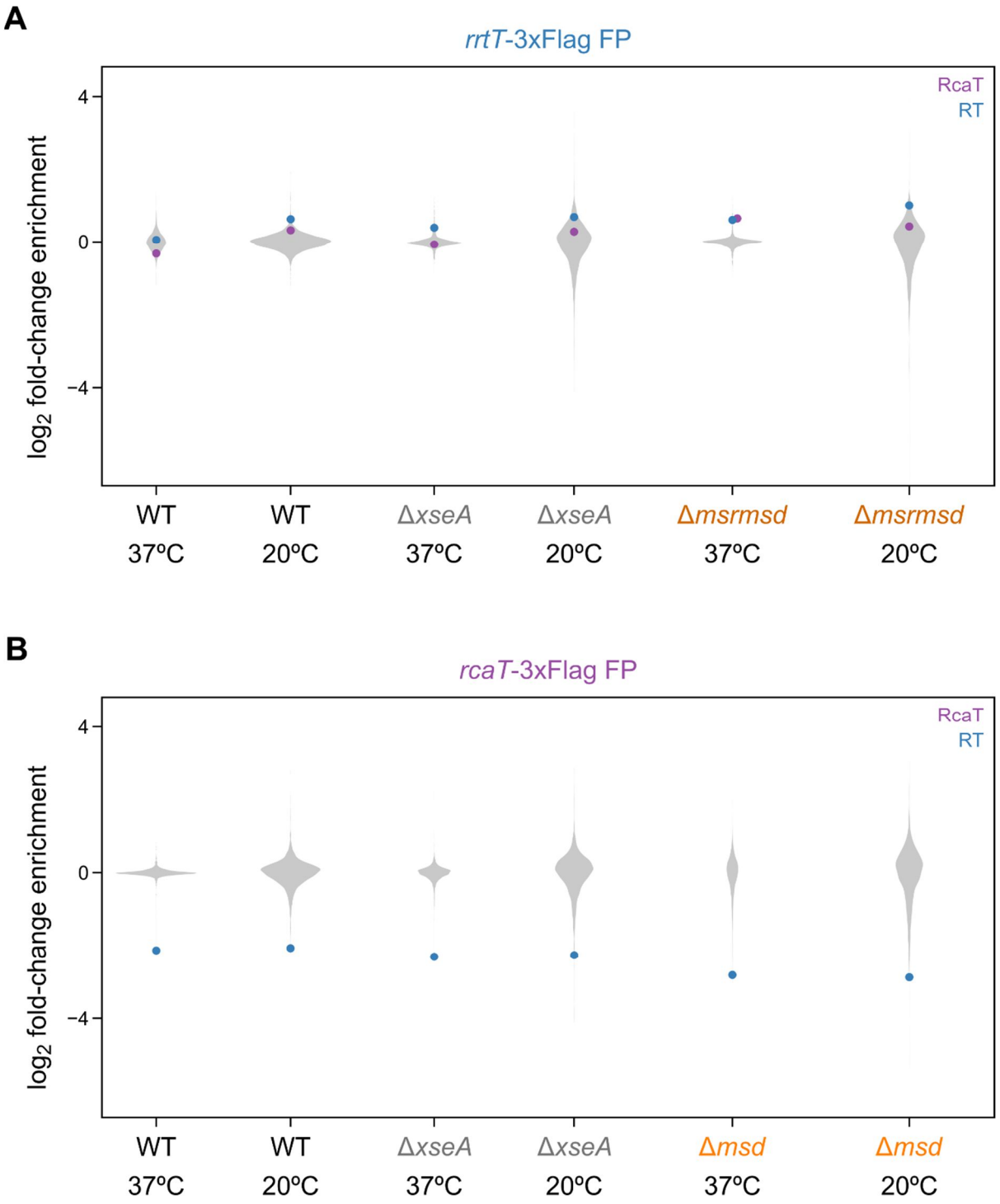

Figure 29. Effects of Flag-tagging on RT/RcaT protein levels.

(A) Flag-tagging RT does not alter retron protein levels. Proteins in input samples of *rrtT*-3xFlag tagged strains (full proteome; FP), used for IPs shown in **Figure 26**, were analyzed by mass spectrometry. Proteins in FP samples of Flag-tagged strains were compared to FP samples of untagged *S*Tm wildtype (y-axis). Data derived from two biological replicates.

(B) Flag-tagging RcaT alters retron protein levels. Experiments were conducted as in panel **A**, but for *rcaT*-3xFlag tagged strains. Data derived from two biological replicates

3.3. RT binds its mature msDNA product.

RT and RcaT interact independently of msDNA, but msDNA synthesis is required to inhibit RcaT. Thus, msDNA itself might also be interacting with some retron component. Notably, msDNA has been previously shown to co-purify with retron-RTs, suggesting the existence of an RT-msDNA interaction (Lampson *et al.*, 1990; Jeong *et al.*, 1997). If msDNA-Sen2 is in a complex with RT-Sen2, they should be co-purifying together. To test this, I first purified a RT-6xHis tagged protein to apparent homogeneity (Figure 30A). The RT-6xHis was co-expressed with its msrmsd-RNA template, in order for msDNA to be produced. His-tagging did not affect the function of the protein, since the RT-6xHis derivative could inhibit RcaT (Figure 30B). Next, I isolated total DNA from the purified RT protein. Indeed, msDNA-Sen2 was extracted from purified RT-6xHis, suggesting a direct RT-msDNA interaction (Figure 30C). Thus, besides RT binding RcaT, RT also binds its mature msDNA product.

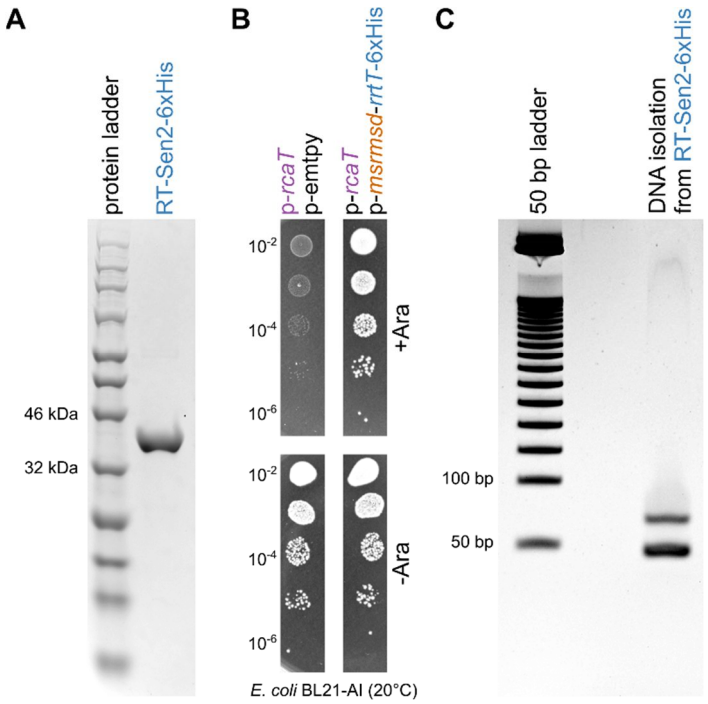

Figure 30. RT interacts with msDNA.

(A) Purification of RT-Sen2. RT-Sen2-6xHis was purified by nickel-column immobilized metal-affinity chromatography, from an *E. coli* BL21 CodonPlus-RIL strain expressing plasmid p-*msrmsd-rrtT*-6xHis. **(B)** RT-Sen2-6xHis is functional. *E. coli* BL21 AI strains carrying combinations of plasmids p-*rcaT*, p-*msrmsd-rrtT*-6xHis, and an empty vector were grown for 5-6 hours in antibiotics-LB/37°C, serially diluted, and spotted on antibiotics-LB plates with or without arabinose. Plates were incubated at 20°C. **(C)** msDNA isolation from pure RT-Sen2. DNA was extracted from 0.5 mg of pure RT-Sen2-6xHis protein, electrophoresed, and EtBr stained. The two bands correspond to immature/mature msDNA.

3.4. The RT-msDNA complex forms the antitoxin.

RT-mediated msDNA synthesis is necessary to inhibit RcaT. It is therefore hard to disentangle whether the msDNA itself, or both the RT and the msDNA, are necessary for antitoxin activity. If msDNA-Sen2 synthesis is sufficient to inhibit RcaT-Sen2, producing msDNA-Sen2 through a non-cognate RT (non -Sen2) would still inhibit RcaT-Sen2. In contrast, if the cognate RT is not only required for synthesizing msDNA, but also for the antitoxin specificity (i.e., the RT-RcaT interaction is required), RcaT would not be inhibited.

RTs between retrons are usually not interchangeable for producing msDNA (Shimamoto *et al.*, 1993; Inouye *et al.*, 1999), unless their *msr* regions are highly similar (Lima and Lim, 1997; Shimamoto *et al.*, 2013). Since the *msr* regions of Retrons-Sen2 and -Eco9 are 85% identical (Figure 22A), I tested whether RT-Sen2 can reverse transcribe msDNA-Eco9, and vice versa. Indeed, the RT-Sen2 and -Eco9 can interchangeably produce their non-cognate msDNA (Figure 31). Notably, while RT-Sen2 produces similar amounts of cognate and non-cognate msDNA, RT-Eco9 is less efficient at producing its non-cognate msDNA (Figure 31). Thus, RT-Sen2 and RT-Eco9 can substitute each other in producing msDNA.

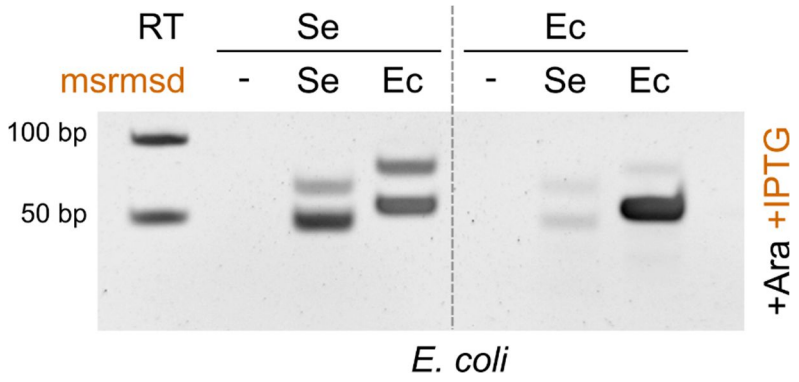

Figure 31. RTs from Retrons-Sen2 and -Eco9 can produce non-cognate msDNA. msDNA were extracted from *E. coli* strains carrying combinations of plasmids p-RT, p-msrmsd, or empty vectors (-), with components originating from Retron-Sen2 (Se) or Retron-Eco9 (Ec). Extracted msDNA were electrophoresed on a TBE-Polyacrylamide gel. Representative results shown from two independent experiments.

Toxins of TA systems, even of the same type, are only inhibited by their cognate antitoxins (Wilbaux *et al.*, 2007). Retron-TAs are more complicated, since RTs usually only reverse transcribe their cognate msrmsd-RNA. Nevertheless, the interchangeable msDNA production between RT-Sen2 (Se) and RT-Eco9 (Ec) can be used to test if RT-RcaT pairs are cognate. If antitoxin activity requires cognate RT-RcaT pairs, then RcaT toxicity should only be alleviated in the cognate combinations.

To test this, I made two sets of plasmids, carrying either msrmsd (Se or Ec), or RT-RcaT pairs (all possible combinations). Inducing RT-RcaT is toxic, unless provided with msrmsd-RNA to make msDNA (Figure 18). Only the toxicity stemming from cognate RT-RcaT pairs (Se-Se, or Ec-Ec) could be inhibited by msDNA production (Figure 32). In contrast, cognate RT-RcaT pairs were inhibited by both cognate and non-cognate msDNA (Figure 32). Therefore, having specific msDNA sequences is not important for inhibition. Inducing msrmsd-Se with IPTG is necessary to inhibit RT-RcaT Ec-Ec, since RT-Ec produces msDNA-Se less efficiently than its own (Figure 31). Therefore, although msDNA is necessary to inhibit RcaT, the RT protein itself provides the antitoxin specificity (facilitated by cognate RT-RcaT interactions).

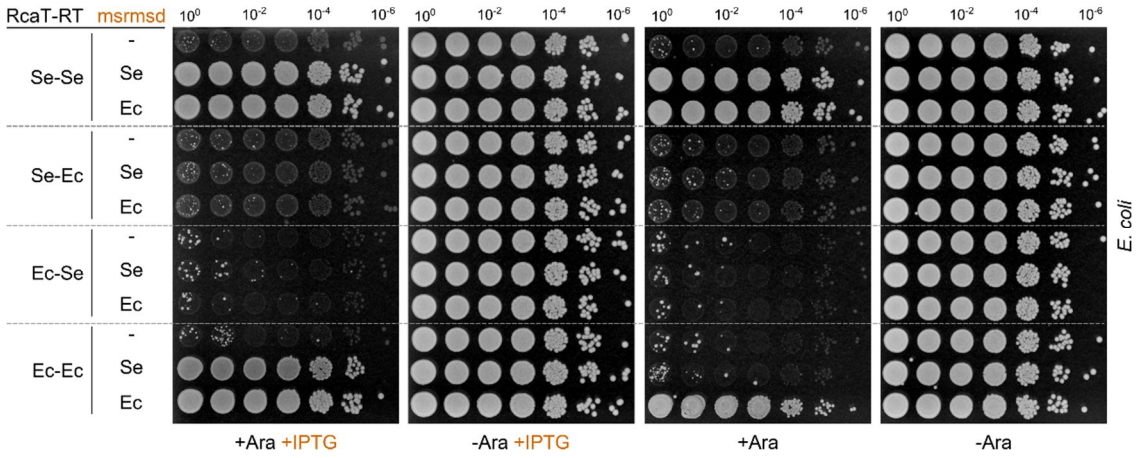

Figure 32. RT-RcaT interactions determine the RT-msDNA antitoxin specificity. *E. coli* B25113 strains carrying combinations of plasmids p-msrmsd (Se, Ec), p-RcaT-RT (combinations), and empty vectors, were grown for 5-6 hours in antibiotics-LB/37°C, serially diluted, and spotted on antibiotics-LB plates with or without arabinose/IPTG. Plates were incubated at 37°C. Representative results shown from two independent experiments.

3.5. Chapter 3 summary and retron-TA mode of action.

- The retron antitoxin does not silence the expression of RcaT.
- The RcaT toxin interacts with the RT through protein-protein interactions, while the RT interacts with the msDNA through protein-DNA interactions.
- The RT and msDNA act in concert as the antitoxin against RcaT (Figure 33).
- The RT-RcaT interaction provides specificity to the antitoxin against its cognate RcaT toxin, while the RT-msDNA interaction enables the antitoxin activity.

Figure 33. The RT-msDNA complex is the antitoxin that inactivates RcaT. The reverse transcriptase of Retron-Sen2 (in blue) bound to its msDNA (orange) binds and inactivates the RcaT toxin (light purple). Events perturbing msDNA synthesis, or the integrity of the reverse transcriptase, activate the RcaT toxin (deep purple), which is active with or without the reverse transcriptase bound to it.

4. Phage proteins block and trigger retron-TAs.

To understand the physiological role of a TA system, it is sufficient to find conditions that modulate its activity. Although these conditions might be complex (e.g., bacteriophage infection), the causal factors should be simple (i.e., effects of specific gene-products on TA systems). I previously found that solely overexpressing RecE triggers Retron-Sen2 toxicity (Figure 21). I therefore wondered how I could expand the search space of overexpressed genes, to find more conditions that affect retrons, and to ultimately understand their biological function.

In Chapter 4

- I describe a high-throughput approach to map single genes that activate or block the Retron-Sen2 TA system, but in principle can be applied onto any TA system (Toxin Inhibition/Activation Conjugation; TIC/TAC) (4.1, 4.2, 4.3).

- I found that several phage-related genes can exogenously trigger or block RcaT toxicity, and mechanistically dissected the action of three of them (4.4, 4.5, 4.6).

Collaborator contributions per figure

Figure 35, Figure 36, Figure 39, Figure 40: I collaborated with **George Kritikos** (EMBL, Heidelberg) to analyze the TIC/TAC fitness data. George also helped in figure design presented in these figures.

Figure 54: I collaborated with **Karin Mitosch** (EMBL, Heidelberg) to explore how RT-Eco1 triggered Retron-Sen2.

Finally, special thanks to **André Mateus** (EMBL, Heidelberg) for teaching me, helping in making, or even directly designing some of the figures found in this thesis.

4.1. TIC/TAC; a new way to find blockers and triggers of TA systems.

All TA systems have a Janus-faced property; toxin expression inhibits growth, and antitoxin co-expression allows growth by inhibiting the toxin. I used this property to develop a fitness-based approach to search for genes that affect TA systems.

To survey as many genes as possible, I employed arrayed strain libraries, containing mobilizable single-gene overexpressing plasmids (library-plasmids). I used the MOB (p1; Saka *et al.*, 2005) and TransBac libraries (p2; Otsuka *et al.*, 2015), which contain individual plasmids carrying nearly every *E. coli* gene (~4000 each). Using high-throughput conjugation on agar plates, I transferred these mobilizable plasmids (Ptac-*gene*X) into *E. coli* wildtype carrying plasmids p-*rcaT* (PBAD-*toxin*) or p-*msrmsd-rcaT-rrtT* (p-retron; PBAD-antitoxin-toxin). Co-inducing the library-plasmids (Ptac) with the toxin/antitoxin plasmids (PBAD) leads to two types of fitness-based screens (Toxin Inhibition/Activation Conjugation; TIC/TAC; Figure 34). TIC identifies blocker genes that permit growth upon toxin overexpression (toxin inhibition), while TAC identifies trigger genes that inhibit growth upon toxin/antitoxin overexpression (toxin activation).

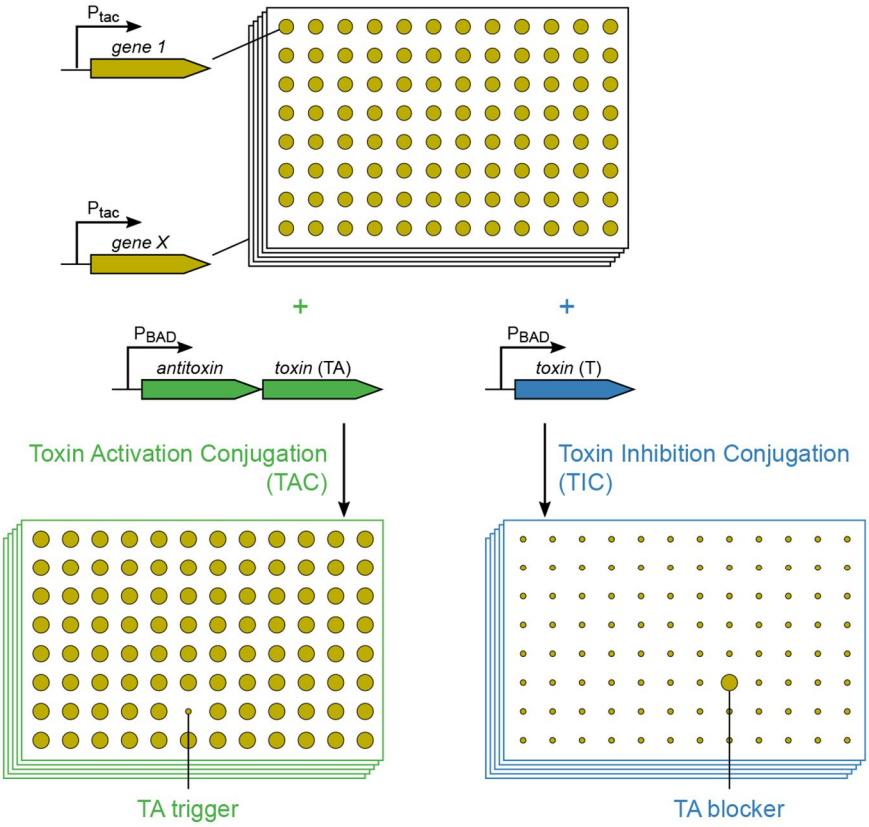

Figure 34. Toxin Inhibition/Activation Conjugation (TIC/TAC); a high-throughput approach to discover TA triggers and blockers. Mobilizable plasmids overexpressing single genes in arrayed conjugative donor strain libraries (Ptac-*gene*1 - Ptac-*gene*X; Saka *et al.*, 2005; Otsuka *et al.*, 2015) are mated with recipient strains carrying plasmids PBAD-*antitoxin-toxin* (PBAD-TA) or PBAD-*toxin* (PBAD-T). Expressing PBAD-TA does not affect growth, while inducing PBAD-T inhibits growth. Co-inducing PBAD-TA with Ptac-*gene*X carrying a TA trigger leads to TA-mediated growth inhibition (TAC), whereas co-inducing PBAD-T with Ptac-*gene*X carrying a TA blocker alleviates T-mediated growth inhibition (TIC).

4.2. Toxin Activation Conjugation (TAC) screen finds retron-TA triggers.

I identified Retron-Sen2 trigger genes by comparing the fitness of *E. coli* strains carrying p-retron (P_{BAD}-TA) and library-plasmids (P_{tac}-*gene*X), across different induction conditions on agar plates. Library-plasmids were induced with either low or high IPTG concentrations. Solely expressing library plasmids should not inhibit growth, but co-expressing the p-retron with its TA-trigger should activate RcaT, and stop growth (Figure 34; TAC). I calculated a triggering standard score (z-score) by comparing individual fitnesses of strains expressing only P_{tac}-*gene*X (IPTG; control plates) and of strains co-expressing P_{BAD}-TA and P_{tac}-*gene*X (arabinose + IPTG; experiment plates). Strains carrying TA-trigger genes should not grow in experiment plates, while being able to grow in control plates. I found 13 triggers from the MOB library (Figure 35A) and 10 triggers from the TransBac library (Figure 35B), by inducing the library-plasmids with high IPTG concentrations. Fewer and largely overlapping triggers were identified by inducing with low IPTG concentrations (Figure 35C-D).

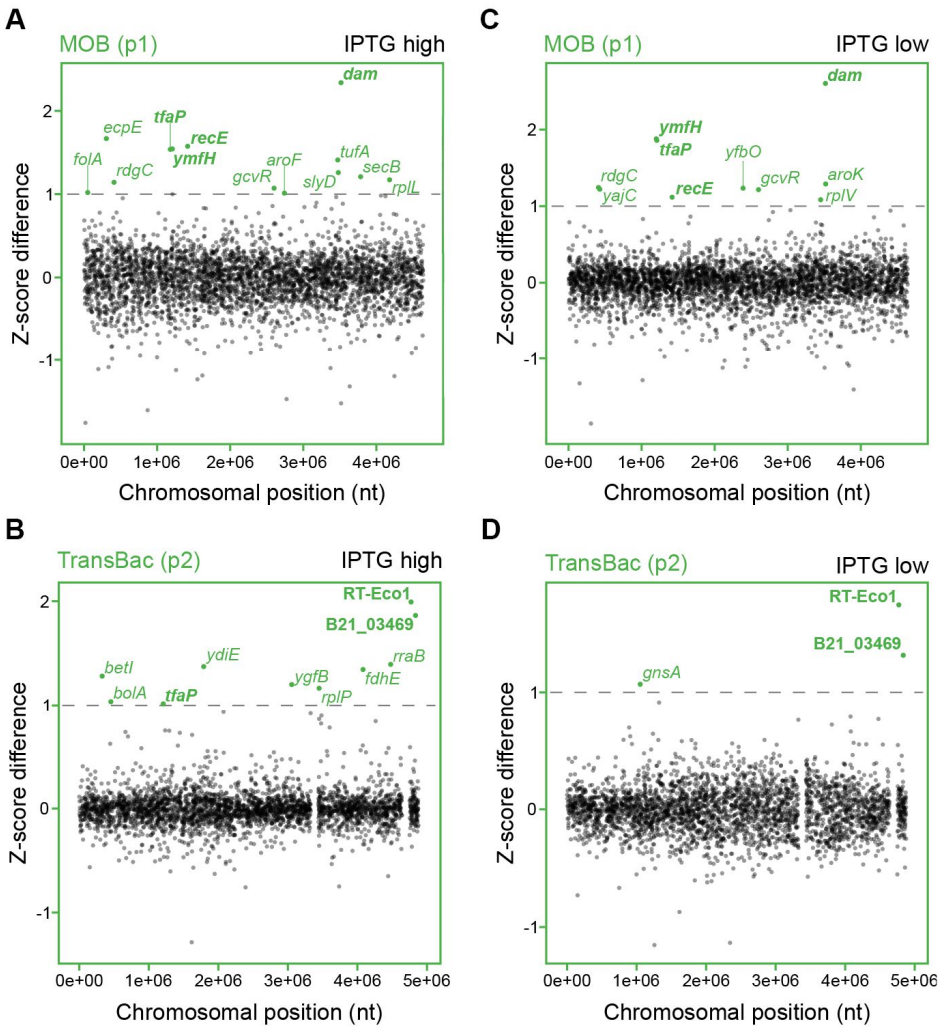

Figure 35. TAC screen identifies multiple Retron-Sen2 triggers. TAC screen by inducing the MOB (p1) and TransBac (p2) library-plasmids with high IPTG **(A-B)** or low IPTG **(C-D)**. Colony arrays of mobilizable plasmid-libraries p1 and p2 (IPTG) were mated with an *E. coli* BW25113 carrying plasmid p-retron (arabinose). Transconjugants carrying both plasmids were selected with appropriate antibiotics, pinned on antibiotics-LB plates containing IPTG (control) or IPTG + arabinose (experiment), and incubated at 37°C. Colony opacities were measured (Kritikos *et al.*, 2017), and mean z-scores per strain (y-axes) were calculated by subtracting z-scores (control – experiment) (n = 2). X-axes denote the chromosomal position of genes carried on library-plasmids based on *E. coli* MG1655 coordinates. Grey line denotes the hit cut-off (z-score difference >1), and phage-related triggers are in bold.

Fitness data acquired from the screens were highly replicable among technical replicates (Figure 36A). There were only a few common triggers between the MOB and TransBac libraries, due to exclusive genes in either library, cloning errors, or expression differences (Figure 36B).

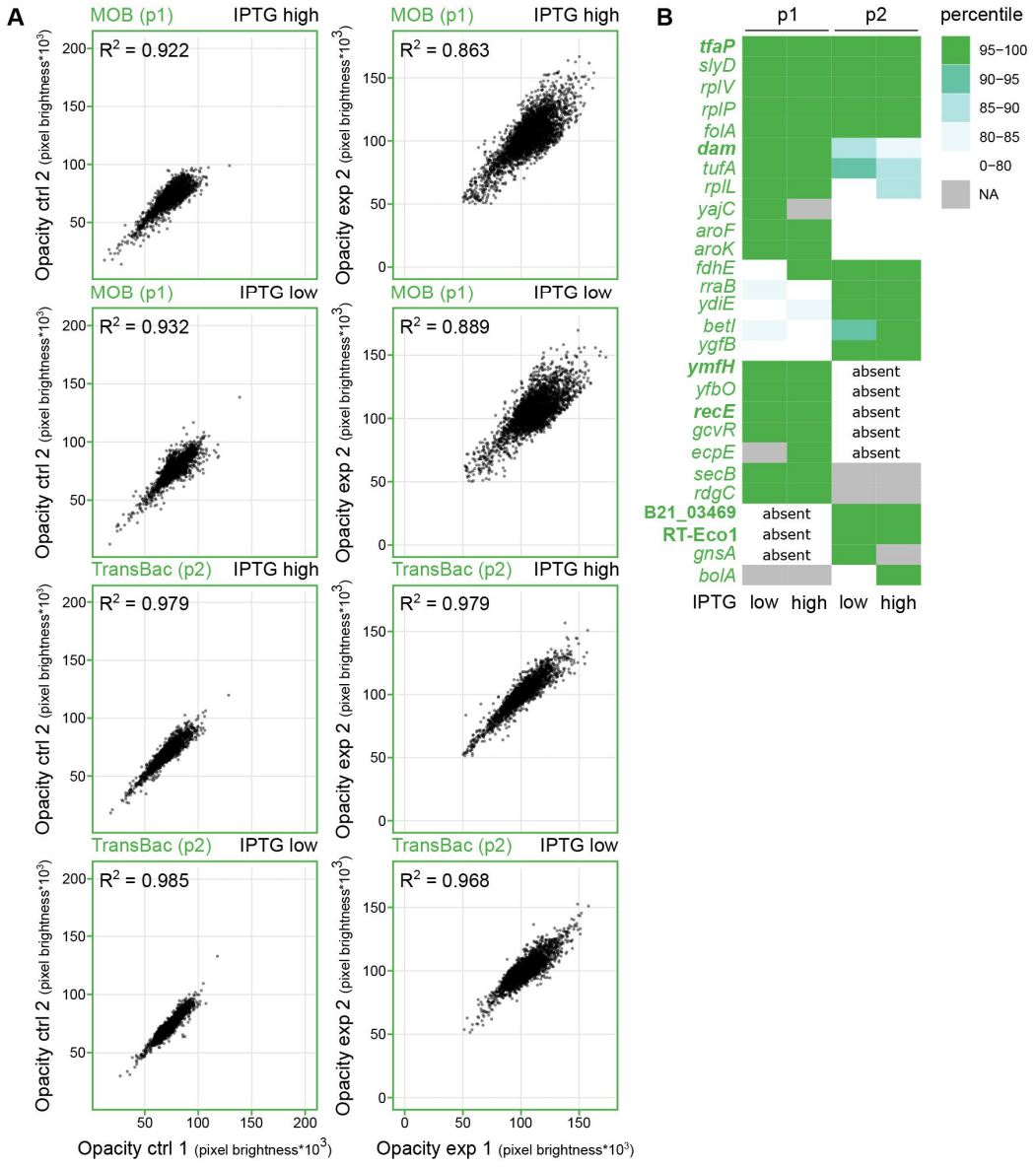

Figure 36. TAC screen reproducibility and trigger conservation between libraries.

(A) TAC screen reproducibility. Unprocessed colony opacity values of strains derived from two replicates of control (ctrl) and experiment (exp) plates, from MOB (p1) or TransBac (p2), were plotted against each other. R^2 denotes the determination coefficients for each plot.

(B) Comparison of triggers between libraries. Triggers identified in each library were rank-ordered in percentiles based on their mean triggering z-scores. NA (in gray) denotes genes that were flagged as problematic. Absent denotes genes not present in one library. Phage-related triggers are in bold.

If the TA-triggers inhibit growth by activating toxin RcaT, they should not be deleterious when co-expressed only with the antitoxin (p-retron-Δ*rcaT*). To assess this, I selected 15 potential triggers, and tested if they inhibit the growth of *E. coli* strains carrying p-retron or p-retron-Δ*rcaT*. All triggers selectively activated RcaT, inhibiting growth only in strains carrying p-retron (Figure 37). Thus, TA-triggers inhibit growth only by activating RcaT, presumably by inactivating the RT-msDNA antitoxin.

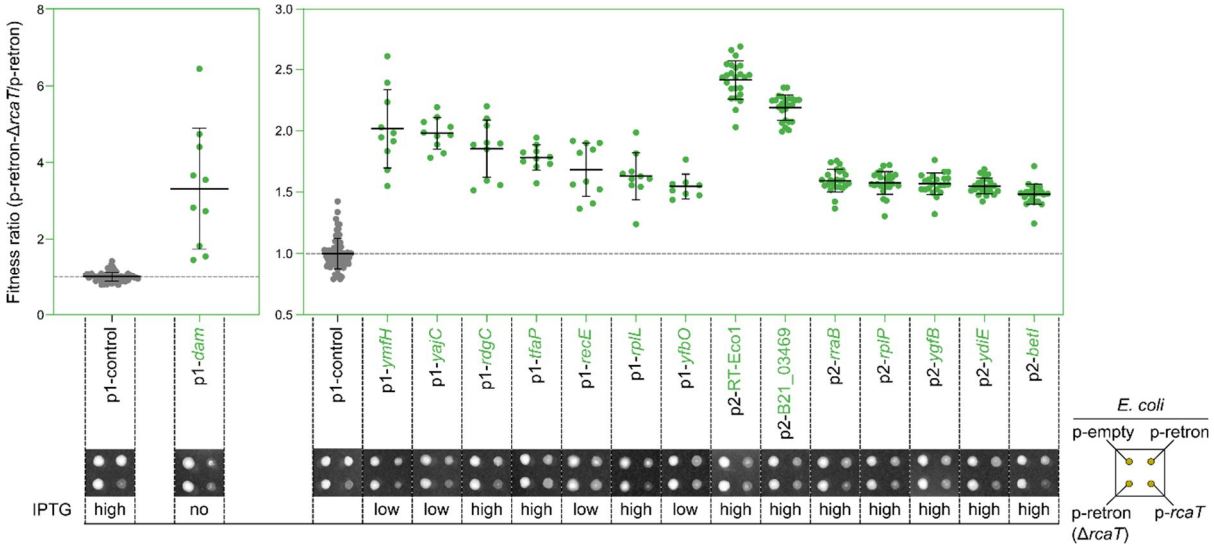

Figure 37. Validation of trigger genes. Plasmids (MOB; p1 or TransBac; p2) containing Retron-Sen2 triggers identified in the TAC screens, were conjugated into *E. coli* BW25113 strains containing plasmids p-retron, p-retron-Δ*rcaT*, p-*rcaT*, or an empty vector. 384 colony-arrays of transconjugant strains were pinned on antibiotics-LB plates containing arabinose, and either no, low, or high IPTG concentrations. The y-axes represent the triggering score for each TA-trigger gene, which is the ratio of the colony opacity values of strains (p-retron-Δ*rcaT* + p1/p2-trigger) divided by strains (p-retron + p1/p2-trigger). p1-control values represent the triggering score of p1-control genes that are not expected to trigger Retron-Sen2 (*n* = 72; 36 biological * 2 technical replicates). Triggering scores for the p1-trigger genes were derived from *n* = 10; 5 biological * 2 technical replicates (except for gene *yfbO*; *n* = 8; 4 biological * 2 technical replicates), while scores for p2-trigger genes were derived from *n* = 24; 12 biological * 2 technical replicates. Representative colonies containing each trigger gene are shown below the graphs for clarity. Horizontal bars denote the average triggering score for each gene, and error bars denote the standard deviation. Grey horizontal line denotes the p1-control triggering score. Trigger *dam* was plotted separately to avoid compressing the scores for the rest of the genes.

Different triggers required different IPTG-induction levels to manifest their effect. For example, the triggering effect of *dam* is already evident from leaky expression levels (no IPTG), while the effect of *rplL* is only apparent in high IPTG concentrations (Figure 38). This suggests that, different TA-triggers require different induction strengths to inactivate the RT-msDNA antitoxin.

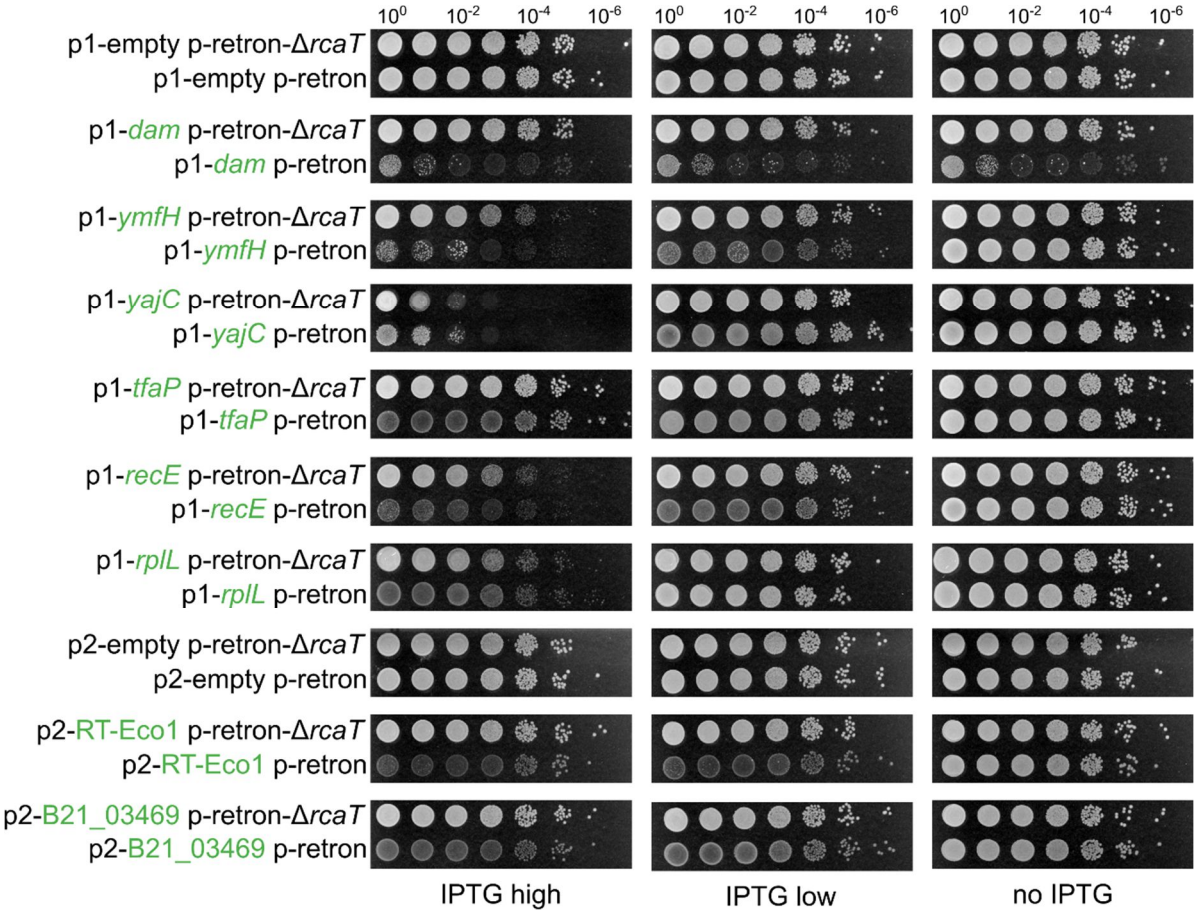

Figure 38. Retron-Sen2 triggers require different IPTG induction levels to activate RcaT. Mobilizable plasmids carrying Retron-Sen2 triggers (p1/p2-*gene*X in green) or empty vectors (p1/p2-empty) were conjugated in *E. coli* BW25113 strains carrying plasmids p-retron or p-retron-Δ*rcaT*. Transconjugants were grown for 5-6 hours in antibiotics-LB/37°C, serially diluted, and spotted on antibiotics-LB plates supplemented with arabinose, and with no, low, or high IPTG concentrations. Plates were incubated at 37°C.

4.2.1. Retron-TA triggers are enriched in prophage genes.

Retron-Sen2 triggers were involved in diverse cellular processes, and several of them (especially strong ones) were genes of cryptic *E. coli* prophages (Table 1). Cryptic prophages are ancient temperate phage insertions into bacterial genomes, that lost their lytic capacity due to mutations (Wang *et al.*, 2010). Retron-TA triggers were significantly enriched in prophage genes (p = 0.01, fold enrichment = 3.6).

Table 1. Description of Retron-Sen2 triggers.

Trigger gene	Trigger score[1]	*p* val[2]	Prophage gene	Function
dam	2.6	5E-23	No	Methylates adenines in 5'-GATC-3' DNA motifs.
RT-Eco1	2	2E-29	Yes	P2*B prophage gene, RT of Retron-Eco1.
ymfH	1.9	7E-13	Yes	e14 prophage gene, unknown function.
B21_03469	1.9	6E-26	Yes	SelC*B prophage gene, unknown function.
tfaP	1.8	1E-12	Yes	e14 prophage gene, unknown function.
ecpE	1.7	2E-08	No	Putative chaperone of *E. coli* common pilus.
recE	1.6	8E-08	Yes	Rac prophage gene, cleaves dsDNA 5'→3'.
tufA	1.4	1E-06	No	Translation elongation factor EF-Tu.
rraB	1.4	2E-15	No	Selective ribonuclease E inhibitor.
ydiE	1.4	6E-15	No	Unknown function.
slyD	1.3	1E-05	No	Peptidyl prolyl cis/trans-isomerase + chaperone.
aroK	1.3	6E-07	No	Involved in chorismate biosynthesis.
fdhE	1.3	2E-14	No	Required for formate dehydrogenase-N activity.
betI	1.3	3E-13	No	DNA-binding transcriptional repressor.
rdgC	1.2	1E-06	No	DNA-binding protein.
secB	1.2	3E-05	No	Chaperone of Sec-mediated protein secretion.
rplL	1.2	5E-05	No	N-acetylated form of 50S ribosomal protein L12.
gcvR	1.2	2E-06	No	DNA-binding transcriptional regulator.
yfbO	1.2	2E-06	No	Unknown function.
yajC	1.2	2E-06	No	Part of Sec translocon accessory complex.
ygfB	1.2	7E-12	No	Unknown function.
rplP	1.2	3E-11	No	50S ribosomal subunit protein L16.
rplV	1.1	2E-05	No	50S ribosomal subunit protein L22.
folA	1	4E-04	No	Dihydrofolate reductase.
aroF	1	4E-04	No	Involved in chorismate biosynthesis.
bolA	1	3E-09	No	DNA-binding transcriptional factor.
gnsA	1	7E-09	No	Unknown function.

1. Trigger score is the mean z-score derived from the TAC screens for each gene (highest z-score was selected between low or high IPTG induction levels).

2. The *p* val is the one-tailed *p* value for z-scores derived from the TAC screens for each gene.

Some triggers encoded in the bacterial core genome were also linked to phage biology. For example, *dam* adenine methyltransferases are commonly found in phages, and share a common evolution with their bacterial counterparts (Hattman *et al.*, 1985). Non-prophage triggers were frequently DNA-binding proteins, chaperones, global transcription/translation players, and orphan genes. Thus, genes triggering Retron-Sen2 are involved in various cellular processes and are enriched in prophage genes.

4.3. Toxin Inhibition Conjugation (TIC) screen finds RcaT blockers.

I identified RcaT blocker genes by comparing the fitness of *E. coli* strains carrying p-*rcaT* (P_{BAD}-T) and library plasmids (Ptac-*gene*X), across different induction conditions. Solely expressing p-*rcaT* inhibits bacterial growth, but co-expressing p-*rcaT* with its blocker should inhibit RcaT, and allow growth (Figure 34; TIC). I calculated a blocking z-score by comparing fitnesses between control and experiment induction plates for the MOB and TransBac libraries. I found 9 blockers from the MOB (Figure 39A) and 4 blockers from the TransBac library (Figure 39B), by inducing the library-plasmids with low IPTG concentrations. More and a few distinct blockers were identified with high IPTG induction from the MOB library (Figure 39C). Thus, TIC screens can identify blocker genes that inhibit RcaT toxicity.

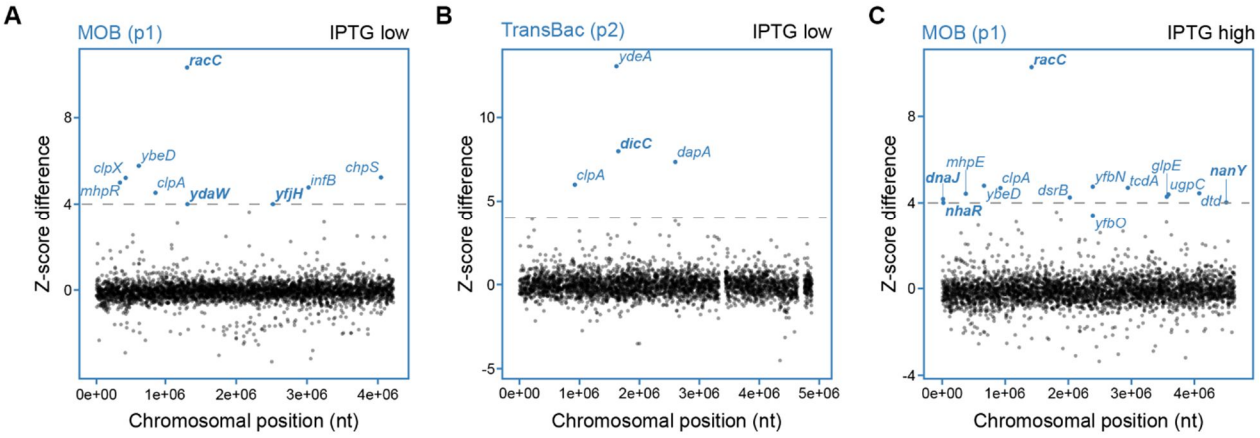

Figure 39. TIC screen identifies multiple Retron-Sen2 blockers. TIC screen by inducing the MOB (p1) and TransBac (p2) library-plasmids with low IPTG **(A-B)** and the MOB library with high IPTG **(C)**. Colony arrays of mobilizable plasmid-libraries p1 and p2 (IPTG) were mated with an *E. coli* BW25113 carrying plasmid p-*rcaT* (arabinose). Procedure carried out as in **Figure 35**, but mean z-scores were calculated by subtracting z-scores (experiment – control) (n = 2). X-axes denote the chromosomal position of genes carried on library-plasmids based on *E. coli* MG1655 coordinates. Grey line denotes the hit cut-off (z-score difference >4), and prophage blockers are in bold.

Replicate correlation was generally high in the TIC screens (Figure 40A). As in the TAC screens, most blockers were specific for one of the two libraries (Figure 40B).

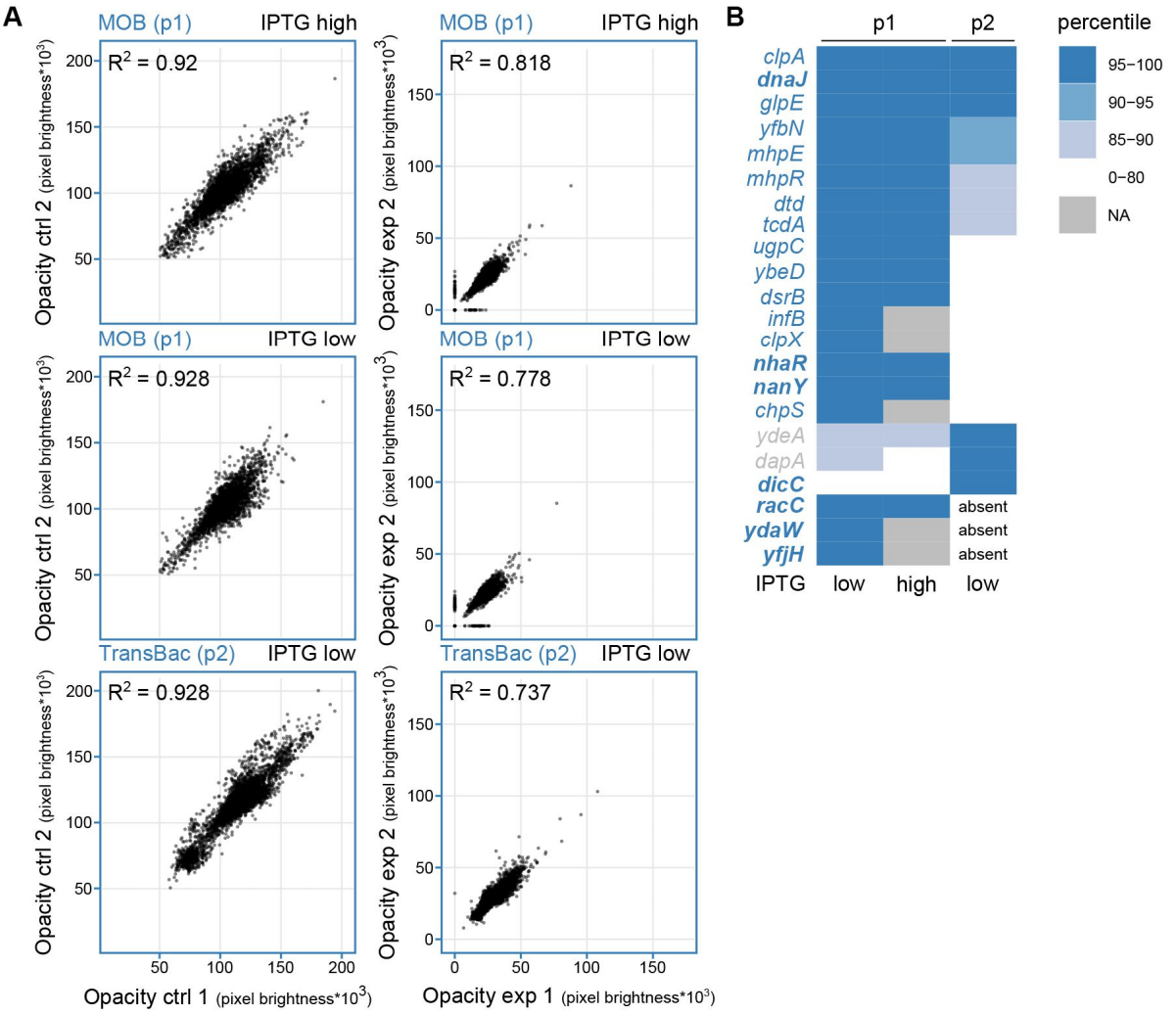

Figure 40. TIC screen reproducibility and trigger conservation between libraries.

(A) TIC screen reproducibility. Unprocessed colony opacity values of strains derived from two replicates of control (ctrl) and experiment (exp) plates, from MOB (p1) or TransBac (p2), were plotted against each other. R^2 denotes the determination coefficients for each plot.

(B) Comparison of blockers between libraries. Blockers identified in each library were rank-ordered in percentiles based on their mean blocking z-scores. NA (in gray) denotes genes that were flagged as problematic. Absent denotes genes not present in one library. Prophage blockers are in bold.

Blockers should specifically alleviate RcaT toxicity, instead of enhancing the overall fitness. To account for this, I selected 11 blockers and introduced them back into *E. coli* strains carrying plasmids p-empty or p-*rcaT*. All blockers selectively inhibited RcaT, while otherwise not affecting growth positively (Figure 41). Thus, blockers allow growth in the presence of RcaT, by specifically inhibiting its toxicity.

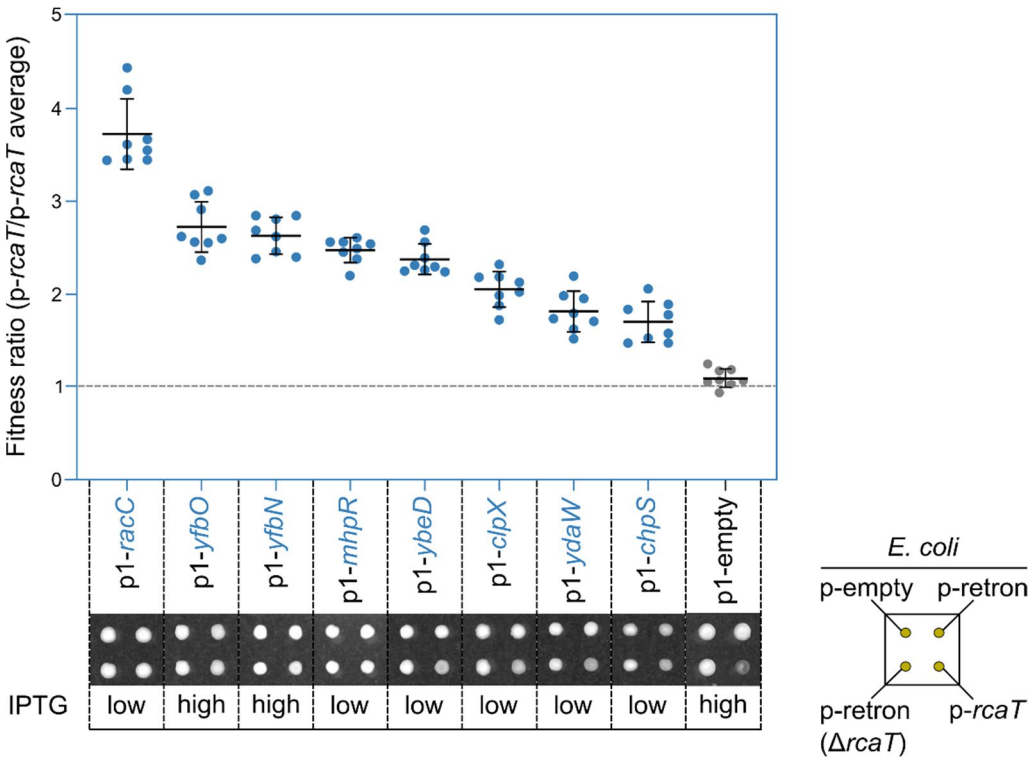

Figure 41. Validation of blocker genes. Plasmids (MOB; p1) containing Retron-Sen2 blockers identified in the TIC screens, were conjugated into *E. coli* BW25113 strains containing plasmids p-*rcaT*, p-retron, p-retron-Δ*rcaT*, or an empty vector. 384 colony-arrays of transconjugant strains were pinned on antibiotics-LB plates containing arabinose, and either no, low, or high IPTG concentrations. The y-axes represent the blocking score for each TA-blocker gene, which is the ratio of the colony opacity values of strains (p-*rcaT* + p1-blocker) divided by the average colony opacity of a strain carrying a control plasmid (p-*rcaT* + p1-control). The mean colony opacity for p1-control was calculated from *n* = 110; 55 biological * 2 technical replicates. The blocking scores were calculated from *n* = 8; 4 biological * 2 technical replicates. Representative colonies containing each blocker gene are shown below the graphs for clarity. Horizontal bars denote the average blocking score for each gene, and error bars denote the standard deviation. Grey horizontal line denotes the expected fitness ratio in the absence of blocking effects.

Different blockers required lower or higher IPTG induction strengths to inhibit RcaT. For instance, RacC blocks in every IPTG concentration, while the blocking effect of *dicC* is only evident at low IPTG, as it is toxic in high IPTG (Figure 42). Thus, different TA-blockers require different induction strengths to allow growth in the presence of RcaT, reflecting different expression-thresholds required to inhibit RcaT, and/or toxicity stemming from high blocker expression.

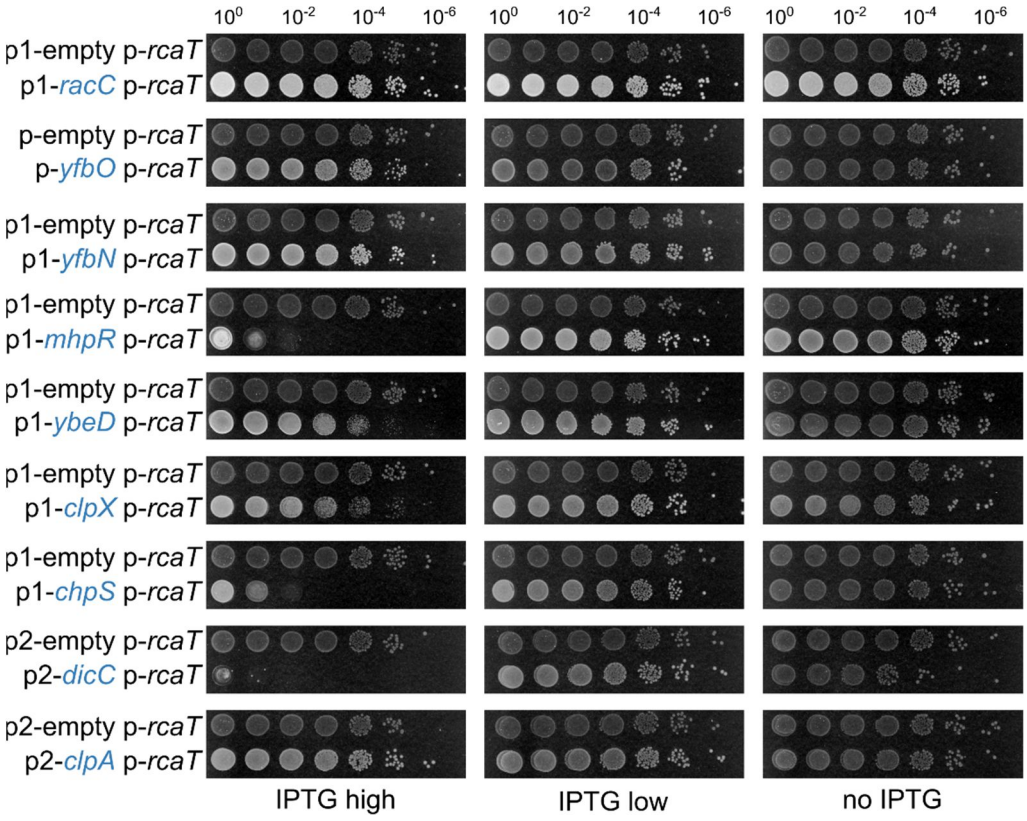

Figure 42. Retron-Sen2 blockers require different IPTG induction levels to inhibit RcaT. Mobilizable plasmids carrying Retron-Sen2 blockers (p1/p2-*gene*X in blue) or empty vectors (p1/p2-empty) were conjugated in *E. coli* BW25113 strains carrying plasmids p-*rcaT*. Transconjugants were grown for 5-6 hours in antibiotics-LB/37°C, serially diluted, and spotted on antibiotics-LB plates supplemented with arabinose, and with no, low, or high IPTG concentrations. Plates were incubated at 37°C.

4.3.1. RcaT blockers are enriched in prophage genes.

RcaT blockers were involved in diverse processes (Table 2), and enriched in prophage genes (p = 0.005, fold enrichment = 5.3). Besides prophage blockers, some were presumably trivial findings affecting arabinose induction or conjugation itself (*ydeA*, *nanY*, *dapA*), with others involved in protein quality control (*clpA*, *clpX*, *infB*, *dnaJ*),

tRNA synthesis (*tcdA*, *dtd*), 3-phenylpropionate synthesis (*mhpR*, *mhpE*), or unknown processes. Thus, individual phage and core genes can alleviate RcaT toxicity.

Table 2. Description of Retron-Sen2 blockers.

Blocker gene	Blocker score[1]	*p* val[2]	Prophage gene	Function
ydeA	13.0	1E-67	No	L-arabinose exporter.
racC	10.3	3E-76	Yes	Rac prophage gene, unknown function.
dicC	8.0	1E-26	Yes	Qin prophage gene, negative regulator of *dicB*
dapA	7.3	8E-23	No	Diaminopimelic acid biosynthesis.
clpA	6.0	9E-16	No	Substrate specifying adaptor for ClpAXP protease.
ybeD	5.8	3E-25	No	Unknown function.
chpS	5.2	4E-21	No	Antitoxin of ChpB/ChpS TA system.
clpX	5.2	6E-21	No	Substrate specifying adaptor for ClpAXP protease.
mhpR	5.0	2E-19	No	DNA-binding transcription factor (3-phenylpropionate).
infB	4.8	7E-18	No	Translation initiation factor IF2
yfbN	4.7	2E-12	No	Unknown function.
tcdA	4.7	4E-12	No	tRNA modification factor.
dtd	4.4	5E-11	No	Aminoacyl-tRNA editing enzyme.
mhpE	4.4	6E-11	No	Class I aldolase (3-phenylpropionate).
ugpC	4.4	8E-11	No	ATP-binding subunit of ABC transporter.
glpE	4.3	2E-10	No	Catalyzes sulfur transfer from thiosulfate to substrates.
dsrB	4.2	3E-10	No	Unknown function.
dnaJ	4.2	6E-10	Yes	Modulator of DnaK chaperone.
nanY	4.0	2E-09	Yes	KpLE2 prophage gene, sugar utilization.
yfjH	4.0	4E-13	Yes	CP4-57 prophage gene, unknown function.
ydaW	4.0	4E-13	Yes	Rac prophage gene, unknown function.
nhaR	4.0	3E-09	Yes	DNA-binding transcription factor.
yfbO	3.4	3E-07	No	Unknown function.

1. Blocker score is the mean z-score derived from the TIC screens for each individual gene (highest z-score was selected between low or high IPTG induction levels, when available).

2. The *p* val is the one-tailed *p* value for z-scores derived from the TIC screens for each gene.

4.4. Dam triggers the retron by directly methylating the msDNA antitoxin.

Combining my grasp on the TA mode of action of Retron-Sen2, and previous functional annotations of genes that I identified as triggers, allowed me to dissect the first triggering molecular mechanisms for any TA system. Trigger Dam is the DNA adenine methyltransferase of *E. coli*, methylating adenines in 5'-GATC-3' genomic motifs (Marinus and Morris, 1973). Dam was the strongest trigger identified in the TAC screen (Figure 35). Since all the triggers were identified through overexpressing Retron-Sen2, it is unclear whether they can activate the native Retron-Sen2 in *S*Tm. Antitoxin deletions in *S*Tm activate RcaT, which inhibits growth in colder temperatures (Figure 8). Therefore, If the triggers interact with the native Retron-Sen2, they should inhibit *S*Tm growth in lower temperatures. Indeed, overexpressing *dam* in *S*Tm inhibited *S*Tm growth in cold in a *rcaT*-dependent manner (Figure 43).

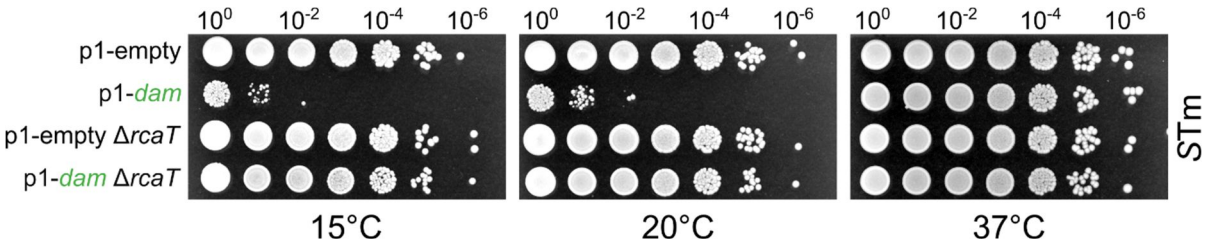

Figure 43. Overexpressing Dam activates the endogenous Retron-Sen2 in *S*Tm. *S*Tm wildtype and *ΔrcaT* strains carrying plasmid p1-*dam* or an empty vector were grown for 5-6 hours in ampicillin-LB/37°C, serially diluted, and spotted on ampicillin-LB plates supplemented with low IPTG concentrations. Plates were incubated at 15°C, 20°C, or 37°C. Representative data shown from four independent experiments.

Dam 5'-GATC-3' methyltransferase homologues are present in other bacteria (e.g., *S*Tm; Torreblanca and Casadesús, 1996), and in phages (e.g., phage P1; Sternberg and Coulby, 1990). Notably, these Dam homologues also trigger the Retron-Sen2 (Figure 44), suggesting that the 5'-GATC-3' adenine methylation activity itself is the triggering signal. Thus, Dam activates the endogenous Retron-Sen2 in *S*Tm, presumably by methylating a double-stranded DNA 5'-GATC-3' sequence.

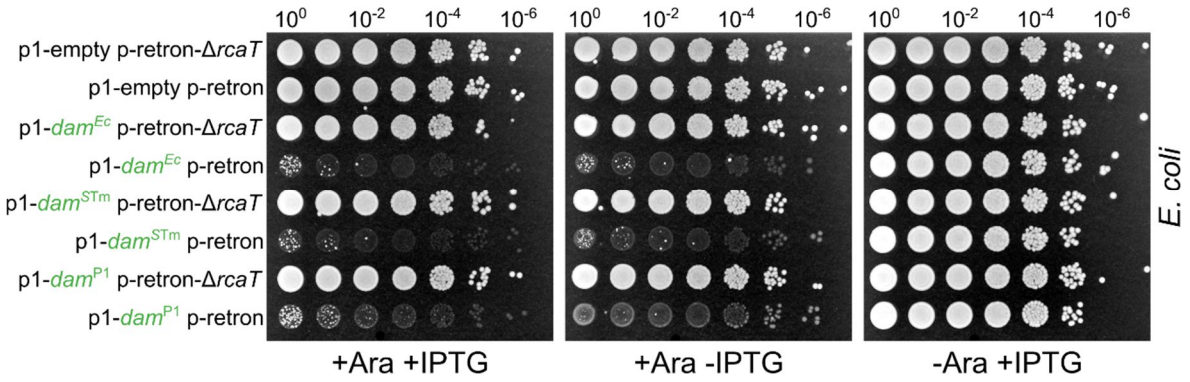

Figure 44. Dam bacterial and phage homologues trigger Retron-Sen2. *E. coli* BW25113 wildtype carrying plasmids p-retron, p-retron-Δ*rcaT* were co-transformed with plasmids carrying *dam* homologues from *E. coli* (p1-dam^{Ec}), from *S*Tm (p1-dam^{STm}), or from phage P1 (p1-dam^{P1}). Strains were grown for 5-6 hours in antibiotics-LB/37°C, serially diluted, and spotted on antibiotics-LB plates with or without arabinose/IPTG. Plates were incubated at 37°C. Representative results shown from two independent experiments.

Since Dam methyltransferases modulate gene expression by methylating DNA (Løbner-Olesen *et al.*, 2005), Dam could be activating RcaT by downregulating the retron antitoxin (either the RT, or the msDNA). If Dam downregulated the RT, there should be a decrease in the amount of msDNA produced. Therefore, I tested whether Dam triggers RcaT through RT/msDNA downregulation, by isolating msDNA from *S*Tm strains carrying either a p1-*dam* or a p1-empty plasmid. Overexpressing Dam did not affect msDNA levels compared to the control (Figure 38). Thus, Dam overexpression does not inactivate the RT-msDNA antitoxin by downregulating RT or msDNA levels.

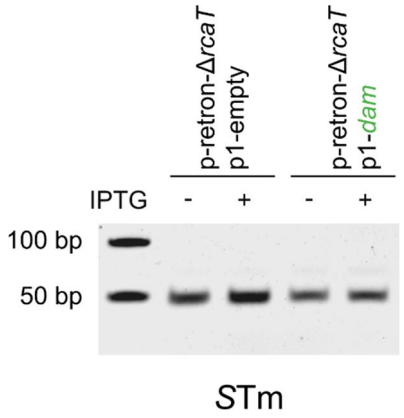

Figure 45. Overexpressing Dam does not downregulate msDNA. msDNA was extracted by *S*Tm wildtype expressing plasmid p-retron-Δ*rcaT* in combination with either a p1-*dam* plasmid or an empty vector (p1-empty). Extracted msDNA was electrophoresed on a TBE-Polyacrylamide gel. A representative gel from three independent experiments is shown.

Another way Dam could be affecting the antitoxin was by directly methylating the msDNA. Dam acts on double-stranded DNA (dsDNA), while msDNA is single-stranded DNA (ssDNA; Simon *et al.*, 2019). Nevertheless, all msDNAs are reverse transcribed from *msd*-RNAs containing inverted repeats, ultimately forming dsDNA (Lampson *et al.*, 2005). I noticed that msDNA-Sen2 has a single 5'-GATC-3' motif in its dsDNA hairpin region, that Dam could recognize. Therefore, I wondered whether Dam activated RcaT by directly methylating this specific motif. To test this, I mutated the 5'-GATC-3' site on msDNA (p-retron^{WT}) towards 5'-GTTC-3' (p-retron^{mut}), which is not recognized by Dam. If msDNA methylation triggered the retron-TA, then p-retron^{mut} should be insensitive to Dam-mediated triggering. Indeed, mutating the Dam motif on msDNA completely abolished Dam-triggering (Figure 46A). The msDNA mutation itself did not affect the function of RcaT, as inducing p-retron^{mut} was toxic in an *E. coli* Δ*xseA* strain (where the antitoxin is inactive) (Figure 46A). The mutation also affected neither the function of msDNA, since RcaT is inhibited when p-retron^{mut} is induced in the wildtype *E. coli* (Figure 46A), nor the produced msDNA levels (Figure 46B). This suggested that Dam activated RcaT by directly methylating the msDNA.

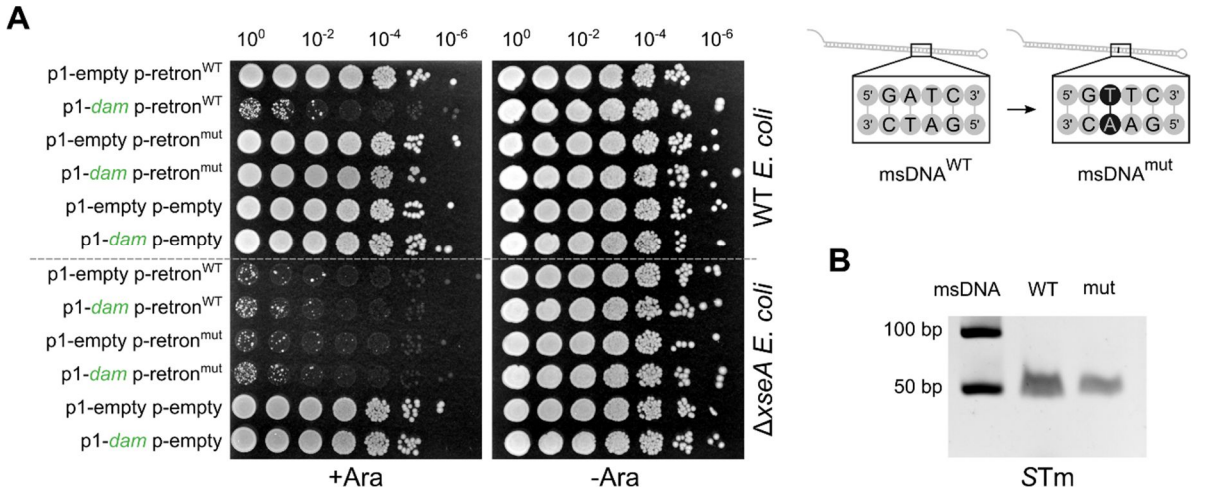

Figure 46. Dam triggers Retron-Sen2 by methylating msDNA.

(A) Mutating the 5'-GATC-3' motif on msDNA abolishes Dam triggering. *E. coli* BW25113 wildtype and Δ*xseA* carrying plasmids p-retron^{WT} (msDNA^{WT}), or p-retron^{mut} (msDNA^{mut}), or an empty vector were combined with p1-*dam* or an empty vector. Strains were grown for 5-6 hours in antibiotics-LB/37°C, serially diluted, and spotted on antibiotics-LB plates with or without arabinose. Plates were incubated at 37°C. Representative results shown from two independent experiments.

(B) p-retron^{mut} produces normal msDNA levels. msDNA were extracted from *S*Tm wildtype expressing p-retron^{WT} or p-retron^{mut}. Extracted msDNA were electrophoresed on a TBE-Polyacrylamide gel.

In order to probe whether Dam methylates the 5'-GATC-3' motif on msDNA, I utilized the restriction enzyme DpnI, which strictly cleaves methylated adenines in 5'-GATC-3' motifs (Geier and Modrich, 1979). I isolated either wildtype (msDNA^{WT}) or mutated msDNA (msDNA^{mut}), from strains carrying either p1-*dam* or a p1-empty plasmid. If Dam methylates msDNA, DpnI should only be able to cleave msDNA^{WT} isolated from strains overexpressing Dam. Indeed, msDNA^{WT} was only cleaved when isolated from a strain overexpressing Dam (Figure 47A). DpnI did not cleave msDNA^{mut} regardless of overexpressing Dam, since the 5'-GATC-3' motif is mutated (Figure 47A). This also proved that chromosomally-produced Dam is not enough to methylate msDNA. This reflects previous findings on higher-copy DNA elements being hypomethylated due to the endogenous Dam protein levels being rate-limiting (Szyf *et al.*, 1984). Thus, Dam activates RcaT by methylating one specific adenine in the stem-loop of msDNA, which then presumably dissociates the RT-msDNA antitoxin complex (Figure 47B).

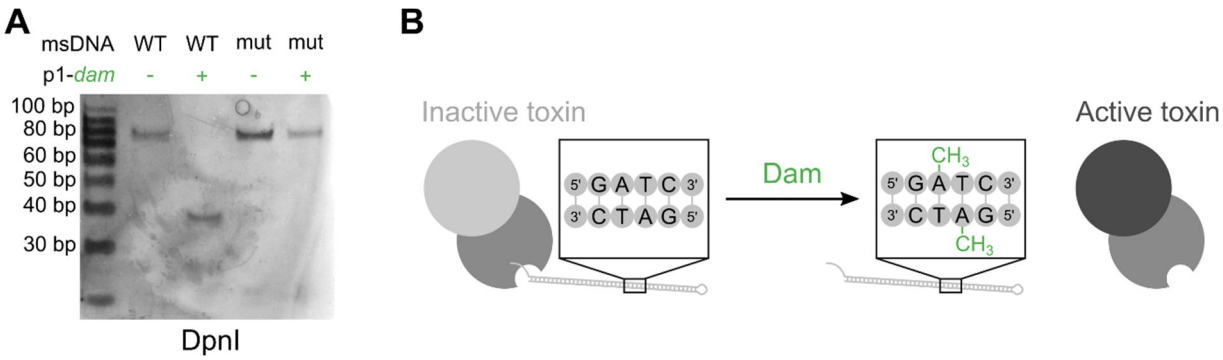

Figure 47. Dam methylates msDNA and inactivates the RT-msDNA antitoxin.

(A) Dam methylates the 5'-GATC-3' site on msDNA-Sen2. msDNA was extracted from *S*Tm strains carrying combinations of plasmids p-retron^{WT}, p-retron^{mut} and plasmids p1-*dam* or an empty vector. Extracted msDNA was further purified by gel extraction, and digested overnight with DpnI. Digests were electrophoresed on a denaturing TBE-Polyacrylamide gel, and DNA were stained with silver.

(B) Schematic model of Dam-mediated Retron-Sen2 triggering. Dam methylates msDNA, activating RcaT (in black). Hypothetically, msDNA methylation inactivates the retron antitoxin, by breaking the RT-msDNA complex.

4.5. RacC-RecE of Rac prophage are a linked blocker/trigger gene pair.

E. coli carries a cryptic Rac prophage, containing among others *recE* and *racC*, two neighbouring prophage genes (Figure 48). RecE triggers Retron-Sen2 (Figure 38), while RacC blocks RcaT-Sen2 (Figure 42). Thus, two neighbouring phage genes exert opposite actions on Retron-Sen2 (blocker/trigger pair).

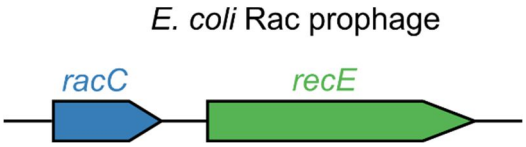

Figure 48. RacC and RecE are a linked blocker/trigger pair. Schematic representation of gene organization in the Rac prophage of *E. coli* BW25113.

The *recE* gene encodes Exodeoxyribonuclease VIII, which recognizes dsDNA and degrades one DNA strand in the 5'→ 3' orientation (Joseph and Kolodner, 1983). Since RecE degrades DNA, and msDNA is necessary for antitoxin activity, I wondered whether msDNA is cleaved by RecE. To assess this, I isolated msDNA from *E. coli* strains carrying either a p1-empty or a p1-*recE* plasmid. I could not retrieve mature msDNA from strains overexpressing RecE, suggesting that RecE degrades msDNA (Figure 49A). Although RecE abolishes mature msDNA production, I noticed a higher molecular weight msDNA being produced. This msDNA is produced in *ΔxseAB* mutants (Figure 10). Notably, immature msDNA is completely resistant to RecE cleavage *in vivo* (Figure 49B), suggesting that only Exo VII-processed msDNA is a substrate for RecE. Thus, RecE inactivates the RT-msDNA antitoxin by degrading mature msDNA, which activates RcaT (Figure 49C).

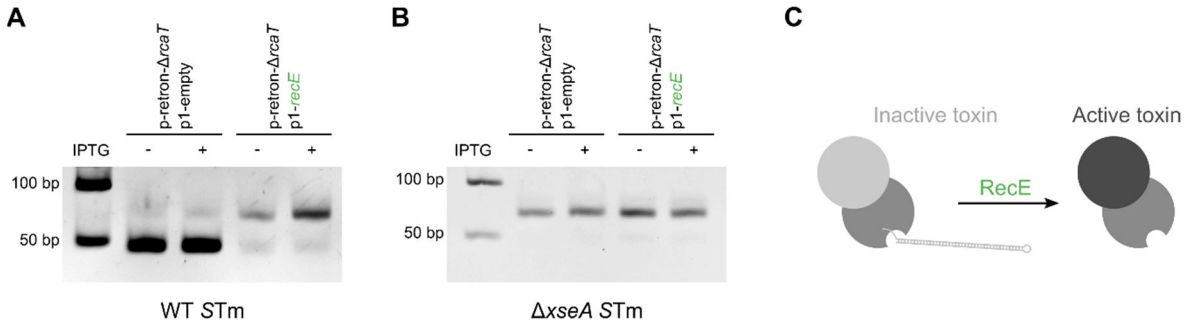

Figure 49. RecE triggers Retron-Sen2 by degrading msDNA.

(A) RecE degrades mature msDNA-Sen2 *in vivo*. msDNA was extracted from *S*Tm wildtype carrying plasmid p-retron-Δ*rcaT*, co-expressed with plasmid p1-*recE* or an empty vector. msDNA were electrophoresed on a TBE-Polyacrylamide gel, and DNA were stained with ethidium bromide. Representative gel shown from three independent experiments.

(B) Immature msDNA-Sen2 is resistant to RecE cleavage. Procedure as in panel **A**, but msDNA were extracted from *S*Tm Δ*xseA* strains. Representative gel shown from two independent experiments.

(C) Schematic model of RecE-mediated Retron-Sen2 triggering. RecE activates RcaT, by inactivating the RT-msDNA antitoxin through msDNA degradation.

RecE also triggers Retron-Eco9 (Figure 50A), the msDNA of which also depends on Exo VII for maturing. This suggests that RecE generally triggers retrons that utilize Exo VII for producing msDNA. Notably, recombinant RecE cleaves both mature and immature msDNA *in vitro*, after they are isolated from cells (Figure 50B). This suggests that a factor besides msDNA sequence/structure protects immature msDNA from RecE (potentially the RNA-branch of msDNA-Sen2 or the RT protein itself). Finally, in contrast to Dam, overexpressing RecE does not trigger the endogenous Retron-Sen2 in *S*Tm, and causes RcaT-independent cold-sensitivity (Figure 50C).

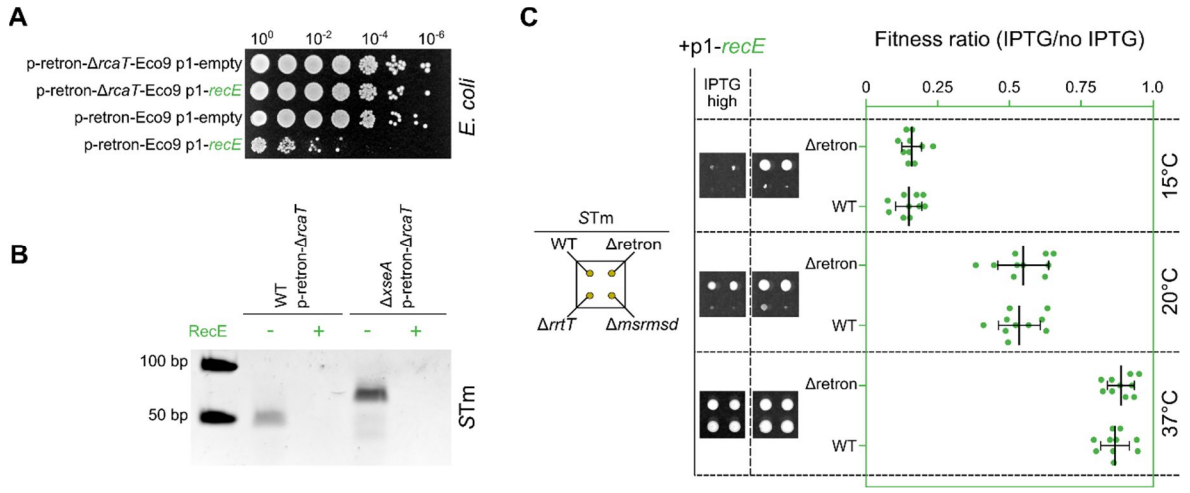

Figure 50. RecE degrades msDNA-Eco9 and immature msDNA *in vitro*.

(A) RecE triggers Retron-Eco9. *E. coli* BW25113 carrying plasmids p-retron-Eco9 or p-retron-Δ*rcaT*-Eco9 were combined with p1-*recE* or an empty vector. Strains were grown for 5-6 hours in antibiotics-LB/37°C, serially diluted, and spotted on antibiotics-LB plates supplemented with arabinose and low IPTG concentrations. Plates were incubated at 37°C. Representative data shown from three independent experiments.

(B) RecE cleaves both mature and immature msDNA *in vitro*. Mature and immature msDNA was extracted from *S*Tm wildtype or Δ*xseA* strains. msDNA extracts were incubated with recombinant RecE, and digests were electrophoresed on a TBE-Polyacrylamide gel, and DNA were stained with ethidium bromide.

(C) RecE does not activate Retron-Sen2 in *S*Tm. *S*Tm wildtype, Δretron, Δ*rrtT*, and Δ*msrmsd* strains carrying plasmid p1-*recE* were pinned on ampicillin-LB plates, with no, or high IPTG concentrations, and plates were incubated at 15°C, 20°C, or 37°C. Colony sizes were quantified, and used to calculate a ratio that reflects the cold sensitivity of the strains (Δretron or WT). Ratios are derived by dividing the colony size of (strain X grown in IPTG) by the colony size of (strain X grown without IPTG) for the three temperatures. Vertical bars denote the average ratio (*n = 10*; 5 biological * 2 technical replicates), and error bars denote the standard deviation. Colonies of the corresponding strains included next to the graphs for clarity.

Prophage gene *racC* lies immediately upstream of *recE*, encoding the small 91-amino acid RacC protein of unknown function. RacC was the strongest RcaT blocker in the TIC screen (Figure 39). Overexpressing RacC in *S*Tm completely reverted RcaT-mediated cold-sensitivity of all retron antitoxin mutants (Figure 51A), in contrast to almost all other blockers (data not shown). This suggested that RacC specifically inhibited the toxicity of RcaT-Sen2. Furthermore, RacC also blocked RcaT-Eco9 (Figure 51B), indicating that it is a promiscuous retron inhibitor. Thus, RacC inhibits retron-mediated toxicity, presumably by directly interacting with RcaT (Figure 51C).

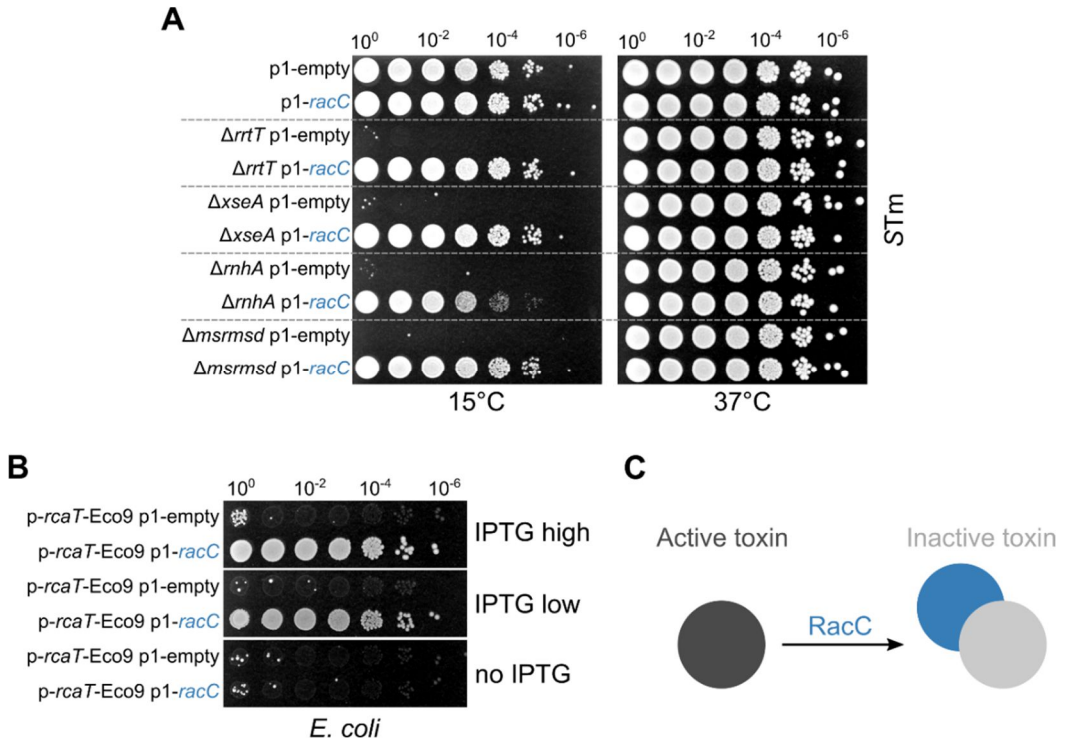

Figure 51. RacC blocks RcaT activity.

(A) RacC reverts the cold-sensitivity phenotype of *S*Tm retron deletion mutants. *S*Tm wildtype and retron deletion mutants, carrying plasmid p1-*racC* or the empty vector, were grown for 5-6 hours in ampicillin-LB/37°C, serially diluted, and spotted on ampicillin-LB plates containing low IPTG concentrations. Plates were incubated at 15°C or 37°C. Representative data shown from two independent experiments.

(B) RacC inhibits RcaT-Eco9. *E. coli* BW25113 carrying plasmid p-*rcaT*-Eco9, was transformed with plasmids p1-*racC* or an empty vector. Strains were grown for 5-6 hours in antibiotics-LB/37°C, serially diluted, and spotted on antibiotics-LB plates containing arabinose, and no, low, or high IPTG concentrations. Plates were incubated at 37°C. Representative data shown from three independent experiments.

(C) Schematic depiction of RacC-mediated RcaT blocking. RacC (in blue) presumably inhibits RcaT activity by directly binding RcaT.

4.5.1. Prophage gene DicC inhibits RcaT by an unknown mechanism.

The Qin prophage gene *dicC* was identified as a blocker through the TIC screen in the TransBac library (Figure 39). Besides RacC, DicC was the only other blocker able to inhibit the native RcaT in *S*Tm (Figure 52). In contrast to RacC, DicC only partially alleviated the cold-sensitivity phenotype of retron mutants, while also conferring a fitness defect of its own at 37°C (Figure 52). This could mean that it only has a partial buffering effect against RcaT toxicity, potentially by interacting with the target of RcaT.

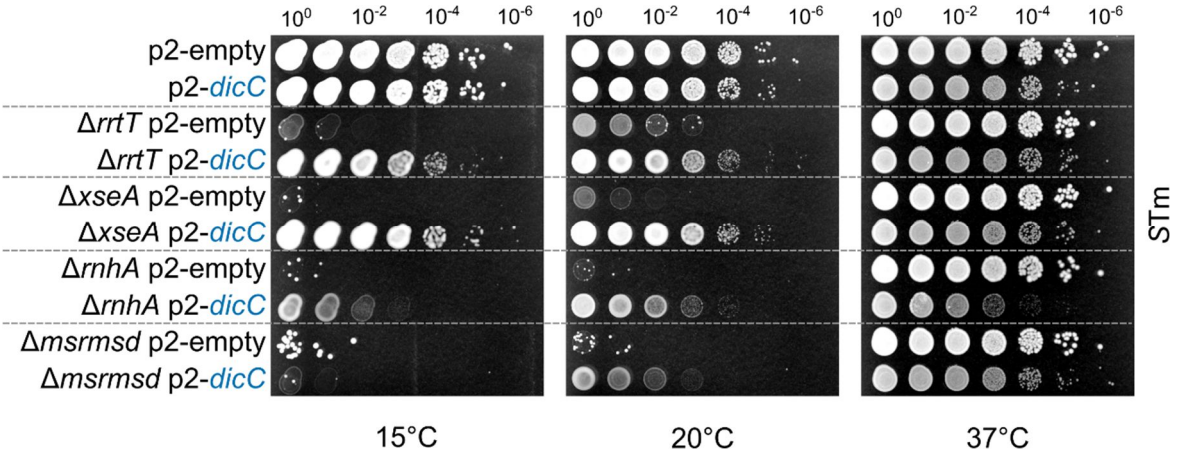

Figure 52. DicC partially restores the cold-sensitivity of *S*Tm retron deletion strains. *S*Tm wildtype and retron deletion strains carrying plasmid p2-*dicC* or an empty vector, were grown for 5-6 hours in tetracycline-LB/37°C, serially diluted, and spotted on tetracycline-LB plates with low IPTG concentrations. Plates were incubated at 15°C, 20°C, or 37°C. Representative results shown from two independent experiments.

4.6. RT-Eco1 triggers Retron-Sen2 by sequestering msDNA.

The *E. coli* species includes quite distinct strains, carrying strain-specific genes. Both the MOB (Saka *et al.*, 2005) and TransBac (Otsuka *et al.*, 2015) overexpression libraries carry genes from the *E. coli* K strain. Additionally, TransBac also contains distinct genes from the *E. coli* B strain (Studier *et al.*, 2009). Prophage gene RT-Eco1 (B21_00839) is among these *E. coli* B genes in the TransBac collection, encoding the retron reverse transcriptase of Retron-Eco1 (retron-Ec86; Kirchner *et al.*, 1992).

RT-Eco1 was the strongest Retron-Sen2 trigger found through the TAC TransBac screen (Figure 35B, D). Overexpressing RT-Eco1 partially activates the endogenous Retron-Sen2 in *S*Tm (while also causing cold-sensitivity of its own), as tested by either colony-fitness (Figure 53A) or spot assays (Figure 53B). This suggested that RT-Eco1

triggers Retron-Sen2 directly. Retron-Sen2 antitoxin activity requires both RT-RcaT and RT-msDNA interactions, one of which RT-Eco1 could be disrupting. Notably, RT-Eco1 triggers Retron-Eco9 from *E. coli* (Figure 53C), suggesting that it interacts with a conserved component between Retrons-Sen2 and -Eco9. It is unlikely that RT-Eco1 breaks the RT-RcaT interaction, since RT-RcaT interactions are cognate within each retron (Figure 32). Since RT-Eco1 is a reverse transcriptase, I presumed that RT-Eco1 triggers Retrons-Sen2 and -Eco9 by disrupting their msDNA biosynthesis. To test this, I isolated msDNA-Sen2 from *E. coli* strains expressing either RT-Eco1 or an empty plasmid. However, overexpressing RT-Eco1 did not affect msDNA levels (Figure 53D), suggesting that RT-Eco1 does not disrupt msDNA biosynthesis.

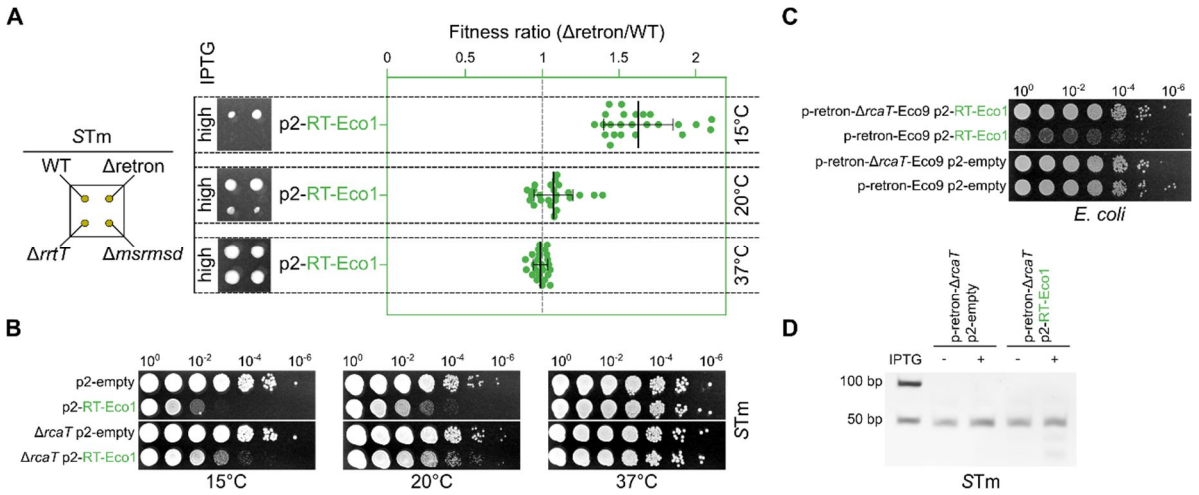

Figure 53. RT-Eco1 triggers Retron-Sen2.

(A) RT-Eco1 partially activates the endogenous Retron-Sen2 in *S*Tm (colony size). Procedure as described in **Figure 50C**. Colony sizes were quantified, and used to calculate a fitness ratio cold-sensitivity between Δretron and WT strains. Ratios are derived by the colony size of (Δretron) by the colony size of (WT) for the three different temperatures. Vertical bars denote the average ratio (n = 24; 12 biological * 2 technical replicates), and error bars denote the standard deviation. Colonies of the corresponding strains included next to the graphs for clarity.

(B) RT-Eco1 partially activates the endogenous Retron-Sen2 in *S*Tm (spots). Procedure as described in **Figure 43**, but for plasmid p2-RT-Eco1. Representative results shown from two independent experiments.

(C) RT-Eco1 triggers Retron-Eco9. *E. coli* BW25113 carrying plasmids p-retron-Eco9 or p-retron-Δ*rcaT*-Eco9 were transformed with plasmid p2-RT-Eco1 or an empty vector. Strains were grown for 5-6 hours in antibiotics-LB/37°C, serially diluted, and spotted on antibiotics-LB plates with arabinose/low IPTG. Plates were incubated at 37°C. Representative results shown from four independent experiments.

(D) RT-Eco1 does not inhibit msDNA biosynthesis. Procedure as described in **Figure 45**, but with plasmid p2-RT-Eco1. Representative gel from two independent experiments shown.

Since RT-Sen2 binds its msDNA (Figure 30), RT-Eco1 could be disrupting the RT-msDNA antitoxin by titrating the msDNA-Sen2. If RT-Sen2 and RT-Eco1 compete for msDNA binding, upregulating msDNA production should alleviate the RT-Eco1 triggering effect. The rate-limiting step to produce msDNA is the msrmsd-RNA template, since RTs can produce more msDNA in the presence of increased substrate. Thus, I supplied more msrmsd-RNA from a third plasmid (p1-*msrmsd*^{WT}), to overproduce msDNA. Indeed, overproducing msDNA completely abolished RT-Eco1-mediated triggering (Figure 54A). To exclude that overexpressing msrmsd-RNA alone is not enough to alleviate triggering, I supplied a msrmsd-RNA point mutant, that cannot be turned into msDNA (p1-*msrmsd*^{mut}). Supplying mutated msrmsd-RNA did not alleviate RT-Eco1 triggering, proving that msDNA production is necessary to mitigate the triggering effect (Figure 54A). Notably, inducing the mutated msrmsd-RNA with high IPTG triggered Retron-Sen2 on its own, possibly by competing with the wildtype msrmsd-RNA. In every case, msrmsd-RNA expression was not toxic by itself, since strains carrying p-retron-Δ*rcaT* did not produce toxicity (Figure 54A). Thus, RT-Eco1 sequesters msDNA-Sen2 from the RT-msDNA antitoxin, and activates RcaT (Figure 54B).

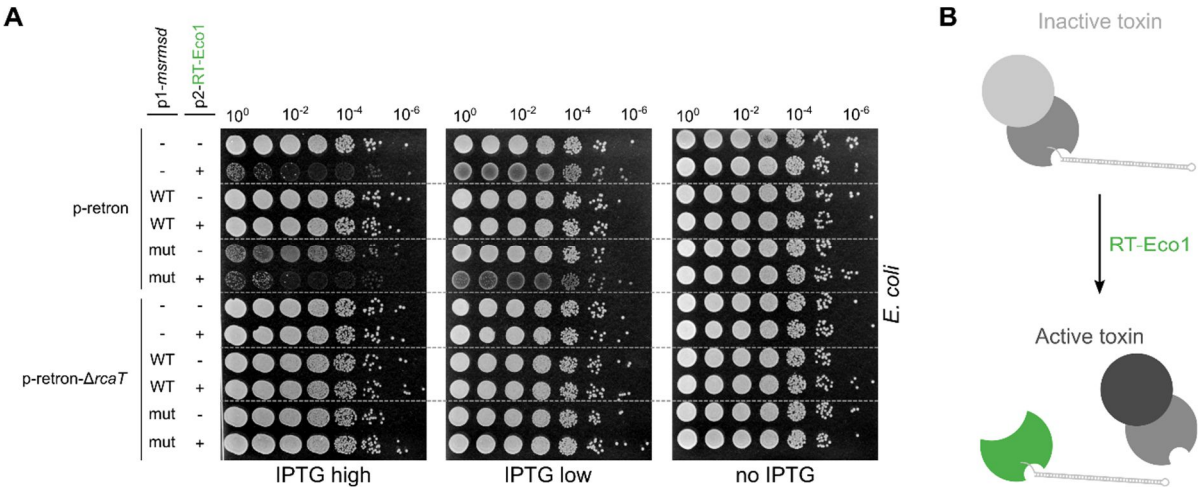

Figure 54. RT-Eco1 triggers Retron-Sen2 by sequestering its msDNA.

(A) Overexpressing msDNA alleviates RT-Eco1 triggering. *E. coli* BW25113 strains carrying combinations of plasmids p-retron or p-retron-Δ*rcaT*, p1-*msrmsd*^{WT} or p1-*msrmsd*^{mut}, p2-RT-Eco1, and empty vectors, were grown for 5-6 hours in antibiotics-LB/37°C, serially diluted, and spotted on antibiotics-LB plate with arabinose, and no, low, or high IPTG concentrations. Plates were incubated at 37°C. Representative results shown of two independent experiments.

(B) Model of RT-Eco1-mediated triggering. RT-Eco1 (green) binds and sequesters msDNA-Sen2 away from its cognate RT-Sen2, and activates RcaT.

4.7. Chapter 4 summary.

- Several phage-related genes can exogenously trigger or block toxicity originating from the Retron-Sen2 TA system. This suggests that retrons respond during phage infection by interacting with specific phage products.

- RcaT toxicity can be triggered through various proteins directly methylating, degrading, or titrating the msDNA-Sen2 in the RT-msDNA antitoxin-complex.

5. Genetic approaches to find the target of RcaT.

The toxins of TA systems can inhibit bacterial growth by targeting diverse essential cellular pathways (1.2). Although I utilized the toxicity of RcaT to understand the function of Retron-Sen2, the cellular target of RcaT remains to be identified. RcaT has no readily-identifiable domains, which makes it hard to design hypothesis-driven experiments to find its target. Thus, in trying to find its target, I opted to use largely-unbiased genetic approaches.

In Chapter 5

- I found that genes involved in RNA-metabolism are involved in RcaT-mediated cold-sensitivity in *S*Tm.
- I found gene-deletions that modulate RcaT-overexpression toxicity in *E. coli*, which acted analogously in *S*Tm.
- I designed a genetic approach to enrich for RcaT-suppressing mutations related to the target of RcaT, rather than for mutations directly inactivating RcaT.

5.1. Deleting RNA-related genes alleviates RcaT toxicity.

Activated RcaT in *S*Tm inhibits growth specifically in lower temperatures (Figure 8), suggesting that RcaT attacks a process necessary for bacterial growth in cold. Bacteria adapt to cold using multiple pathways, encoded by a multitude of genes (Inouye and Phadtare, 2008; Barria *et al.*, 2013). In order to link RcaT toxicity with specific cold-adaptation pathways, I searched for epistasis between RcaT-mediated cold-sensitivity (Δ*rrtT*) and deletions of cold-related genes in *S*Tm. If RcaT toxicity was linked to a certain pathway affected by geneX, epistatic genetic interactions should occur in double deletion mutants Δ*rrtT* ΔgeneX. Through P22 transduction, I combined 33 gene-deletions (Table 3) with Δ*rrtT*, and profiled the growth of all single and double mutants in lowering temperatures on plates. I selected these genes based on (1) literature connecting them to the cold-shock response, and, (2) on their respective deletion mutants having a fitness defect in lower temperatures (Pfalz, 2017).

Table 3. Genes tested for epistatic interactions with Δ*rrtT*.

Gene name	STM gene name	*S* score (room temp.)[1]	Function
bipA	STM14_4822	-11	Ribosome-binding GTPase, necessary for growth in cold.
cspA	STM14_4399	0	Cold shock protein A, RNA chaperone upregulated in cold.
cspB	STM14_2420	0	Cold shock-like protein.
cspC	STM14_2220	-1	Cold shock-like protein.
cspE	STM14_0732	-1	Cold shock-like protein.
dbpA	STM14_2001	0	RNA helicase, late-stage biogenesis of 50S ribosome.
deaD	STM14_3962	-12	DEAD-box RNA helicase, assists degrading RNA in cold.
hfq	STM14_5242	-1	Global RNA-binding protein, affects small RNA function.
nlpI	STM14_3963	-5	Lipoprotein, regulates peptidoglycan hydrolases.
pnp	STM14_3964	-3	PNPase, member of the RNA degradosome.
ppdC	STM14_3612	0	Unknown function (negative control).
recF	STM14_4629	-6	Involved in RecA-mediated recombination.
rhlB	STM14_4712	-1	RNA-helicase, member of the RNA degradosome.
rhlE	STM14_0951	0	DEAD-box RNA helicase.
rimI	STM14_5476	-6	Alanine acetyltransferase of ribosomal protein S18.
rluC	STM14_1359	-1	rRNA pseudouridine synthase, affects Δ*bipA* cold sens.
rnd	STM14_2196	0	Ribonuclease D, tRNA maturation.
rnr	STM14_5250	-1	Ribonuclease R, mRNA, rRNA, and tRNA maturation.
rodZ	STM14_3095	-6	Cell shape maintenance.
secB	STM14_4461	-5	Protein chaperone involved in SecYEG protein export.
secG	STM14_3976	0	Member of the SecYEG preprotein translocase.
smpB	STM14_3294	0	Component of trans-translation.
srmB	STM14_3240	-8	DEAD-box RNA helicase, biogenesis of 50S ribosome.
tig	STM14_0529	-1	Protein chaperone, alleviates Δ*secB* cold sensitivity.
xseA	STM14_3077	-18	Exonuclease VII, large subunit.
ycaR	STM14_1116	-9	Unknown function (deletion cold sensitive).
yggX	STM14_3756	-8	Unknown function (deletion cold sensitive).
yifL	STM14_4747	-8	Unknown function (deletion cold sensitive).
yjgA	STM14_5328	-10	Unknown function (deletion cold sensitive).
yrdD	STM14_4106	-10	Putative DNA topoisomerase (deletion cold sensitive).
-	STM14_3826	-6	Unknown function (deletion cold sensitive).
-	STM14_4069	-8	Unknown function (deletion cold sensitive).
-	STM14_5071	-4	Unknown function (deletion cold sensitive).

[1] *S* scores <-3 denote deletion strains impaired in growing in LB at room temperature (Pfalz, 2017).

In order to be able to assess the presence of epistatic interactions, I arrayed colonies of the various strains on plates, and quantified their fitness in lower temperatures. The Δ*rrtT* cold-sensitivity phenotype was partially alleviated upon deleting genes encoding ribonuclease R (*rnr*), ribonuclease D (*rnd*), or a non-coding RNA chaperone (*hfq*) (Figure 55A). The remaining gene deletions did not exhibit epistatic interactions with Δ*rrtT* (data not shown). The triple deletion mutant Δ*rrtT* Δ*rnr* Δ*rnd* was equally alleviating to Δ*rrtT* Δ*rnr*/Δ*rnd* double mutants, while the Δ*rrtT* Δ*rnr* Δ*hfq* was more alleviating (Figure 55B). This suggests that deleting ribonuclease R or D alleviate RcaT toxicity through the same pathway, while deleting Hfq acts through a different pathway. The epistatic effects were also reproduced with targeted spot growth-assays (Figure 55C). Thus, deleting genes involved in intracellular RNA metabolism (RNase R and D), or small RNA function (Hfq) partially alleviates RcaT toxicity.

I did not follow up on the epistatic effects of these RNA-metabolism genes on RcaT toxicity for two reasons. First, although RNAses R/D and Hfq are certainly involved in RNA-related functions, all three of them have multiple cellular RNA targets (Table 3). This makes it difficult to make connections to any specific RNA-targets. Second, the alleviating effect of all three gene-deletions was only partial. Partial phenotypes complicate genetic analyses, which usually depend on growth/non-growth selection magnitudes in order to be successful. Nevertheless, these findings suggest that the cellular target of RcaT is an RNA-molecule, potentially upregulated when *rnr*/*rnd*/*hfq* are deleted, which might be leading to the observed partial buffering phenotypic effects.

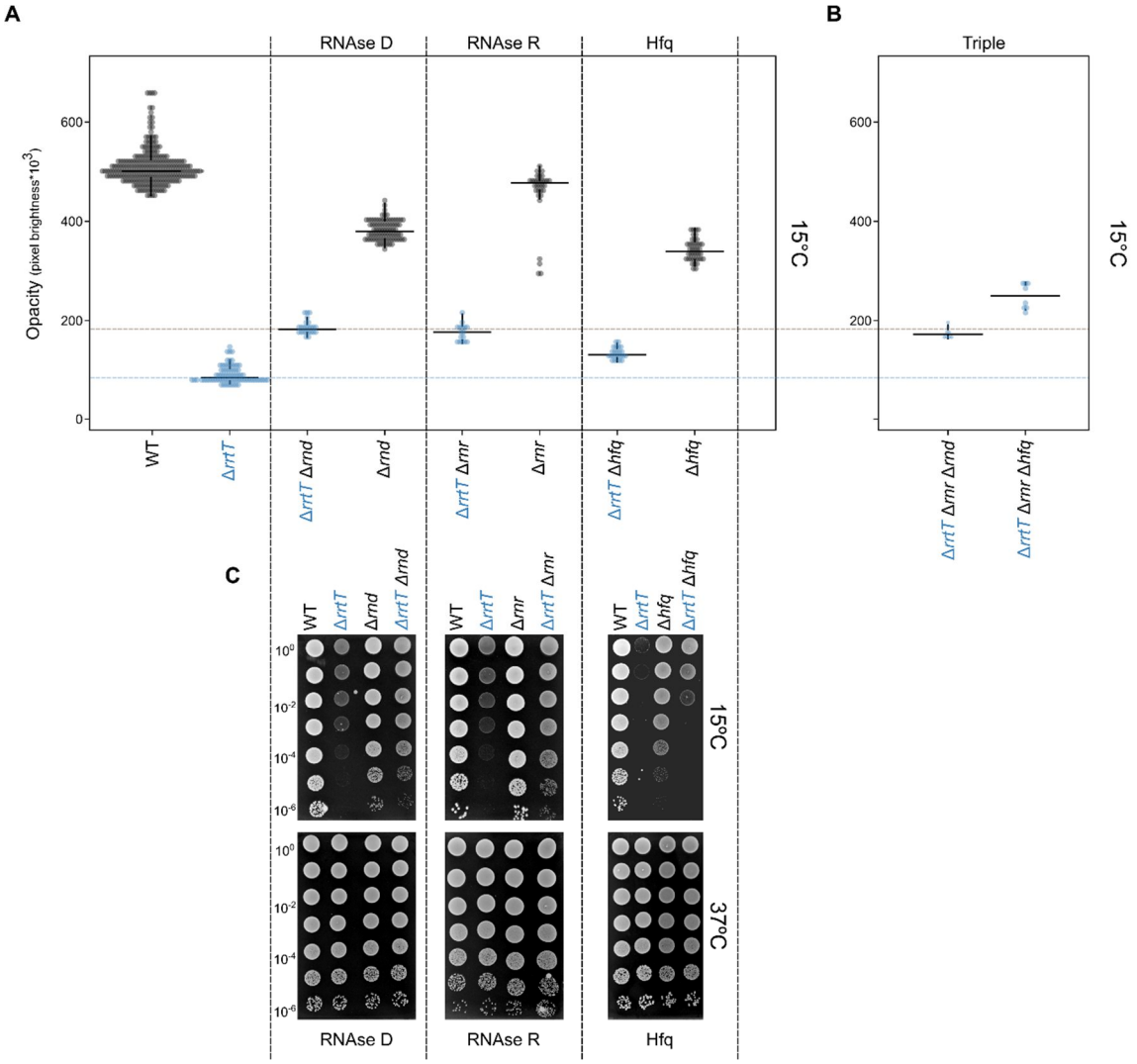

Figure 55. Deleting RNAse R, D, or Hfq alleviates RcaT cold-sensitivity.

(A) Epistatic interactions in *rnd*, *rnr*, *hfq* deletions with Δ*rrtT* (colony assays). Genes *rnd*, *rnr*, or *hfq* were deleted in *S*Tm wildtype or Δ*rrtT* strains. Resultant strains were pinned on LB plates, and plates were incubated at 15°C. Colony integral opacities were quantified, and the raw values are plotted. WT (*n* = 260; 65 biological * 4 technical replicates), Δ*rrtT* (*n* = 76; 19 biological * 4 technical replicates), Δ*rnd* (*n* = 84; 21 biological * 4 technical replicates), Δ*rnr* (*n* = 36; 9 biological * 4 technical replicates), Δ*hfq* (*n* = 40; 10 biological * 4 technical replicates) Δ*rrtT* Δ*rnd* (*n* = 24; 6 biological * 4 technical replicates), Δ*rrtT* Δ*rnr* (*n* = *16*; 4 biological * 4 technical replicates), and Δ*rrtT* Δ*hfq* (*n* = 24; 6 biological * 4 technical replicates). Horizontal bars denote the average colony opacity value per strain, and error bars denote standard deviation. Blue horizontal bar denotes the average colony opacity value of Δ*rrtT*, and the gray bar of Δ*rrtT* Δ*rnd*.

(B) Δ*rnd* and Δ*rnr* alleviate RcaT through the same pathway. Procedure as described in panel **A**. Triple mutants (*n* = 8; 2 biological * 4 technical replicates).

(C) Epistatic interactions in *rnd*, *rnr*, *hfq* deletions with Δ*rrtT* (spot assays). Same strains as in panel **A** were grown for 5-6 hours in LB/37°C, serially diluted, and spotted on LB plates. Plates were incubated at 15°C or 37°C. Representative results shown from three independent experiments.

5.2. Genome-wide RcaT toxicity screen in *E. coli* to find RcaT target.

Deleting non-essential genes in *S*Tm alleviates RcaT toxicity (Figure 55), which could provide indirect cues to find the molecular target of RcaT. To systematically identify RcaT-alleviating non-essential gene deletions, I induced RcaT in *E. coli* strains of the Keio single-gene deletion library (Baba *et al.*, 2006). Since expressing RcaT is toxic in *E. coli* (Figure 16), gene knockouts alleviating RcaT toxicity should grow better than average. I could then simply identify the alleviating deletions, by quantifying their fitness while inducing RcaT. Indeed, many *E. coli* single-gene deletion strains were partially protected from RcaT toxicity (Figure 56).

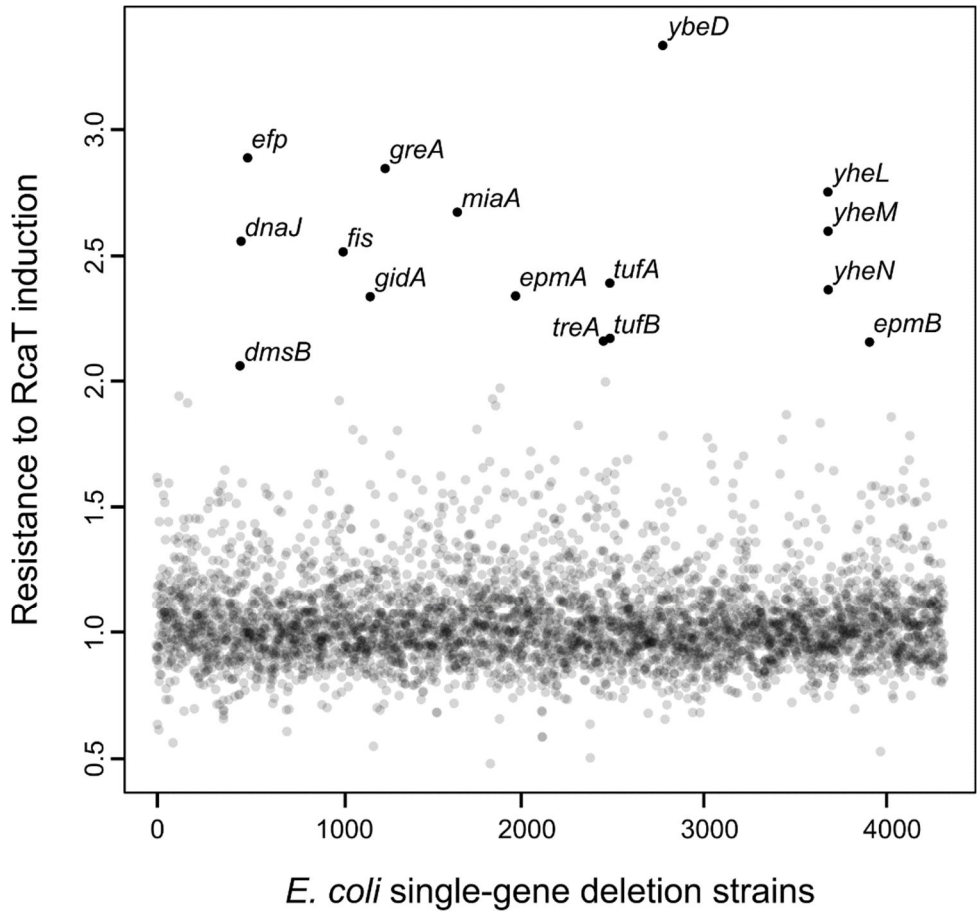

Figure 56. RcaT induction in deletion libraries identifies RcaT-alleviating gene deletions. Plasmid p-*rcaT* was conjugated in the Keio library (Baba *et al.*, 2006), and transconjugants were pinned on spectinomycin-LB plates with or without arabinose. Plates were incubated at 37°C. For every strain, per plate (n = 2) normalized colony integral opacities were quantified. Mean opacity values were calculated for the two biological clones within the Keio library. These values from (strain X in plates with no arabinose) were divided by the values from (strain X in plates with arabinose), to produce a score that increases with increased resistance towards RcaT induction. On the y-axis, the mean value of two such ratios are presented per strain. X-axis represents the *E. coli* gene deletion strains of the Keio library.

Notably, deleting translation factor EF-P (Δ*efp*), or genes affecting EF-P activity (Δ*epmA*/Δ*epmB*), alleviated RcaT toxicity. Furthermore, deleting tRNA modifying enzymes (Δ*miaA*, Δ*yheL*, Δ*yheM*, Δ*yheN*), or even genes of unknown function (Δ*ybeD*), also led to resistance against RcaT. Since many of these genes were involved in translation, RcaT toxicity could be connected to inhibiting protein synthesis. To validate these findings from *E. coli*, I deleted the orthologous genes in *S*Tm and tested whether they alleviate RcaT-mediated cold sensitivity. Indeed, deleting *efp*, *ybeD*, *miaA*, or *epmA*, partially alleviated the cold sensitivity phenotype arising from Δ*msrmsd* (Figure 57). Thus, RcaT-alleviating gene deletions identified in *E. coli*, also alleviate RcaT-mediated cold sensitivity in *S*Tm.

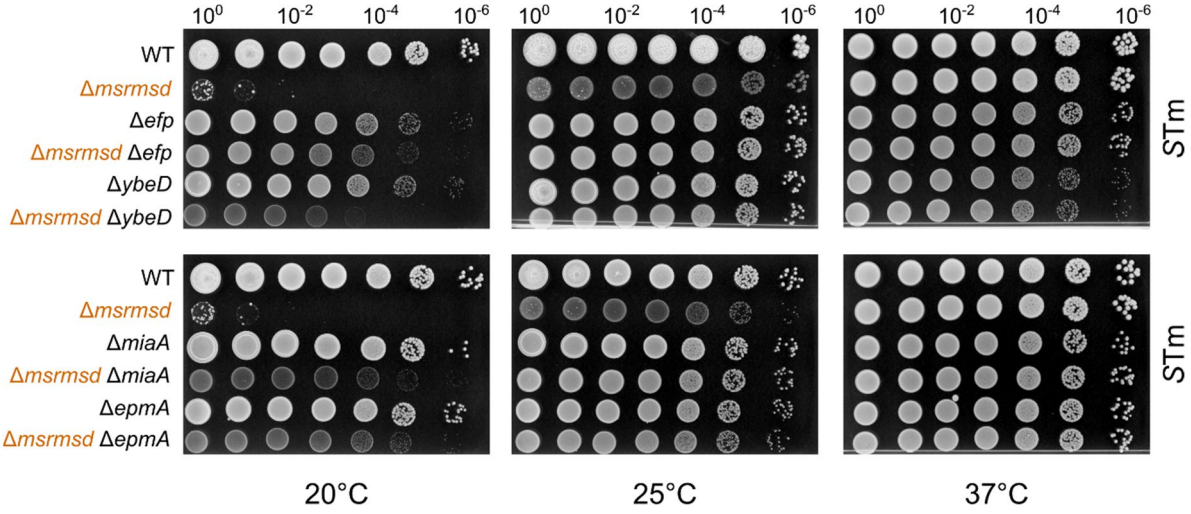

Figure 57. Gene deletions identified in *E. coli* alleviate RcaT-mediated cold-sensitivity in *S*Tm. Genes *efp*, *ybeD*, *miaA*, and *epmA* were deleted in *S*Tm wildtype and Δ*msrmsd* strains. Resultant strains were grown for 5-6 hours in LB/37°C, serially diluted, and spotted on LB plates. Plates were incubated at 20°C, 25°C, or 37°C.

EF-P promotes the translational rate of proteins containing polyproline stretches (Doerfel *et al.*, 2013; Ude *et al.*, 2013), and MiaA affects expression of certain proteins by modifying tRNAs (Thompson and Gottesman, 2014). Therefore, instead of RcaT targeting translation through these factors, it is instead possible that they are necessary for RcaT expression. The cold sensitivity alleviation could be explained if RcaT protein levels are downregulated in the absence of these genes. Indeed, RcaT protein levels were decreased upon deleting *efp*, *ybeD*, *miaA*, or *epmA* (Figure 58). This suggests that these genes are not related to the target of RcaT, but rather affect

its translation rates. These observations can be plausibly explained for EF-P, since RcaT has a motif with two prolines, but it is less clear how MiaA and YbeD affect RcaT translation. In contrast, previously identified RcaT-alleviating gene deletions of RNases D and R (Figure 55) do not downregulate RcaT protein levels (Figure 58), suggesting that these are related to the target of RcaT. Thus, the RcaT toxicity screen in the *E. coli* knockout library preferentially identifies factors needed for translating RcaT, instead of pathways related to the mode of action of RcaT.

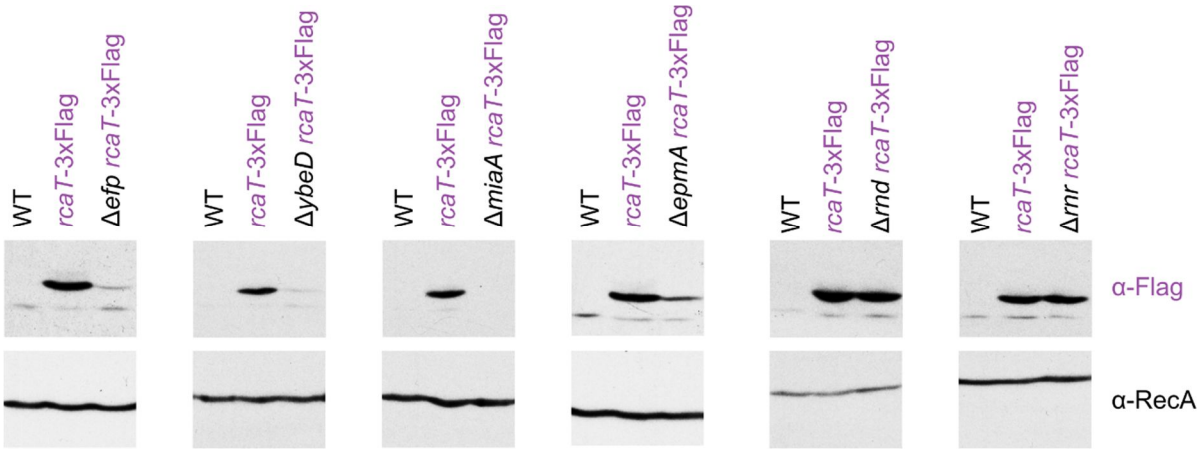

Figure 58. Deleting *efp*, *ybeD*, *miaA*, and *epmA* downregulates RcaT in *S*Tm. Genes *efp*, *ybeD*, *miaA*, and *epmA* were deleted in *S*Tm wildtype and *rcaT*-3xFlag tagged strains. These strains, along with *S*Tm wildtype, were grown until OD_{595} = 0.4-0.6 in LB/37°C, lysed, and proteins were separated by SDS-PAGE and immunoblotted against RcaT. RecA protein levels were used as a loading control.

5.3. Selection of target-related RcaT suppressors by phage transduction.

I originally identified RcaT by isolating spontaneous suppressor mutants of retron antitoxin deletion strains in cold (Figure 13). The same approach could be used, in principle, to find mutations related to the target of RcaT. Previously, I sequenced 29 suppressor strains, and all of them contained mutations either inactivating or downregulating RcaT (Figure 13). Thus, without counter-selecting for RcaT mutations, it is unlikely to find suppressors related to the target of RcaT.

To enrich for RcaT target-related mutants, I triaged RcaT suppressors by transducing back the wildtype RcaT sequence by phage transduction (Figure 59). First, I isolated spontaneous suppressors of a Δ*xseA* *S*Tm strain at 15°C. Most alleviating mutations would map on RcaT (toxin loss of function mutations), and only few could occur in

distant genomic loci (target-related mutations). After pooling the suppressors together, I transduced the Δ*msrmsd* RcaT-3xFlag sequence to all of them, flanked by a kanamycin and chloramphenicol resistance genes (Figure 59). Phage P22 transfers a maximum of 48 kb of DNA from donor to target strains (Ebel-Tsipis *et al.*, 1972). Transductants were then selected on kanamycin-chloramphenicol plates at 15°C, and the only strains able to grow under these conditions, were those that (1) carried kanamycin and chloramphenicol resistance cassettes (i.e., carry wildtype 3xFlag-tagged *rcaT*), and, (2) could grow in the presence of active RcaT (i.e., carry target-related mutations in genetic loci away from Retron-Sen2; Figure 59). Through this approach I isolated five potential RcaT target-related suppressors, which I have not sequenced yet. To exclude mutations that affect RcaT expression, RcaT-3xFlag levels can be assessed in the suppressors by immunoblotting. Overall, I present here an easy genetic approach to distinguish toxin-target mutations from trivial toxin-inactivating mutations.

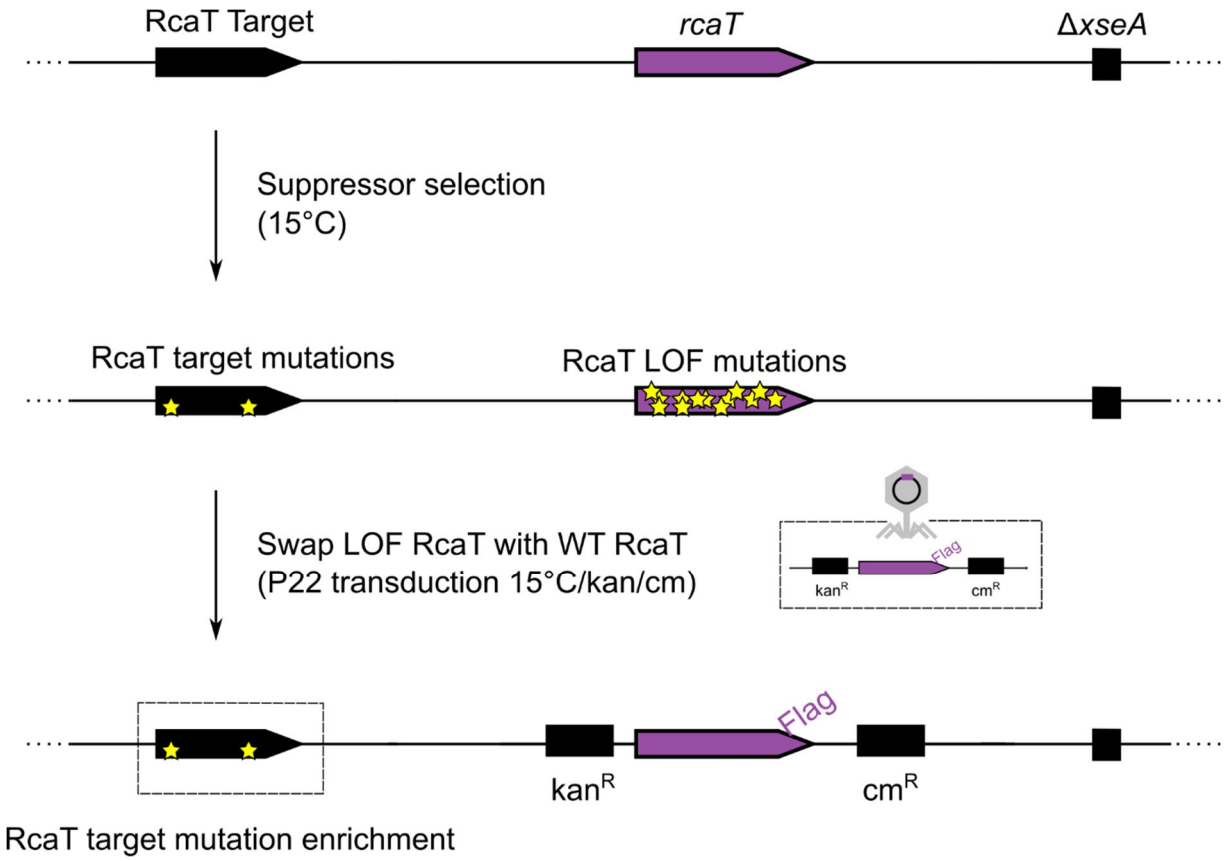

Figure 59. A strategy to isolate suppressing mutations related to the target of RcaT. Mutations suppressing RcaT-mediated cold-sensitivity are denoted with golden stars. This genetic strategy would not work if the loci amassing suppressor mutations are genetically linked (<20 kb) to Retron-Sen2.

5.4. Chapter 5 summary.

- Deleting RNAse D, RNAse R, or Hfq partially alleviates the RcaT-mediated cold-sensitivity in *S*Tm.

- Screening gene-deletion libraries for RcaT resistance yielded many genes that regulate the expression of RcaT in *S*Tm.

- Phage transduction can be used to select spontaneous suppressing mutations that are connected to the cellular target of RcaT.

6. Discussion

6.1. Retron-Sen2 is the prototypical member of a new toxin/antitoxin type.

The biological function of bacterial retrons remained an enigma for thirty years. By starting from a retron-dependent phenotype in *Salmonella enterica* ser. Typhimurium (*S*Tm), I discovered that Retron-Sen2 is a novel tripartite toxin/antitoxin system (TA). The toxin RcaT is inhibited by protein-protein interactions with its bipartite antitoxin, the RT-msDNA protein-DNA complex (Figure 33).

6.1.1. Retron-TAs represent a novel type of toxin/antitoxin systems.

Retron-TAs are substantially different from other TA systems. The msDNA is the key feature separating retron-TAs from all other known TA systems. Although protein- or RNA-antitoxins have been described before (Figure 4), retron-TAs are the first example where an extrachromosomal DNA (msDNA) is a functional part of an antitoxin. Furthermore, the msDNA is not only produced by the RT, but goes through a complex maturation process by two host enzymes (RNAse H and Exo VII; Figure 3). The msDNA maturation is essential for antitoxin activity, since RNAse H or Exo VII mutations elicit RcaT toxicity in *S*Tm (Figure 8) or in *E. coli* (Figure 18C). No other TA system has been shown to require the action of host enzymes to support a functional antitoxin. Even disregarding the added complexity of host enzymes, almost all known TA systems are bipartite (toxin/antitoxin) (Harms *et al.*, 2018), while retron-TAs are tripartite (RcaT/RT-msDNA). Thus, retron-TAs are unique among TA systems, consisting a novel type of their own.

6.1.2. Retron-TAs display similarities to known toxin/antitoxin systems.

Retron-TAs are similar to type II TA systems. Antitoxins of type II systems inhibit their toxins by directly binding them (Figure 4) (Page and Peti, 2016). For instance, toxin CcdB of the *ccdB*/*ccdA* TA system is inactivated by forming a protein complex with its CcdA antitoxin (Maki *et al.*, 1996). Analogously, toxin RcaT of Retron-Sen2 also forms a protein complex with its cognate RT (Figure 26), although the RT-RcaT interaction by itself is not sufficient to inhibit RcaT. Similarly to type II TAs, where antitoxins specifically inhibit only their cognate toxins (Wilbaux *et al.*, 2007), only the toxicity of cognate RT-RcaT pairs can be inhibited by concomitant msDNA production (Figure 32). This suggests that the retron-RTs can only bind their cognate RcaT toxins, which

determines the antitoxin specificity. Remarkably, similar to the RT-msDNA interaction of retron-TAs, the antitoxins of type II TA systems also bind DNA. It has been long known that type II toxin/antitoxin complexes (e.g., CcdB/CcdA) autoregulate their transcription by binding their own DNA promoters (de Feyter *et al.*, 1989). For instance, although the C-terminus of the antitoxin CcdA is enough to bind and neutralize the toxin CcdB (Bernard and Couturier, 1991), the CcdA-CcdB complex also binds the *ccdB*/*ccdA* promoter through a DNA-binding domain at the N-terminus of CcdA, and inhibits the transcription of the TA operon (Afif *et al.*, 2001). This transcriptional autoregulation phenomenon has been observed in multiple type II TAs (Johnson *et al.*, 1996; Magnuson and Yarmolinsky, 1998; Monti *et al.*, 2007; Overgaard *et al.*, 2008). In contrast to retron-TAs, the antitoxin-DNA interaction of type II TAs is not involved in inactivating the toxin, since breaking the antitoxin-DNA interactions upregulates, but does not activate the toxins (LeRoux *et al.*, 2020). Since type II TAs are not homologous to retrons, the antitoxin-DNA interaction seems to have evolved independently in the two systems. Overall, although retron-TAs are distinct from all other TAs, their antitoxicity mechanism has analogies to that of type II TAs.

6.1.3. Outstanding questions to be addressed on the retron-TA mechanism.

I resolved several aspects of the retron-TA mechanism, but there are still outstanding questions to be addressed.

- First, since the msDNA does not mediate the RT-RcaT interaction (Figure 27), it is not clear how msDNA enables the antitoxin activity by binding the RT (Figure 30). It is possible that RcaT also binds the msDNA as part of the tripartite complex. This RcaT-msDNA interaction could itself inhibit RcaT, with the msDNA being brought in close-enough proximity to RcaT through the RT-RcaT interaction. Alternatively, when the msDNA is bound to the RT, it could be altering its structure in such a way as to enable the antitoxin activity against RcaT.

- Second, it is still unclear where the msDNA binds the RT, as well as which domain of the RT interacts with which domain of RcaT. Since non-cognate msDNAs can inhibit cognate RT-RcaT pairs (Figure 32), it is likely that different RTs can bind multiple msDNAs (as long as they can produce them). On the other hand, since

non-cognate RT-RcaT pairs cannot form functional antitoxins (Figure 32), the interaction surface between RT-RcaT should vary across retrons. Thus, the antitoxicity mechanism of RT-msDNA, and the specific RT/RcaT domains that enact the relevant interactions, remain to be elucidated.

6.1.4. RcaT displays atypical and recurring features with other toxins.

The RcaT toxin also displays similarities and distinct features to other toxins. Notably, RcaT exhibits the unusual feature of inhibiting growth more efficiently in specific growth conditions – cold temperatures (Figure 8) and anaerobic conditions (Figure 9). In cells growing aerobically at 37°C, RcaT is only toxic when overexpressed (Figure 16). In contrast, toxins of most well-studied TA systems usually inhibit growth irrespectively of growth conditions. In fact, this property renders antitoxins essential genes, which has been used in the past to screen for novel TA systems (Sberro *et al.*, 2013). Nevertheless, a type II TA system of *Pseudomonas putida* named GraT/GraA encodes a similar-acting toxin to RcaT. Although GraT shares no homology with RcaT, it also inhibits growth of *P. putida* specifically in colder temperatures (Tamman *et al.*, 2014). The GraT toxin belongs to the family of RelE/HigB toxins (Pandey and Gerdes, 2005), which are mRNA-targeting ribonucleases (Pedersen *et al.*, 2003). In accordance, GraT was also recently shown to be a ribonuclease (Talavera *et al.*, 2019), although its RNA targets, and why it preferentially inhibits bacterial growth in cold, remain to be investigated. At present, the cellular target of RcaT is unclear, but its shared conditional activity with GraT raises the hypothesis that it might be also a ribonuclease. Supporting this notion, deletions in RNA-related genes partially alleviate the RcaT-mediated cold-sensitivity in *S*Tm (Figure 55). Finally, RcaT is unique in also inhibiting bacterial growth specifically in anaerobic conditions, a conditional phenotype that has not been reported for any other toxin. Therefore, RcaT could also have a distinct cellular target compared to known toxins. Thus, RcaT displays unique and shared features among other toxins, and its activity and cellular targets await to be elucidated.

6.2. TIC/TAC; retron-TA mechanism to biological function, and back.

Understanding the mechanism through which a TA system operates does not help in finding its physiological function. TA systems can be beneficial for their hosts, insofar as they can be activated to inhibit bacterial growth under certain conditions. The holy grail of the TA field has been to find these activating conditions, and to mechanistically understand how TAs are triggered. I found both the activating conditions and triggering mechanisms of Retron-Sen2 by developing a simple reverse genetics approach, which I call Toxin Inhibition/Activation Conjugation (TIC/TAC) (Figure 34). Importantly, TIC/TAC can be used to do the same for any TA system.

6.2.1. TIC/TAC can be applied to virtually any TA system.

TIC/TAC employs systematic single-gene overexpression libraries to find molecular blockers (gene products inhibiting the toxin activity) and triggers (gene products that activate the toxin, when the antitoxin is present). As genes are artificially overexpressed, TIC/TAC can identify the role of genes that are normally repressed in standard growth conditions. Although overexpression libraries from any organism may be used, the advantage of using *E. coli* overexpression libraries lies on the extensive functional characterization of the *E. coli* genes (Keseler *et al.*, 2017), which facilitates mechanistic studies on potential hits. The only requirement to apply TIC/TAC is for the TA system to be functional in *E. coli* (i.e., toxin overexpression inhibits growth, and toxin/antitoxin overexpression inhibits the toxin). Since *E. coli* is the workhorse of molecular biology, the function of diverse TA systems from various phyla is routinely assessed in *E. coli* (Blower *et al.*, 2012; Sberro *et al.*, 2013; Kato *et al.*, 2019; Jimmy *et al.*, 2020). Thus, TIC/TAC can be applied to find blockers/triggers for the majority of known TA systems, which could potentially provide hints for their biological function.

6.2.2. The biological function of retrons is to respond against phage attack.

By applying TIC/TAC to Retron-Sen2, I found multiple triggers (Table 1) and blockers (Table 2) of diverse functions. Many hits, especially the strongest ones, were related to phages or were even prophage genes themselves. Bacteria are under constant attack by bacteriophages, which do not always lyse their prey, but can also become latent prophages, by integrating their genomes into bacterial genomes (Harrison and Brockhurst, 2017). Phage-related and prophage genes (*dam*, *recE*, RT-Eco1,

B21_00839, *ymfH*, *tfaP*) encoded proteins that acted as Retron-Sen2 triggers (p = 0.01, fold enrichment = 3.6 among hits), indicating that the condition where RcaT inhibits growth may be when phages infect bacteria. The active toxin would then inhibit the growth of the phage-infected bacterium, which would stop the phage propagation at the site of infection. This suggested that the biological function of retron-TAs is to defend against phages through abortive infection (Abi; Figure 6). Accordingly, prophage genes (*racC*, *dicC*, *ydaW*, *yfjH*, *yjhC*) also encoded proteins that acted as RcaT blockers (p = 0.005, fold enrichment = 5.3 among hits), suggesting that phages defend against retrons by encoding products that directly inhibit the retron-toxins. Thus, retron-TAs are triggered and blocked by specific phage products, hinting that their biological function is to act as Abi systems against phages.

6.2.3. Retron triggers are phage blockers against early anti-phage systems.

Phage-related Retron-Sen2 triggers, such as Dam and RecE, have been shown to inhibit early anti-phage defense systems. Restriction-Modification (R-M) and CRISPR-Cas systems, are termed “early” phage-defense systems, since they attack the DNA of the incoming phages upon entry (Deveau *et al.*, 2010; Vasu and Nagaraja, 2013). For instance, R-M systems usually have two genes, and act similarly to TA systems (Mruk and Kobayashi, 2014); the R subunit cuts specific DNA sequences, while the M subunit modifies the same DNA sequences, protecting them against the R subunit. When unmodified phage DNA (or plasmid DNA) enters an R-M-containing cell, the R subunit cleaves the phage DNA, protecting the bacterium. In response to early anti-phage defenses, phages have evolved a stunning array of anti-restriction (Tock and Dryden, 2005) and anti-CRISPR mechanisms (Davidson *et al.*, 2020). Phages carry Dam methyltransferases in efforts to mimic the M subunit of type II R-M systems (Hattman, 1970). Furthermore, the phage-protein RecE counters type III R-M systems (Handa and Kobayashi, 2005), and a plasmid-homologue of RecE blocks both type I R-M and CRISPR-Cas systems (Roy *et al.*, 2020). I showed that Dam and RecE trigger Retron-Sen2 by directly methylating msDNA (Figure 46) or degrading msDNA (Figure 49). Thus, retron-TAs directly sense phage products meant to block early-defense systems, and stop the phage infection by inhibiting the growth of the phage-infected bacterium (Figure 60).

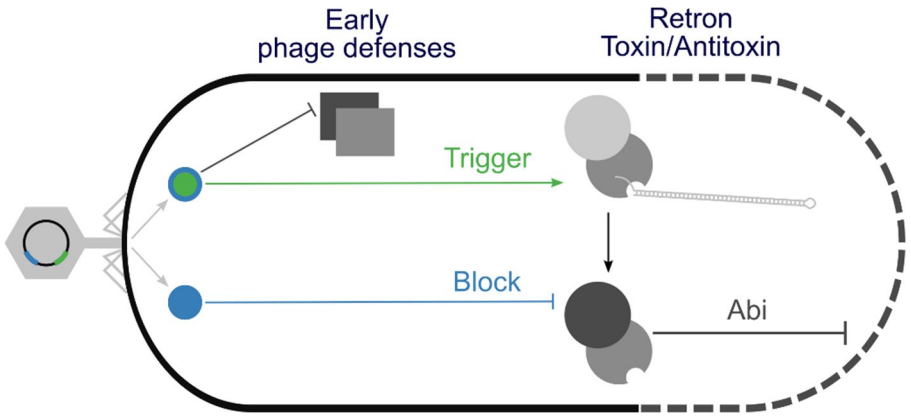

Figure 60. Retron-TAs defend bacteria against phages. Phages encode proteins that circumvent early phage-defense systems (green-blue circle; e.g., Dam, RecE). These phage proteins trigger retron-TA systems by inactivating their RT-msDNA antitoxins. Then, the activated retron-toxin (deep purple) inhibits the growth of the infected bacterium, which indirectly stops phage propagation (abortive infection; Abi). Therefore, phage proteins are simultaneously blockers for early phage-defenses, while being triggers of secondary Abi systems (hence green-blue color). As a response, phages also encode blocker proteins (blue circle; e.g., RacC, DicC), that directly inhibit the activity of retron-toxins.

6.2.4. The first example of blocker-trigger genetic linkage in phages.

While RecE triggers Retron-Sen2 (Figure 35), RacC blocks Retron-Sen2 (Figure 39). Notably, genes *recE* and *racC* are genetically linked in the Rac prophage (Figure 48), which means they were linked in the original phage as well. This example suggests that phages couple the expression of TA triggers with TA blockers for the same TA, in order to counter the detrimental effects of abortive infection. Bacterial anti-phage defense systems (e.g., R-M, CRISPR-Cas, Abi) are frequently clustered; a property that has been used to find novel defense systems (Doron *et al.*, 2018). On the flip side, the phage defence mechanisms against bacterial systems (anti-restriction, anti-CRISPR) were recently suggested to also cluster together in the phage genomes (Pinilla-Redondo *et al.*, 2020). Since these same phage defense mechanisms can trigger Abi systems (6.2.3), it is plausible that phages also cluster Abi-blockers in these phage defense islands. Thus, the *racC-recE* linkage represents the first example of a TA-blocker colocalizing with a TA-trigger in phage genomes.

6.2.5. How do non-phage-related proteins trigger and block Retron-Sen2?

Retron-Sen2 was triggered by overexpressing genes of the core genome of *E. coli* (i.e., not phage genes; Table 1). If retron-TAs are anti-phage abortive systems, why do these phage-unrelated core-genes activate Retron-Sen2?

- First, there are cases of core-genes, like *dam*, that have clear homologues in phage genomes (Murphy *et al.*, 2013). These cases can be explained due to having similar functions to their phage-counterparts. For instance, the Dam-homologue of phage P1 also triggers Retron-Sen2 (Figure 44). By analogy, a phage homologue of the *rdgC* core-gene that triggers Retron-Sen2 (Figure 37) is also found on the genome of phage P1, genetically linked to the phage-Dam homologue (Łobocka *et al.*, 2004).
- Second, RcaT is inhibited by the RT-msDNA through a complex mechanism, requiring both the RT-msDNA and the RT-RcaT interaction to remain intact (Figure 33). Overexpressing core-genes with DNA- or protein-binding capabilities might be non-specifically affecting the RT-msDNA/RT-RcaT interactions, and thus leading to antitoxin disruption. Supporting this, many core-genes that trigger Retron-Sen2 bind DNA (*betI*, *gcvR*, *bolA*) or are protein chaperones (*ecpE*, *slyD*, *secB*).
- Third, some core-proteins might be disrupting the msrmsd-RT-RcaT complex by differentially affecting the expression of msrmsd, RcaT, or RT. For example, a translation factor could trigger Retron-Sen2 if it upregulated RcaT over msrmsd/RT, or if it downregulated msrmsd/RT. Supporting this idea, there are triggers directly involved in the translation apparatus (*tufA*, *rplL*, *rplP*, *rplV*).

It is important to note that, although these core-genes trigger the overexpressed Retron-Sen2, only Dam could activate the endogenous Retron-Sen2 in *S*Tm (Figure 43). Overall, core-genes might be triggering Retron-Sen2 due to their similarity with phage genes, or by interacting non-specifically with the RT-msDNA antitoxin, but more work is needed to exclude or verify these hypotheses.

On the other side, RcaT was also blocked by overexpressing core-genes. It is intuitive that phages encode defense genes to inhibit RcaT-mediated Abi (e.g., RacC), but not why core-proteins would alleviate RcaT-toxicity (Table 2). First, some of these proteins

could be alleviating the toxicity of RcaT by being connected to its cellular target. Finding these potential proteins would be interesting, as the target of RcaT is unknown. For instance, the antitoxin ChpS of the *chpB*/*chpS* type II TA system is partially alleviating the toxicity of RcaT (Figure 41). Since ChpS binds and inhibits its cognate ChpB toxin (Masuda *et al.*, 1993), it is tempting to speculate that ChpS directly binds and inhibits RcaT. ChpB is a ribonuclease toxin, hinting again to RcaT being possibly also able to degrade RNAs. In support of this idea, overexpressing genes encoding tRNA modification factors (*tcdA*, *dtd*) alleviate the toxicity of RcaT (Figure 39). Finally, an additional tRNA-modification factor, TilS (Soma *et al.*, 2003), and an RNA-repair and tRNA-splicing protein, RtcB (Tanaka *et al.*, 2011), also alleviate RcaT toxicity when overexpressed (Figure 61), although both were not above the strict cut-off used for hit-calling (z-score cut-off 4, *tilS* z- score 3.9, *rtcB* z-score 3). Thus, combining these observations with complementing ones I made earlier (6.1.4), it is likely that RcaT is a ribonuclease that specifically targets and cleaves tRNAs. More work is needed to exclude or verify this hypothesis.

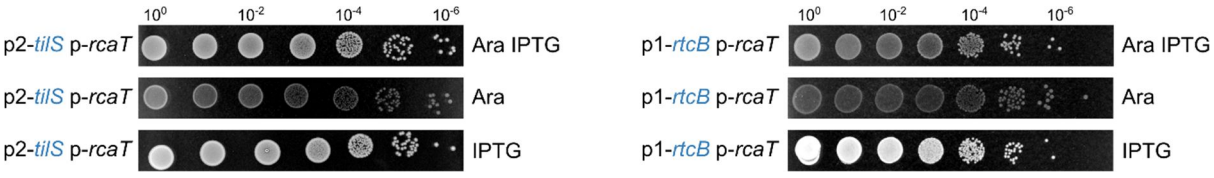

Figure 61. Genes involved in tRNA-modification or tRNA-repair alleviate RcaT toxicity. *E. coli* BW25113 carrying combinations of plasmids p-*rcaT*, p2-*tilS*, or p1-*rtcB* were grown for 5-6 hours in antibiotics-LB/37°C, serially diluted, and spotted on antibiotics-LB plates containing combinations of arabinose and IPTG. Plates were incubated overnight at 37°C.

A second group of core-proteins could be lowering the levels of RcaT or the conjugation efficiency during the TIC/TAC process. For instance, YdeA is an arabinose efflux exporter (Bost *et al.*, 1999), hence overexpressing it lowers the intracellular arabinose levels, on which the induction of the p-*rcaT* plasmid relies on. Similarly, it is intuitive that overexpressing protease adaptors (*clpA*, *clpX*) could also lead to increased RcaT degradation rates, which would alleviate RcaT-mediated toxicity. A different example is that of *dapA*; a metabolic gene involved in making precursors of diaminopimelic acid (DAP). Since the TransBac plasmid donor strains are DAP auxotrophs (Otsuka *et al.*, 2015), *dapA* would increase their overall growth, and thus increase the conjugation efficiency of these specific strains, potentially explaining its

blocking phenotype. Finally, there are also genes of unknown function that block the effect of RcaT. For example, the genetically linked orphan genes *yfbO* and *yfbN* both block RcaT (Figure 41). Interestingly, while *yfbO* blocks RcaT when overexpressed with high IPTG concentrations (Figure 42), it triggers Retron-Sen2 when overexpressed with low IPTG concentrations (Figure 37). More work is needed to understand these effects. In summary, core-proteins that block RcaT (1) might be connected to the target of RcaT, (2) might be affecting RcaT levels and/or aspects of the TIC/TAC procedure, and, (3) are involved in other undefined processes.

6.3. Recent studies confirm that retrons are anti-phage defense systems.

While our work was underway (Bobonis *et al.*, 2020a; Bobonis *et al.*, 2020b), two recent studies independently showed that retrons are indeed anti-phage defense systems (Gao *et al.*, 2020; Millman *et al.*, 2020). These two groups independently observed that RTs of various families (1.1) cluster frequently with anti-phage defense systems (e.g., R-M, CRISPR). Among these RTs there were also retrons, which when cloned and expressed conferred protection against diverse phage families (Gao *et al.*, 2020; Millman *et al.*, 2020). Confirming the hypothesis of this work (Figure 60), retrons defend against phages through abortive infection, by regulating their accessory genes (Millman *et al.*, 2020). It is tempting to speculate that the deep understanding of the Retron-Sen2 mechanism gained through my work (Figure 33) will be generalizable across all retrons; retron accessory proteins bind to their RTs, and the RT-msDNA complexes regulate them (Bobonis *et al.*, 2020a). These studies also exemplify the power of TIC/TAC in uncovering the biological function of TA systems only through their toxicity phenotype. TIC/TAC not only allowed me to assign a general biological function to retrons (i.e., systems that respond to phage infection), but also a specific role in being triggered by phage products meant to inhibit early anti-phage defenses (Figure 60) (Bobonis *et al.*, 2020b). Analogously, Retron-Eco6 [Ec48] which defends against multiple phages (λ, T2, T4, T5, T7) is triggered by specific phage proteins meant to inhibit the early phage defense system RecBCD (Millman *et al.*, 2020), through an unclear mechanism. Thus, my work combined with recent ones, unravel retrons as a novel class of prokaryotic anti-phage defense systems.

Incongruities between the studies may reflect differences in how retrons regulate their accessory proteins. In Retron-Sen2, abolishing the msDNA production activates the toxin RcaT, which inhibits bacterial growth (Figure 18). In contrast, inhibiting msDNA production in Retron-Eco1 [Ec86] (Gao *et al.*, 2020), Retron-Eco3 [Ec73], or Retron-Eco6 [Ec48] (Millman *et al.*, 2020), abolishes phage defense, but does not inhibit bacterial growth. These same systems have been shown to defend against phages through abortive infection (Millman *et al.*, 2020). This suggests that, unlike RcaT, the accessory proteins of other retrons require the presence of msDNA in order to exert their toxicity upon being triggered. Another difference is that, while Retron-Sen2 is activated by deleting Exonuclease VII (Figure 8), Retron-Eco6 is activated by deleting a different exonuclease, RecB (Millman *et al.*, 2020). Furthermore, a different study showed that an unnamed retron, with a similar accessory protein to Retron-Eco6, is activated by deleting yet another exonuclease, Exonuclease I (Rousset *et al.*, 2020). Overall, it seems that different retrons are translating the RT-msDNA (or accessory protein-msDNA) interaction differently, due to different msDNAs interacting with different host exonucleases. The apparent complexity of retrons (variations in RT-msDNA-Accessory structure, in msDNA sequence, or in the exonucleases associated with them) may allow them to easily evolve new ways to sense incoming phages.

Different retrons containing various accessory genes (Figure 2) exhibited markedly specific anti-phage specificities. For example, Retron-Eco1 [Ec86] only provided resistance against phage T5 in both studies (Gao *et al.*, 2020; Millman *et al.*, 2020), while one study reported Retron-Eco2 to protect only against phage T5, but not T2 (Millman *et al.*, 2020) and the other reported that Retron-Eco2 does protect against T2 (Gao *et al.*, 2020). Since these studies overexpress the retrons using different vectors, it is possible that incongruent phage specificities are partially driven by different retron expression levels. For instance, RexAB – the first Abi system ever described – is unable to abort phage T4 from its native expression levels, but aborts T4 when overexpressed (Shinedling *et al.*, 1987). On a different note, the native Retron-Sen2 in *S*Tm only inhibits bacterial growth in cold temperatures (Figure 8) and anaerobic conditions (Figure 9) (Elfenbein *et al.*, 2015). It is thus tempting to speculate that retrons only protect against phages under specific growth conditions. Finally, there are multiple retrons for which the phage-sensitivity is not known. For example, Retron-Sen2 did not defend against any tested phages (Millman *et al.*, 2020). This could be

due to phages carrying toxin-blockers (e.g., RacC), which can be major determinants of specifying whether they can counter specific retrons. Thus, more work is required to understand how retrons protect bacteria against phages in their native environment.

6.4. How are chromosomal-TAs triggered and why are they so many?

TA systems exert their biological function in conditions that trigger their growth inhibition ability. Plasmid TAs promote the fitness of their host plasmid by addicting its bacterial host to it (1.2.1), and are triggered by bacterial proteases that degrade their labile antitoxins faster than their toxins (Van Melderen *et al.*, 1994; Lehnherr and Yarmolinsky, 1995). Inspired by the plasmid TAs, chromosomal-TAs have been largely thought to be triggered by stress-induced host proteases that degrade their antitoxins (Muthuramalingam *et al.*, 2016). This has been supported by observing that chromosomal TA systems are transcriptionally upregulated in specific environmental conditions (e.g., starvation, heat, antibiotics) (Christensen *et al.*, 2001; Christensen *et al.*, 2004; Christensen-Dalsgaard *et al.*, 2010; Janssen *et al.*, 2015). Recently it has been shown that, proteases indeed mediate TA upregulation under stress, but they do not trigger growth inhibition by the toxin (LeRoux *et al.*, 2020). Upregulation does not equal triggering, since the proteases relieve the TA auto-regulation (6.1.2) by cleaving free antitoxins; but antitoxins bound to their toxins are resistant to proteases, and maintain their toxins inactive (LeRoux *et al.*, 2020). My work reveals for the first time how TA systems can be triggered. In the retron-TA, the RT-msDNA antitoxin is directly inactivated by triggers that methylate (Figure 46), degrade (Figure 49), or simply bind (Figure 54) its msDNA component. Thus, instead of TAs being triggered indirectly by a stress-induced bacterial system (e.g., proteases), TAs are triggered by specific products that directly inactivate their antitoxins.

The extravagant number of chromosomal-TAs per bacterial genome is also under debate (Van Melderen, 2010). Why would *Mycobacterium tuberculosis* need to have 88 type II TA systems? (Ramage *et al.*, 2009). Since TAs are “addictive”, it has been hypothesized that TAs are selfish systems that propagate in high numbers for their own benefit (Van Melderen and De Bast, 2009; Ramisetty and Santhosh, 2017; Rosendahl *et al.*, 2020). However, even mobile selfish systems like group II introns are only found two times per genome on average (Waldern *et al.*, 2020). By combining

multiple studies showing various TAs having anti-phage activity (1.2.1), it is tempting to speculate that chromosomal-TAs are mostly anti-phage abortive infection defense systems (Figure 6). The specificity of Retron-Sen2 triggers I identified here provides one potential reason for the high numbers of TAs per genome. Specifically, the Dam trigger can only activate retron-TAs that have a 5'-GATC-3' duplex in their msDNA (Figure 46). Analogously, RecE can only degrade msDNAs cleaved by Exonuclease VII (Figure 49), and most msDNAs are not recognized by Exonuclease VII. Therefore, multiple TAs per genome provides an advantage, since even TAs of the same type are likely activated by distinct phage triggers.

There is a simple explanation on why phages encode proteins that trigger TA systems. A phage needs to bypass all the early and all the abortive infection systems (including TA systems) to successfully infect a bacterium and propagate. From the bacterial side, the early anti-phage systems evolve in multiple ways to attack phages directly (R-M, CRISPR/Cas), and phages evolve numerous proteins to inactivate these early systems (anti-R-M, anti-CRISPR). These very same numerous phage proteins that inactivate the early systems, simultaneously trigger TA systems (e.g., Dam, RecE), and phages as a response encode different proteins to block the triggered TA systems (e.g., RacC) (Figure 60). Thus, bacteria encode TA systems to counter the early phage defenses directed against the bacterial early anti-phage defenses. It is also possible (even likely) that the TA blockers for one TA system are simultaneously triggers for another TA system. These would create an ever-expanding arms-race survival game; bacteria would need to encode an ever-increasing number of TAs to counter phages that try to bypass early anti-phage systems, and phages an ever-increasing number of TA blockers to bypass the TAs (Figure 62). A scenario like this explains both the high number of TAs in bacteria, and the vast number of uncharacterized small proteins in phage genomes. Thus, it is a brave new world for retrons and toxin/antitoxin systems and I am very much looking forward to see what comes next.

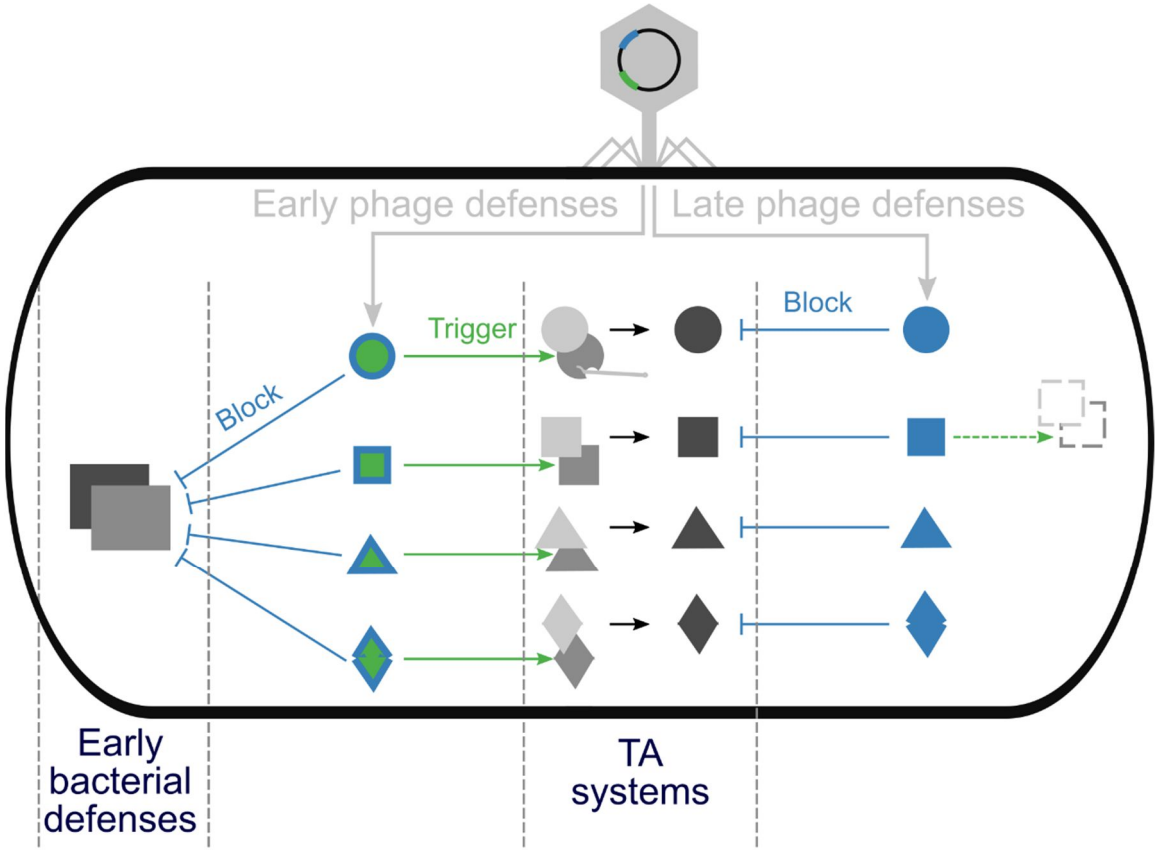

Figure 62. The arms-race between phages and toxin/antitoxin systems. Phages encode diverse proteins (early phage defenses; blue-green shapes) that block early-bacterial defenses (R-M, CRISPR/Cas), and these proteins simultaneously trigger toxin/antitoxin systems (TAs). Phages then encode blocker proteins (late phage defenses; blue shapes) to block the active toxins (in dark grey). Some TA-blockers are likely also triggering other TA systems (dotted green line), although this has not been shown thus far. This creates an ever-expanding arsenal of TA systems (in bacteria) to counter the early-phage defenses, as well as an ever-increasing diversity of TA-blocker genes (in phages) to counter the toxin/antitoxin systems.

7. Methods

7.1. Bacterial strains, plasmids, primers, and growth conditions.

- The genotypes of the bacterial strains, descriptions of plasmid construction, and primers used can be found in Tables S3-S6 in (Bobonis *et al.*, 2020a) and in Tables S3-S6 in (Bobonis *et al.*, 2020b).

- Bacteria were grown in Lysogeny Broth (LB; Tryptone 10 g/L, Yeast Extract 5 g/L, Sodium Chloride 5 g/L – Lennox formulation). LB-Agar plates (LB plates) were prepared by mixing liquid 2x-LB with separately autoclaved molten Agar (2% final concentration).

- All experiments involving strains carrying plasmids were conducted in the presence of the appropriate antibiotics, in order to maintain the plasmids. Strains carrying chromosomally-inserted antibiotic resistance markers were assayed in the absence of antibiotics, but streaked out from glycerol stocks on antibiotics-LB plates.

- Antibiotics were used in the following concentrations: Ampicillin (50 μg/mL), Tetracycline (10 μg/mL), Spectinomycin (100 μg/mL), Kanamycin (30 μg/mL) and Chloramphenicol (10 μg/mL for chromosomal cassettes or 20 μg/mL for plasmid-based markers). The growth of diaminopimelic acid (DAP) auxotrophic strains was supplemented with 0.3 mM DAP. Plasmids carrying inserts controlled by P_{BAD} promoters were induced with D-Arabinose (0.2%), while P_{tac} promoters were induced with low (0.1 mM) or high (1 mM) concentrations of isopropyl β-D-1-thiogalactopyranoside (IPTG). Inducers were only added when growth tests or other tests were conducted (i.e., Ara or IPTG were included in LB plates for spot tests, but not in the plates used for streaking-out the strains).

- Cold-sensitive strains (*S*Tm Retron-Sen2 antitoxin deletions) were freshly streaked-out from glycerol stocks, and kept only at 37°C before every experiment, in order to prevent suppressor mutations from arising. To assay growth in colder temperatures, strains were incubated on plates for 24 hours (25°C), 48 hours (20°C), or 72 hours (15°C).

7.2. Genetic techniques.

- Most gene-deletion strains of *Salmonella enterica* subsp. *enterica* ser. Typhimurium str. 14028s (*S*Tm) were acquired from the *S*Tm single-gene strain deletion library (Porwollik *et al.*, 2014). I deleted *S*Tm genes *rnhA*, *xseB*, *msrmsd*, and *araBAD* deleted through λ-red recombineering (Datsenko and Wanner, 2000), with primer sequences as described in Table S5 (Bobonis *et al.*, 2020a). *Escherichia coli* BW25113 (*E. coli*) deletion strains of genes *xseA*, *xseB*, and *rnhA* were acquired from the *E. coli* single-gene deletion library (Baba *et al.*, 2006).

- To remove secondary genomic mutations, I re-transduced every gene deletion (acquired from libraries or newly-made) in wildtype *S*Tm or *E. coli* strains by P22 or P1 transduction, respectively. To minimize polar effects originating from recombineering, I flipped out the antibiotic resistance cassettes from *S*Tm gene-deletion strains by using the yeast flippase-encoding pCP20 plasmid (Cherepanov and Wackernagel, 1995).

- I constructed double gene deletion strains by transducing antibiotic resistance cassettes (linked to a deleted locus) in deletion strains which already had the first resistance marker flipped out.

- Non-mobilizable plasmids were transformed in *E. coli* BW25113 or *E. coli* MFDpir strains through TSS (Chung *et al.*, 1989), and in *E. coli* BL21 or *S*Tm strains through electroporation (Chassy *et al.*, 1988). Mobilizable plasmids were introduced in strains through conjugation (7.4).

- Directed deletions in the *msd* region (Figure 15) were made in two stages. First, I designed and constructed the scarless *msd* deletions in plasmids. Second, I amplified the scarless deletions from the plasmids, and replaced the chromosomal *msd* locus with them through *ccdB*-recombineering (Wang *et al.*, 2014).

- The p-retron^{mut} plasmid (*msd*: GATC → GTTC; Figure 46) was constructed by mutating a source plasmid (p-retron^{WT}) through PCR mutagenesis by using a kit (NEB; Q5-Site-Directed Mutagenesis Kit, catalogue number: E0554S). Mutagenic primers used (JB433 and JB434) can be found in Table S6 of (Bobonis *et al.*, 2020b).

7.3. Spot growth tests.

1) Single bacterial colonies were inoculated in 2 mL LB and incubated aerobically at 37°C in a roller drum until the cultures reached their maximum yield (~6-7 hours, OD_{595}~5-6).

2) These cultures were then serially diluted eight times (in ten-fold steps). For this, I used a 96 deep-well plate containing 900 µL of LB in each well, and added 100 µL of the individual cultures in the wells of the top row (maximum 12 strains per deep-well). Next, by using a 12-span multi-channel pipette, I transferred 100 µL from the first row to the second row of the deep-well plate, and repeated this until the last row. It is important to change tips for every dilution step.

3) Next, I transferred 200 µL of all dilutions in a normal 96-well plate. To do this, I used the multi-channel pipette to transfer the diluted cultures starting from the bottom row of the 96 deep-well (more dilute) to the top row (more dense cultures), without changing tips between rows.

4) Subsequently, I used a 96-pinner (V&P Scientific, catalogue number: VP 404) to spot an equal volume (~10 µL) of the dilutions in the 96-well plate onto rectangular Singer LB-plates. To do this, I first sterilized the 96-pinner by bleaching it. Three glass tanks were filled with enough volume to cover the pins of the 96-pinner, containing either ten-fold diluted bleach solution (Sodium Hypochlorite, Sigma, catalogue number: 1056142500), or sterile/distilled water. The 96-pinner was dipped 8-10 times in bleach and subsequently washed twice by dipping it 8-10 times in the water tanks. Between each dipping-step, the pins were thoroughly dried on paper towels. Next, the pins were submerged in 100% isopropanol, and isopropanol was removed by flaming the 96-pinner over a Bunsen-burner. Finally, the 96-pinner was allowed to cool off on top of a sacrificial Singer LB-plate for 1 min, submerged in the 200 µL of the dilutions in the 96-well plate, and pinned on top of target LB-plates. For every target LB-plate, the pinner was repeatedly submerged in the dilutions before-hand.

5) The LB plates were incubated for appropriate times based on temperature, as described in 7.1.

7.4. Conjugation of mobilizable plasmids in target strains.

The steps for low-throughput plasmid conjugation reported here were described in (Bobonis *et al.*, 2020b).

1) Mobilizable plasmids were introduced in *E. coli* or *S*Tm strains through conjugation. Donor strains were either *E. coli* JA200 (Clarke and Carbon, 1976), *E. coli* BW28029 (Otsuka *et al.*, 2015), *E. coli* MFDpir (Ferrières *et al.*, 2010), or *E. coli* CAG60056 (BW25113 pseudoHfr::(*trp bla* (-))). The donor selected depends on the *oriT* sequences of the mobilizable plasmids (for example, plasmids carrying the RP4 *oriT* can be conjugated by *E. coli* MFDpir, but not by *E. coli* CAG60056).

2) Single-colonies of both donor and recipient strains were grown in LB overnight at 37°C in a roller-drum. The LB medium was supplemented with appropriate antibiotics (depending on the resistance markers on plasmids) and with auxotrophies (donors *E. coli* MFDpir and BW28029 are DAP auxotrophs).

3) Next, 200 µL of diluted 1:10 overnight cultures (OD_{595}~0.5) of the donors were spread on LB-plates (supplemented with DAP if needed), and the plates were incubated at 37°C in a dry incubator for 1 hour.

4) Subsequently, 10 µL of diluted 1:10 overnight cultures (OD_{595}~0.5) of the recipients were spotted on top of the lawn of the donor strains, and these conjugation plates were incubated for 6 hours in a moist incubator at 37°C (this incubation can also be left overnight). At this stage, the donor strains grow together with the recipients, while donating their mobilizable plasmids to them (transconjugant strains).

5) Finally, transconjugants were selected by streaking them out from the area where the recipients were spotted, in either double-antibiotic selection plates, or in single-antibiotic plates without auxotrophies. Selection plates were incubated at 37°C overnight, and transconjugants were single-colony purified for further use.

7.5. Growth and viability curves.

The bacterial growth monitoring approaches reported here were described in (Bobonis *et al.*, 2020a). The anaerobic growth curves were acquired in collaboration with **Sarela Garcia-Santamarina** (EMBL, Heidelberg), who conducted the experimental part taking place within the anaerobic chamber.

- Bacterial growth curves in anaerobic conditions (Figure 9, Figure 14) were conducted within an anaerobic chamber (2% H2, 12% CO2, 86% N2; Coy Laboratory Products). The LB medium was pre-reduced in the chamber for two days before usage. Transparent flat-bottomed 96-well plates containing 90 µL of pre-reduced LB were inoculated with *S*Tm strains that were grown overnight in LB (aerobically at 37°C) to a final OD_{595}=0.01 (as read in a table-top cuvette-spectrophotometer). The inoculated 96-well plates were sealed with a breathable membrane (Breathe-easy), and incubated at 37°C in the anaerobic chamber (without shaking). The growth of the strains was monitored by periodic OD_{578} measurements of the wells (EON Biotek microplate-spectrophotometer).

- To obtain growth curves in aerobic conditions (Figure 9), plates containing the same strains were incubated in a microplate reader with shaking (200 rpm) at 37°C, and their OD_{578} was periodically measured (Tecan Safire2 microplate-spectrophotometer).

- To obtain *S*Tm growth and viability curves at 15°C (Figure 17A-B), overnight cultures of the appropriate strains were inoculated at a final OD_{595}=0.01 in flasks containing LB. Cultures were incubated at 15°C in a refrigerated incubator (Infors Multitron HT) with shaking (180 rpm). To monitor growth, the OD_{595} of the cultures was periodically measured. To monitor viability, culture samples were periodically taken, serially diluted, plated on LB-plates, and Colony Forming Units per culture volume (CFU/mL) were calculated after incubating the plates overnight at 37°C.

- To obtain *E. coli* viability curves (Figure 17C), the appropriate strains were incubated until OD_{595}=0.4 at 37°C with shaking (180 rpm), and then cultures were transferred at a refrigerated incubator at 15°C with shaking (180 rpm). Next, plasmids were induced by adding arabinose (0.2%), and strain viability was

measured by periodically plating culture-portions on ampicillin LB-plates. Plates were incubated overnight at 37°C and CFU/mL were calculated for each strain per timepoint.

7.6. Extraction of msDNA from cells.

I isolated msDNA by applying the alkaline lysis method (Green and Sambrook, 2016) adapted for small DNA molecules. In order to be able to isolate msDNA from small culture volumes, I overproduced msDNA by overexpressing the reverse transcriptase along with its *msrmsd* gene through arabinose-inducible plasmids carrying msrmsd-RT.

1) Appropriate *S*Tm strains carrying plasmids overexpressing msrmsd-RT (and deleted in *araBAD* to allow efficient arabinose-induction) were inoculated in 20 mL LB with appropriate antibiotics and 0.2% arabinose (starting OD_{595}=0.01). The cultures were then incubated for 5-6 hours at 37°C (180 rpm). From this step onwards, cells were always kept in ice.

2) Cultures of equal densities (OD ~ 4) and volume (10 mL) were then centrifuged (4,000 rpm/15 min/4°C), and the pellets were washed once with ice-cold PBS. After complete removal of the PBS, the cells were re-suspended with vigorous vortexing in 200 µL of ice-cold Alkaline lysis solution I (50 mM glucose, 25 mM Tris-Cl pH 8.0, 10 mM EDTA pH 8.0), and transferred in Eppendorf tubes. After this step, it is important to not vortex the contents of the tube (as this will shear the genomic DNA, producing short DNA fragments that will contaminate the msDNA preparation).

3) Next, 400 µL of freshly prepared alkaline solution II (0.2 N NaOH, 1% w/v SDS) were added to each bacterial suspension. The tubes were closed tightly, and the contents were mixed by inverting the tube rapidly ten times.

4) Subsequently, 300 µL of alkaline solution III (60 mL of 5M potassium acetate, 11.5 mL of Glacial acetic acid, 28.5 mL of H_2O) were added in each tube, the caps were closed, and the tubes inverted rapidly ten times to disperse the liquid thoroughly across the cells. The tubes were stored in ice for 5 minutes.

5) Next, the suspensions were centrifuged (14,000 rpm/20 min/4°C) in a micro-centrifuge, and 700 µL of the supernatant were transferred to fresh Eppendorfs.

6) To separate the proteins from the nucleic acids, an equal volume (700 µL) of Phenol: Chloroform: Isoamylalcohol (25:24:1, pH 8.0) was added in the supernatants. The organic and aqueous phases were mixed by vigorously vortexing for 30 seconds (the correct vortex requires two tubes smashing against each other), and then the tubes were centrifuged in a micro-centrifuge (14,000 rpm/20 min/4°C). From these tubes, 600 µL of the upper aqueous phase (containing the nucleic acids) were transferred in fresh Eppendorfs.

7) Next, the nucleic acids were extracted once again with Phenol: Chloroform: Isoamylalcohol, to remove the residual proteins. This time 600 µL of Phenol were added, instead of 700 µL. After mixing, vortexing, and spinning (as in step 6), 500 µL of the upper aqueous phase were transferred in fresh Eppendorfs.

8) To precipitate the nucleic acids from the solution, an equal volume (500 µL) of 100% isopropanol was added to the protein-free aqueous phases. The mixes were vigorously vortexed (~20 seconds), and the nucleic acids were left to precipitate overnight in the fridge (4°C). This extended precipitation time is important due to the small size of msDNA (and can be extended over 2-3 days if necessary, although the DNA yields will not change).

9) The next morning, the precipitated nucleic acids were collected by centrifugation (14,000 rpm/60 min/4°C) in a micro-centrifuge. The extended centrifugation times are crucial to increase the msDNA yield, due to the small size of msDNA.

10) Following centrifugation, there should be a small white pellet at the bottom of the tubes (mostly salt and nucleic acids). The supernatants were removed gently by aspirating with a P1000, and any residual volumes were removed with a P20.

11) The msDNA were ethanol-precipitated by adding 1 mL of 70% ethanol to the pellet. The tubes were then inverted 8-10 times (the pellet should be mixed with the ethanolic solution), and the nucleic acids were recovered by centrifugation (14,000 rpm/60 min/4°C) in a micro-centrifuge.

12) After the centrifugation, all of the remaining ethanol was removed by aspiration (P1000 for most of the volume and P20 for residual volumes), and the open tubes were left at room temperature for 15 minutes, in order for the residual ethanol to evaporate. If any visible beads of ethanol remain in the tubes, paper towels can be used to remove them.

13) Finally, the pellets containing the nucleic acids (DNA and RNA) were re-suspended in 10 µL of water containing 20 µg/mL of DNAse-free RNAse A. The tubes were then incubated at 37°C for 30 minutes. At this point the msDNA preparations can be used for downstream procedures, or stored at -20°C indefinitely.

7.7. Electrophoresis of msDNA in non-denaturing TBE-Polyacrylamide.

Due to their small sizes, msDNA can only be visualized adequately in polyacrylamide gels, which have superior resolving capacities compared to agarose gels. An appropriate acrylamide concentration can be used (maximum 20%), based on the size of DNA fragments one needs to resolve. I used 12% polyacrylamide gels to visualize msDNA-Sen2.

1) In order to make non-denaturing 12% TBE-Polyacrylamide gels (enough for two), mix:
   - 9.84 mL of water,
   - 8 mL of 30% Acrylamide/Bis-acrylamide solution (Sigma, catalogue number: A3574),
   - 2 mL of 10x Tris Borate Buffer (TBE; 108 g of Tris, 54 g of boric acid, 20 mL of 0.5 M EDTA pH 8.0),
   - 140 µL of Ammonium Persulfate (APS), and,
   - 20 µL of Tetramethylethylenediamine (TEMED).

   Quickly pour the contents of the non-polymerized TBE-acrylamide solution between two ethanol-cleaned supporting glass plates, until the gap is filled to the brim. Insert 10- or 15-well combs and allow the gels to polymerize for 1 hour at room temperature.

2) After polymerization, the TBE-Polyacrylamide gel should be pre-run (with no samples loaded) with 1xTBE buffer at 70V for 30 min – 1 hour. This pre-run step removes residual acrylamide in the bottom parts of the gels, which ultimately adds noise to the signal if allowed to stay. After the pre-run, the wells should be pre-rinsed with 1xTBE to remove residual acrylamide from the wells.

3) The msDNA samples (10 µL) were mixed with standard DNA loading dye (without SDS), and the entire volume was loaded on the TBE-Polyacrylamide gels. The DNA ladder used was a 50 bp step ladder from Promega (catalogue number: G4521).

4) The msDNAs were electrophoresed at 70V for ~3 hours or until the red/pink dye (NEB, Gel Loading Dye, catalogue number: B7025S) was close to the edge of the gel.

5) Finally, the polyacrylamide gels were stained in a 1 µg/mL Ethidium Bromide (EtBr) water bath for 30 minutes and visualized under ultraviolet (UV) light using a UV transilluminator.

7.8. Purification of msDNA from polyacrylamide gels.

Although msDNA can be extracted from cells using the alkaline lysis method (7.6), this method also extracts the plasmid DNA used to overexpress msDNA. Therefore, these extracts are not appropriate for downstream purposes, such as cutting msDNA with restriction enzymes to ascertain its size (Figure 11) or its methylation status (Figure 47). For these purposes I purified msDNA further from polyacrylamide gels.

1) msDNA were extracted from 200 mL of culture (as described in 7.6) and electrophoresed in non-denaturing 12% TBE-Polyacrylamide gels (ran for 70V for 4 hours). In order to increase the efficiency of msDNA elution from the gel, I loaded the equivalent of 60 mL of culture per well (normally, the equivalent of 10 mL is loaded).

2) Gels were stained with EtBr and gel-slices containing the msDNA were transferred to Eppendorfs.

3) Next, the gel-slices were crushed against the wall of the tubes using a pipette tip, as described in (Green and Sambrook, 2019).

4) The crushed acrylamide crumps were suspended in two gel-slice volumes of acrylamide elution buffer (10 mM magnesium acetate tetrahydrate, 0.5 M ammonium acetate, 1 mM EDTA pH 8.0), vortexed, and the tubes were incubated by sticking them in the 37°C roller-drum overnight.

5) The tubes were then centrifuged (14,000 rpm/10 min/RT) and the supernatants (containing the nucleic acids) were transferred to fresh tubes. It is important here to use drawn-out Pasteur pipettes, to avoid carrying over acrylamide with the supernatants.

6) An additional one gel-slice volume of acrylamide elution buffer was added, and after centrifugation (14,000 rpm/10 min/RT) the supernatant was joined with the supernatant from the first round. This step is performed to increase the recovery efficiency of the msDNA elution.

7) Subsequently, the procedure is identical as starting from step 9 of section (7.6).

- Following purification of the msDNAs from the acrylamide gels, I digested them overnight either with Sau3AI (NEB; catalogue number R0169S) for experiments shown in (Figure 11) or with DpnI (NEB; catalogue number R0176S) for experiments shown in (Figure 47).

7.9. Electrophoresis of msDNA in denaturing TBE-Polyacrylamide gels.

In order to be able to ascertain the true size of the msDNA, I needed to electrophorese them in denaturing TBE-Polyacrylamide gels. This is due to the extensive secondary structures that the msDNA adopts (Figure 3), which alter its electrophoretic mobility in non-denaturing gels.

1) In order to make denaturing 20% TBE-Urea-Polyacrylamide gels (enough for two), mix:

- Add 3 mL of water,
- Add 4.8g of Urea*,
- 13.3 mL of 30% Acrylamide/Bis-acrylamide solution (Sigma, catalogue number: A3574),
- 2 mL of 10x Tris Borate Buffer (TBE; 108 g of Tris, 54 g of boric acid, 20 mL of 0.5 M EDTA pH 8.0),
- Fill with water up to 20 mL,
- 140 µL of Ammonium Persulfate (APS), and,
- 20 µL of Tetramethylethylenediamine (TEMED).

*Before adding APS and TEMED, mix the ingredients of the solution well enough for the urea to be completely dissolved.

2) Quickly pour the contents of the non-polymerized TBE-acrylamide solution between two ethanol-cleaned supporting glass plates, until the gap is filled to the brim. Insert 10- or 15-well combs and allow the gels to polymerize for 1 hour at room temperature.

3) After polymerization, the denaturing TBE-Polyacrylamide gel should be pre-run (with no samples loaded) with 1xTBE buffer at 70V for 1 hour at 55°C. I achieved the higher electrophoresis temperature by inserting the running apparatus in an incubator set at 55°C (Infors Multitron HT). This pre-run step removes residual acrylamide and urea in the bottom parts of the gels, which ultimately adds noise to the signal if allowed to stay. After the pre-run, the wells should be pre-rinsed with 1xTBE to remove residual acrylamide from the wells (as well as the urea that has certainly crept in the wells).

4) To load the msDNA samples in the denaturing gels, 2x formamide loading buffer (90% formamide, 0.5% EDTA, 0.1% xylene cyanol, 0.1% bromophenol blue) is mixed with the msDNA samples, and the formamide-containing samples were heated to 95°C for 15 min, and then quickly transferred in ice. This step is crucial to break the secondary structure of the msDNA (so that it is loaded as a single-stranded DNA in the denaturing gels).

5) The heated formamide-msDNA samples were loaded in the denaturing gel (flush out the urea again from the wells before loading the msDNA) and electrophoresed for 3 hours at 60 V (at 55°C).

6) Finally, the gels were stained with silver, using the silver stain kit from Roth (article number L533.1), following the procedure as described in (Bassam and Gresshoff, 2007). The msDNA were not stained with EtBr, since EtBr preferentially stains double-stranded DNA (while silver stains efficiently stains single-stranded DNA). A 10-bp step DNA ladder was used from Promega (catalogue number; G4471).

7.10. SDS-PAGE and immunoblotting.

1) Culture samples from 3xFlag-tagged strains (*rrtT*-3xFlag, *rcaT*-3xFlag) and control *S*Tm strains were suspended in 1x Laemmli sample buffer and heated to 95°C for 10 minutes.

2) Proteins were separated by SDS-PAGE (Sodium Dodecyl Sulphate – PolyAcrylamide Gel Electrophoresis) at 80 V for 2 hours, and the gel was blotted to a PVDF membrane (100 V for 1.5 hours) at 4°C.

3) The membranes were blocked for 1 hour at RT in TBS-T containing 5% skimmed-milk (TBS-TM) and probed overnight at 4°C in TBS-TM containing 1:1000 of an anti-Flag antibody (Sigma-Aldrich; catalogue No F3165), or in TBS-TM containing 1:10000 of an anti-LpoA antibody as a loading control (Typas *et al.*, 2010). Wherever applicable, the membranes were cut, and one half was probed with anti-LpoA, while the other half with anti-Flag antibody, respectively).

4) Next, the membranes were washed, and incubated for 1 hour with HRP-conjugated secondary antibodies (1:5000, anti-mouse, Sigma-Aldrich Catalogue No A9044; Flag, or 1:10000, anti-rabbit, Merck, Catalogue No GENA934; LpoA) in TBS-TM.

5) After washing with TBS-T, chemiluminescence substrate (GE-Healthcare) was added, and the signal was detected using X-ray films (Advantsta). X-ray films were then scanned at 300x300 dpi. Digital images were cropped, and adjusted in Inkscape. Signal quantifications were done in ImageJ.

7.11. Protein-RNA UV-crosslinking *in vivo*.

The UV-crosslinking procedure to identify RT-msrmsd-RNA complexes shown in (Figure 12) was adapted from (Holmqvist *et al.*, 2016).

1) Over-night cultures of rrtT-3xFlag tagged strains (and controls) were inoculated at OD595=0.01 in 100 mL of LB, and grown until OD595 ~ 1.2.

2) Cultures were split in half, and centrifuged (5000 rpm/10 min/4°C), washed with 50 mL of ice-cold distilled water (dH2O), and centrifuged again (5000 rpm/10 min/4°C).

3) Pellets were re-suspended in 7 mL dH2O, and the suspensions were poured in pre-cooled 100 mm x15 mm Petri-dishes, covering their surface. One half of each culture was UV-crosslinked at λ=254 nm (5 J/cm2; Spectrolinker XL-1500 UV crosslinker), while the other halves were not crosslinked. Crosslinked and non-crosslinked suspensions were centrifuged again (5000 rpm/10 min/4°C), and cells were re-suspended in Lysis Buffer, and lysed as described in the Immunoprecipitation section.

4) Samples from the cleared lysates were mixed with 2x Laemmli Buffer, heated at 70°C for 20 min, and analysed by immunoblotting (described in SDS-PAGE and Immunoblot section).

- For RNase/DNase treatment, samples (100 µL) from the cleared lysates were incubated either with 10 ng/mL RNase A (R5503, Sigma-Aldrich), or with 2 U/mL Turbo DNase (AM2238, Thermo Fisher) for 30 min at 37°C, and 10 µL samples were analysed by immunoblotting.

7.12. Whole genome sequencing.

The steps described here were reported in (Bobonis et al., 2020a). The genomic DNA-libraries were prepared and sequenced by the EMBL Gene Core facility. The whole-genome sequencing analysis part was performed by **Marco Galardini** (TWINCORE, Hannover).

- The genomic DNAs from cold-sensitivity suppressor mutants of *S*Tm retron-antitoxin deletion mutants were isolated using a kit (NucleoSpin Tissue, Mini kit for DNA from cells and tissue; REF 740952.50), by following the instructions of the provider.

- For preparing the genomic DNA-libraries, 1 µg of input DNA was sonicated for 2 min, and libraries were constructed by using a kit (NEB Ultra DNA library kit for Illumina; catalogue number E7370L), according to the manufacturer's instructions. The 30 genomic libraries (29 suppressors and the wildtype strain) were sequenced using a NextSeq Illumina platform with a 150 base pairs paired-end configuration.

- Genetic variants in the suppressors were called by using breseq v0.28.0 (Deatherage and Barrick, 2014), by using the *S*Tm genome as reference (RefSeq ID: NC_016856.1). The genotypes of suppressor strains can be found in Table S2 of (Bobonis *et al.*, 2020a).

7.13. Protein immunoprecipitations (IP)

This section describes the experimental approach to immunoprecipitate the RT or RcaT proteins from STm (Figure 26, Figure 27).

1) Two biological replicates of *S*Tm strains 3xFlag-tagged in either *rrtT* (RT-3xFlag) or *rcaT* (RcaT-3xFlag) genes, along with the analogous untagged strains, were inoculated in 100 mL LB (OD_{595}=0.02) from overnight cultures. Cultures were incubated at 37°C with shaking (180 rpm) until OD_{595}= 1.1 – 1.5.

2) Cultures were then split in half, and one half was transferred to a refrigerated incubator (Infors Multitron HT) set at 20°C with shaking (180 rpm) for 5 hours. The other half was used to prepare the 37°C samples. After this stage, samples were always kept on ice.

3) A volume of 50 mL/OD_{595} = 1.5 from each culture was transferred to 50 mL Falcons, centrifuged (5,000 rpm/10 min/4°C), and the medium supernatant was discarded. It is important at this stage to normalize all strains per OD_{595}, in order to have an equal amount of total protein across all samples.

4) Cell pellets were washed once with 50 mL of ice-cold PBS, cells were centrifuged once more (5,000 rpm/10 min/4°C), and the PBS supernatant was discarded. The remaining liquid was removed with a P1000 pipette, and pellets were flash-frozen and put at -80°C until further processing.

5) Next, pellets were thawed on ice, suspended in 1.2 mL of Lysis Buffer (50 µg/ml lysozyme, 0.8% NP-40, 1 mM MgCl2, 1x protease inhibitors [Roche; cOmplete Protease Inhibitor Cocktail] in PBS), and transferred to fresh 1.5 mL Eppendorfs.

6) Cells were then lysed by ten freeze-thaw cycles using liquid nitrogen. Specifically, the 1.5 mL tubes fit just correctly in the metallic racks used for cuvettes. These racks containing the tubes were submerged in liquid nitrogen, until the cells were completely frozen. Subsequently, the cells were thawed in a tube incubator set at 25°C with mixing (1400 rpm) for 5 minutes. This process was repeated ten times.

7) The lysates were then centrifuged (14,000 rpm/60 min/4°C) in order to remove intact cells and other insoluble components. The same volume (1 mL) of clear lysates was transferred to fresh Eppendorfs. Samples from the clear lysates were taken (input samples; 40 µL). These input samples were then later used to analyze the full proteome of the samples, representing the proteome state prior to immunoprecipitation.

8) Subsequently, agarose beads coated with Flag-peptide (ANTI-FLAG® M2 Affinity Agarose Gel; Sigma-Aldrich) were washed twice (20x the beads volume) with Wash Buffer (0.8% NP-40 in PBS) and 25 µL of washed beads were added to each of the 1 mL of cleared lysates. Lysates were then incubated with the beads overnight in a table-top roller at 4°C.

9) Next, the beads were centrifuged (8,200 rcf/10 min/RT) and the lysate-supernatants were thoroughly discarded. It is important to let the agarose beads to sit for 1 minute after centrifugation, in order to avoid aspirating beads along with the supernatants.

10) The beads were then washed four times with 1 mL of Wash Buffer. For each wash, the Wash Buffer was dispersed and mixed thoroughly with the beads through a 2-

minute incubation in a table-top roller. Beads were centrifuged at 8,200/2 min/RT per wash, and left to sit in the tubes for 1 minute, before aspirating and discarding the Wash Buffer after each wash. After the fourth wash, the beads were centrifuged for a longer time (8,200 rcf/15 min/RT) and the supernatants were thoroughly discarded, leaving the agarose beads as dry as possible.

11) To elute the proteins from the beads, 50 µL of Elution Buffer (150 µg/mL 3xFlag peptide [Sigma-Aldrich], 0.05% Rapigest [Waters], 1x protease inhibitors in PBS) was added to the agarose Flag-beads and the proteins were eluted for 2 hours on a table-top roller at 4°C.

12) Finally, the samples were centrifuged (8,200 rcf/15 min/RT) and 50 µL of eluates were retrieved (carefully, while avoiding to aspirate beads), and transferred to Eppendorf tubes (Immunoprecipitation samples; IP).

7.14. Proteomic analysis of IPs.

The process is described here as reported in (Bobonis *et al.*, 2020a). The entire analysis described below was conducted by **André Mateus** (EMBL, Heidelberg).

1) The proteins in the IP samples were digested by following a modified SP3 protocol (Hughes *et al.*, 2019). Approximately 2 µg of proteins were diluted in 20 µL of water and added to the bead suspension (10 µg of beads (Thermo Fischer Scientific—Sera-Mag Speed Beads, CAT# 4515-2105-050250, 579 6515-2105-050250) in 10 µL 15% formic acid and 30 µL ethanol). The beads were incubated for 15 min with shaking at room temperature, and then the beads were washed four times with 70% ethanol.

2) Subsequently, the proteins were digested overnight by adding 40 µL of digest solution (5 mM chloroacetamide, 1.25 mM TCEP, 200 ng trypsin, and 200 ng LysC in 100 mM HEPES pH 8).

3) Next, the digested proteins were eluted from the beads, vacuum-dried, re-suspended in 10 µL of water, and labelled with 17 µg of TMT10plex dissolved in 4 µL of acetonitrile (Thermo Fisher Scientific) for 30 min at room temperature. The

labelling reaction was quenched with 4 µL of 5% hydroxylamine and the IP experiments that belong to the same group were combined in the same mass spectrometry run.

4) The samples were desalted with solid-phase extraction on a Waters OASIS HLB µElution Plate (30 µm) and fractionated under high pH conditions prior to analysis with liquid chromatography coupled to tandem mass spectrometry (Q Exactive Plus; Thermo Fisher Scientific), as described previously (Mateus *et al.*, 2018).

5) The mass spectrometry raw files were processed with isobarQuant and peptides/proteins were identified with Mascot 2.5.1. (Matrix Science) against the STm UniProt FASTA (Proteome ID: UP000001014), modified to include known contaminants and the reversed protein sequences (search parameters: trypsin; missed cleavages 3; peptide tolerance 10 ppm; MS/MS tolerance 0.02 Da; fixed modifications were carbamidomethyl on cysteines and TMT10plex on lysine; variable modifications included acetylation on protein N-terminus, oxidation of methionine, and TMT10plex on peptide N-termini).

- The fold-enrichment of pulled-down proteins in IP samples were compared to negative controls (*S*Tm strains without 3xFlag-tagged proteins), and statistical significance was evaluated through limma analysis (Ritchie *et al.*, 2015). A similar analysis was conducted on the input samples (proteome state before IP), in order to ensure that the enriched proteins in the IP were not overexpressed in the Flag-tagged strains. The complete data can be found in Table S1 of (Bobonis *et al.*, 2020a).

7.15. RT-Sen2 purification and msDNA-isolation from pure RT-Sen2.

The process is described here as reported in (Bobonis *et al.*, 2020a). The protocol to purify RT-Sen2 was optimized collaboratively with **Joel Selkrig**, **Anna Sueki**, **Jacob Scheurich**, and **Kim Remans** (EMBL, Heidelberg).

1) An *E. coli* BL21 (DE3) CodonPlus-RIL strain, carrying plasmid pJB120 (pET28α-*msrmsd-rrtT*-6xHis; described in Tables S3-4 in (Bobonis *et al.*, 2020a) was inoculated at ~OD_{595}=0.02 in 100 mL of Auto-Induction Medium (TB-FB, 1.5%

lactose, 0.05% glucose, 100 µg/mL kanamycin, 20 µg/mL chloramphenicol, 2 mM $MgSO_4$). The culture was incubated until OD_{595}=0.8 – 1 at 37°C with shaking (180 rpm).

2) The culture was then transferred in a refrigerated incubator set at 18°C for 16 hours. The final OD_{595} of the culture should be ~15-20. The cells were then centrifuged (4,000 rpm/10 min/4°C), washed once with 50 mL of ice-cold PBS, and the dried pellets were flash-frozen with liquid nitrogen, and stored at -80°C until further use.

3) The pellets were re-suspended in 40 mL of Lysis Buffer (50 mM Tris pH 8.0, 500 mM NaCl, 20 mM Imidazole, 10% glycerol, 1x protease inhibitors [Roche; cOmplete Protease Inhibitor Cocktail in water] and 2 U/mL of DNAse I [NEB; catalogue number, M0303S) and lysed by passaging them 6 times through a micro-fluidizer.

4) To remove intact cells and other insoluble parts, the lysates were centrifuged (35,000 rpm/25 min/4°C).

5) The cleared lysates were filtered through a 0.45 µm filter and added to 100 µL of washed Ni-NTA Agarose Beads (Thermo Fisher; catalogue number, R90101). Proteins were bound to the beads by passing the lysate through a gravity flow column with the packed 100 µL bead-bed.

6) After discarding the flow through, the beads were washed thrice with 5 mL of Lysis Buffer, and the bound proteins were subsequently eluted in four fractions with a total of 1 mL of Elution Buffer (50 mM Tris pH 8.0, 500 mM NaCl, 500 mM Imidazole pH 8.0, 10% glycerol, and 1x protease inhibitors). It is important to add some imidazole in the tube that the first elution fraction is collected (e.g., 50 µL of 2M imidazole), due to the RT-Sen2 protein precipitating when present in high concentrations.

- In order to isolate msDNA from purified RT-Sen2 (Figure 30C), I isolated total DNA from 500 µg of RT-Sen2 protein. For this, the procedure was identical as for isolating msDNA (7.6), but starting from step 6 of the process.

7.16. Toxin Inhibition/Activation Conjugation (TIC/TAC) procedure.

The process is described here as reported in (Bobonis *et al.*, 2020b).

1) I used two plasmid gene-overexpression libraries as plasmid-donors, the MOB library (carried in an *E. coli* JA200 F^+ plasmid-donor strain; Saka *et al.*, 2005) and the TransBac library (carried in an *E. coli* BW38029 F^+ *dapA*$^-$ plasmid-donor strain; Otsuka *et al.*, 2015). 384-colony arrays of the libraries were pinned from liquid glycerol-stocks on ampicillin-LB or tetracycline-DAP-LB plates, respectively, by using a Singer ROTOR and 384-density long-pin Singer RePads, and the colonies were growth overnight.

2) The recipient strains (*E. coli* BW25113; Baba *et al.*, 2006) carried either a p-*rcaT* plasmid (for TIC) or a p-retron plasmid (for TAC), with both plasmids encoding a spectinomycin resistance marker (plasmids described in Tables S4-5 of Bobonis *et al.*, 2020b). The recipients were grown overnight in 5 mL of spectinomycin-LB, and 200 μL of diluted cultures (OD_{595}=0.5) were spread using sterile glass beads on rectangular Singer LB plates (for MOB), or on Singer LB-DAP plates (for TransBac). These plates were incubated in a non-humid incubator for 1 hour at 37°C.

3) Subsequently, the donor 384-colony arrays were pinned on top of the LB-plates containing the lawns of recipient strains, using 384 short-pin Singer RePads. The donor and recipients were allowed to conjugate for 6 hours in a humid incubator at 37°C.

4) Next, cells from the conjugation plates were pinned onto double-antibiotic-selection plates, using 384 short-pin Singer RePads, in order to select for BW25113 transconjugants carrying both plasmids (p-rcaT/p-retron + library-plasmids). The double-selection plates contained ampicillin-spectinomycin for the MOB library, and tetracycline-spectinomycin for the TransBac library. The transconjugants were then allowed to grow for ~20 hours in a humid incubator at 37°C. After this first selection, the colonies will not be uniformly grown (irregular shapes), due to the non-uniform nature of conjugation.

5) The transconjugants were then subjected to a second round of selection on double-antibiotic plates, and were also re-arrayed in a 1536-colony format. 1536-colony transconjugant plates were incubated for 10 hours at 37°C, and then each plate was pinned (using 1536-density short-pin Singer RePads) on two replicates of double-antibiotic selection plates (third-round of selection; “source-plates”).

6) The source plates were incubated for 4-5 hours overday at 37°C and these were used to pin onto double-selection LB-plates (“test-plates”), using 1536-density short-pin Singer RePads. The test-plates contained either no inducers, only arabinose (inducing the p-*rcaT*/p-retron), only IPTG (low or high; inducing the library-plasmids), or combinations of both inducers. Finally, the test plates were incubated for 13 hours at 37°C and imaged afterwards using a Canon EOS Rebel T3i camera under controlled lighting settings (S&P robotics).

- The high-throughput conjugation experiments in the *E. coli* single-gene deletion library (Keio; Baba *et al.*, 2006) shown in (Figure 19 and Figure 56) were carried essentially the same way as described above for TIC/TAC. The only difference was that the recipient strains were the Keio library strains, and the donor strains were *E. coli* CAG60056 F^+ strains, carrying plasmids p-retron (Figure 19) or p-*rcaT* (Figure 56). The p-retron/p-*rcaT* plasmids are mobilizable by *E. coli* F^+ donors.

7.17. TIC/TAC data analysis.

The process is described here as reported in (Bobonis *et al.*, 2020b). The computational analysis was conducted by **George Kritikos** (EMBL, Heidelberg).

1) Bacterial colony morphological features for each strain were quantified by using the Iris image-analysis platform (Kritikos *et al.*, 2017). The colony integral opacity values were used as a fitness proxy for each strain. In order to account for the effects of inducing the library-plasmids on bacterial fitness, we used plates containing only low or high IPTG concentrations as control plates. The strain opacities in control plates were compared with the strain opacities of analogous strains in the experiment plates, where the library-plasmids and the p-*rcaT*/p-retron plasmids were co-induced with IPTG and arabinose, respectively.

2) For quality control, we empirically derived cut-offs for strains that were a) growth-inhibited in the control plates (opacity values < 50,000), b) mucoid in the control plates (colony densities of both replicates > 51; Kritikos et al., 2017), and c) noisy strains in control and/or experiment plates (standard deviation for opacity values > 23,000 – median opacities were: TAC control - 103,820, TAC experiment – 71,680, TIC control – 106,941, TIC experiment – 24,357). Any strains exceeding these cut-off values in the control plates were flagged and removed from the final reported dataset, but they are visible on Table S2 of (Bobonis *et al.*, 2020b).

3) Plate exterior opacity values (four outermost rows and columns) were each multiplicatively corrected to match the mean growth of the interior of the plate. Plate-to-plate biases were also multiplicatively corrected to the same mean. Subsequently, z-scores of those corrected opacity values were calculated per condition, and mean z-scores were calculated per mutant across technical replicates. The final reported score is calculated as the difference between the mean z-scores of each mutant in the experiment and the control plates. All raw and processed data from the TIC/TAC analysis can be found in Table S2 of (Bobonis *et al.*, 2020b).

8. Bibliography.

Aakre, C.D., Phung, T.N., Huang, D., and Laub, M.T. (2013) A Bacterial Toxin Inhibits DNA Replication Elongation through a Direct Interaction with the β Sliding Clamp. *Mol Cell* **52**: 617–628 https://linkinghub.elsevier.com/retrieve/pii/S1097276513007569.

Afif, H., Allali, N., Couturier, M., and Melderen, L. Van (2001) The ratio between CcdA and CcdB modulates the transcriptional repression of the ccd poison-antidote system. *Mol Microbiol* **41**: 73–82 http://doi.wiley.com/10.1046/j.1365-2958.2001.02492.x

Ahmed, A.M., and Shimamoto, T. (2003) msDNA-St85, a multicopy single-stranded DNA isolated from *Salmonella enterica* serovar Typhimurium LT2 with the genomic analysis of its retron. *FEMS Microbiol Lett* **224**: 291–297. https://academic.oup.com/femsle/article-lookup/doi/10.1016/S0378-1097(03)00450-6

Arambula, D., Wong, W., Medhekar, B.A., Guo, H., Gingery, M., Czornyj, E., *et al.* (2013) Surface display of a massively variable lipoprotein by a legionella diversity-generating retroelement. *Proc Natl Acad Sci U S A* **110**: 8212–8217. http://www.pnas.org/cgi/doi/10.1073/pnas.1301366110

Baba, T., Ara, T., Hasegawa, M., Takai, Y., Okumura, Y., Baba, M., *et al.* (2006) Construction of *Escherichia coli* K-12 in-frame, single-gene knockout mutants: The Keio collection. *Mol Syst Biol* **2**: 2006.0008 https://onlinelibrary.wiley.com/doi/abs/10.1038/msb4100050

Baltimore, D. (1970) RNA-dependent DNA Polymerase in Virions of RNA Tumour Viruses. *Nature* **226**: 1209–1211. http://www.nature.com/articles/2261209a0

Barria, C., Malecki, M., and Arraiano, C.M. (2013) Bacterial adaptation to cold. *Microbiol (United Kingdom)* **159**: 2437–2443. https://www.microbiologyresearch.org/content/journal/micro/10.1099/mic.0.052209-0

Bassam, B.J., and Gresshoff, P.M. (2007) Silver staining DNA in polyacrylamide gels. *Nat Protoc* **2**: 2649–2654 http://www.nature.com/articles/nprot.2007.330.

Belfort, M., and Lambowitz, A.M. (2019) Group II Intron RNPs and Reverse Transcriptases: From Retroelements to Research Tools. *Cold Spring Harb Perspect Biol* **11**: a032375 http://cshperspectives.cshlp.org/lookup/doi/10.1101/cshperspect.a032375.

Bernard, P., and Couturier, M. (1991) The 41 carboxy-terminal residues of the miniF plasmid CcdA protein are sufficient to antagonize the killer activity of the CcdB protein. *MGG Mol Gen Genet* **226**: 297–304. http://link.springer.com/10.1007/BF00273616

Bernard, P., and Couturier, M. (1992) Cell killing by the F plasmid CcdB protein involves poisoning of DNA-topoisomerase II complexes. *J Mol Biol* **226**: 735–745. https://linkinghub.elsevier.com/retrieve/pii/002228369290629X

Bleibtreu, A., Clermont, O., Darlu, P., Glodt, J., Branger, C., Picard, B., and Denamur, E. (2014) The rpoS Gene Is Predominantly Inactivated during Laboratory Storage and Undergoes Source-Sink Evolution in *Escherichia coli* Species. *J Bacteriol* **196**: 4276–4284 http://jb.asm.org/cgi/doi/10.1128/JB.01972-14.

Blower, T.R., Short, F.L., Rao, F., Mizuguchi, K., Pei, X.Y., Fineran, P.C., *et al.* (2012) Identification and classification of bacterial Type III toxin-antitoxin systems encoded

in chromosomal and plasmid genomes. *Nucleic Acids Res* **40**: 6158–6173 https://academic.oup.com/nar/article-lookup/doi/10.1093/nar/gks231.

Bobonis, J., Mateus, A., Pfalz, B., Garcia-Santamarina, S., Galardini, M., Kobayashi, C., *et al.* (2020a) Bacterial retrons encode tripartite toxin/antitoxin systems. *bioRxiv* 2020.06.22.160168 https://doi.org/10.1101/2020.06.22.160168.

Bobonis, J., Mitosch, K., Mateus, A., Kritikos, G., Elfenbein, J.R., Savitski, M.M., *et al.* (2020b) Phage proteins block and trigger retron toxin/antitoxin systems. *bioRxiv* 2020.06.22.160242 https://doi.org/10.1101/2020.06.22.160242.

Bordes, P., Cirinesi, A.M., Ummels, R., Sala, A., Sakr, S., Bitter, W., and Genevaux, P. (2011) SecB-like chaperone controls a toxin-antitoxin stress-responsive system in *Mycobacterium tuberculosis*. *Proc Natl Acad Sci U S A* **108**: 8438–8443. http://www.pnas.org/cgi/doi/10.1073/pnas.1101189108

Bost, S., Silva, F., and Belin, D. (1999) Transcriptional Activation of ydeA, Which Encodes a Member of the Major Facilitator Superfamily, Interferes with Arabinose Accumulation and Induction of the *Escherichia coli* Arabinose PBADPromoter. *J Bacteriol* **181**: 2185–2191 https://jb.asm.org/content/181/7/2185.

Butland, G., Peregrín-Alvarez, J.M., Li, J., Yang, W., Yang, X., Canadien, V., *et al.* (2005) Interaction network containing conserved and essential protein complexes in *Escherichia coli*. *Nature* **433**: 531–537 http://www.nature.com/articles/nature03239.

Cavalier-Smith, T. (1991) Intron phylogeny: a new hypothesis. *Trends Genet* **7**: 145–148 https://linkinghub.elsevier.com/retrieve/pii/0168952591903773.

Chase, J.W., and Richardson, C.C. (1974) Exonuclease VII of *Escherichia coli*. Mechanism of action. *J Biol Chem* **249**: 4553–61 http://www.ncbi.nlm.nih.gov/pubmed/4602030.

Chassy, B., Mercenier, A., and Flickinger, J. (1988) Transformation of bacteria by electroporation. *Trends Biotechnol* **6**: 303–309 https://linkinghub.elsevier.com/retrieve/pii/016777998890025X.

Cherepanov, P.P., and Wackernagel, W. (1995) Gene disruption in *Escherichia coli*: TcR and KmR cassettes with the option of Flp-catalyzed excision of the antibiotic-resistance determinant. *Gene* **158**: 9–14 https://linkinghub.elsevier.com/retrieve/pii/037811199500193A.

Chopin, M.C., Chopin, A., and Bidnenko, E. (2005) Phage abortive infection in lactococci: Variations on a theme. *Curr Opin Microbiol* **8**: 473–479. https://linkinghub.elsevier.com/retrieve/pii/S1369527405000809

Christensen-Dalsgaard, M., Jørgensen, M.G., and Gerdes, K. (2010) Three new RelE-homologous mRNA interferases of *Escherichia coli* differentially induced by environmental stresses. *Mol Microbiol* **75**: 333–348 http://doi.wiley.com/10.1111/j.1365-2958.2009.06969.x.

Christensen, S.K., Maenhaut-Michel, G., Mine, N., Gottesman, S., Gerdes, K., and Melderen, L. Van (2004) Overproduction of the Lon protease triggers inhibition of translation in *Escherichia coli*: involvement of the yefM-yoeB toxin-antitoxin system. *Mol Microbiol* **51**: 1705–1717 http://doi.wiley.com/10.1046/j.1365-2958.2003.03941.x.

Christensen, S.K., Mikkelsen, M., Pedersen, K., and Gerdes, K. (2001) RelE, a global

inhibitor of translation, is activated during nutritional stress. *Proc Natl Acad Sci* **98**: 14328–14333 http://www.pnas.org/cgi/doi/10.1073/pnas.251327898.

Chung, C.T., Niemela, S.L., and Miller, R.H. (1989) One-step preparation of competent *Escherichia coli*: transformation and storage of bacterial cells in the same solution. *Proc Natl Acad Sci* **86**: 2172–2175 http://www.pnas.org/cgi/doi/10.1073/pnas.86.7.2172.

Clarke, L., and Carbon, J. (1976) A colony bank containing synthetic Col EI hybrid plasmids representative of the entire *E. coli* genome. *Cell* **9**: 91–99. https://linkinghub.elsevier.com/retrieve/pii/0092867476900556

Coq, J. Le, and Ghosh, P. (2011) Conservation of the C-type lectin fold for massive sequence variation in a Treponema diversity-generating retroelement. *Proc Natl Acad Sci* **108**: 14649–14653 http://www.pnas.org/cgi/doi/10.1073/pnas.1105613108.

Coray, D.S., Wheeler, N.E., Heinemann, J.A., and Gardner, P.P. (2017) Why so narrow: Distribution of anti-sense regulated, type I toxin-antitoxin systems compared with type II and type III systems. *RNA Biol* **14**: 275–280 http://dx.doi.org/10.1080/15476286.2016.1272747.

Crick, F. (1970) Central Dogma of Molecular Biology. *Nature* **227**: 561–563 http://link.springer.com/10.1007/978-1-4020-6754-9_2672.

Datsenko, K.A., and Wanner, B.L. (2000) One-step inactivation of chromosomal genes in *Escherichia coli* K-12 using PCR products. *Proc Natl Acad Sci U S A* **97**: 6640–6645. http://www.pnas.org/cgi/doi/10.1073/pnas.120163297

Davidson, A.R., Lu, W., Stanley, S.Y., Wang, J., Mejdani, M., Trost, C.N., *et al.* (2020) Anti-CRISPRs: Protein Inhibitors of CRISPR-Cas Systems. *Annu Rev Biochem* **89**: 309–332 https://www.annualreviews.org/doi/10.1146/annurev-biochem-011420-111224.

Davies, J.F., Hostomska, Z., Hostomsky, Z., Jordan, S.R., and Matthews, D.A. (1991) Crystal structure of the ribonuclease H domain of HIV-1 reverse transcriptase. *Science (80-)* **252**: 88–95. https://www.sciencemag.org/lookup/doi/10.1126/science.1707186

Deatherage, D.E., and Barrick, J.E. (2014) Identification of Mutations in Laboratory-Evolved Microbes from Next-Generation Sequencing Data Using breseq. In *Engineering and Analyzing Multicellular Systems: Methods and Protocols*. Sun, L., and Shou, W. (eds). Springer New York, New York, NY. pp. 165–188 https://doi.org/10.1007/978-1-4939-0554-6_12.

Dedrick, R.M., Jacobs-Sera, D., Bustamante, C.A.G., Garlena, R.A., Mavrich, T.N., Pope, W.H., *et al.* (2017) Prophage-mediated defence against viral attack and viral counter-defence. *Nat Microbiol* **2**: 16251 http://www.nature.com/articles/nmicrobiol2016251.

Deveau, H., Garneau, J.E., and Moineau, S. (2010) CRISPR/Cas System and Its Role in Phage-Bacteria Interactions. *Annu Rev Microbiol* **64**: 475–493. http://www.annualreviews.org/doi/10.1146/annurev.micro.112408.134123

Dhundale, A., Lampson, B., Furuichi, T., Inouye, M., and Inouye, S. (1987) Structure of msDNA from *Myxococcus xanthus*: Evidence for a long, self-annealing RNA precursor for the covalently linked, branched RNA. *Cell* **51**: 1105–1112 https://linkinghub.elsevier.com/retrieve/pii/0092867487905964.

Dodd, I.B., and Egan, J.B. (1996) The *Escherichia coli* retrons Ec67 and Ec86 replace DNA between the cos site and a transcription terminator of a 186-related prophage. *Virology* **219**: 115–124. https://linkinghub.elsevier.com/retrieve/pii/S0042682296902287

Doerfel, L.K., Wohlgemuth, I., Kothe, C., Peske, F., Urlaub, H., and Rodnina, M. V. (2013) EF-P is essential for rapid synthesis of proteins containing consecutive proline residues. *Science (80-)* **339**: 85–88. https://www.sciencemag.org/lookup/doi/10.1126/science.1229017

Doron, S., Melamed, S., Ofir, G., Leavitt, A., Lopatina, A., Keren, M., *et al.* (2018) Systematic discovery of antiphage defense systems in the microbial pangenome. *Science (80-)* **359**: eaar4120 https://www.sciencemag.org/lookup/doi/10.1126/science.aar4120.

Doulatov, S., Hodes, A., Dai, L., Mandhana, N., Liu, M., Deora, R., *et al.* (2004) Tropism switching in *Bordetella* bacteriophage defines a family of diversity-generating retroelements. *Nature* **431**: 476–481 http://www.nature.com/articles/nature02833.

Dy, R.L., Przybilski, R., Semeijn, K., Salmond, G.P.C., and Fineran, P.C. (2014) A widespread bacteriophage abortive infection system functions through a Type IV toxin-antitoxin mechanism. *Nucleic Acids Res* **42**: 4590–4605. https://academic.oup.com/nar/article-lookup/doi/10.1093/nar/gkt1419

Ebel-Tsipis, J., Botstein, D., and Fox, M.S. (1972) Generalized transduction by phage P22 in *Salmonella* Typhimurium. I. Molecular origin of transducing DNA. *J Mol Biol* **71**: 433–448. https://linkinghub.elsevier.com/retrieve/pii/0022283672903610

Elfenbein, J.R., Endicott-Yazdani, T., Porwollik, S., Bogomolnaya, L.M., Cheng, P., Guo, J., *et al.* (2013) Novel determinants of intestinal colonization of *Salmonella enterica* serotype Typhimurium identified in bovine enteric infection. *Infect Immun* **81**: 4311–4320. https://iai.asm.org/content/81/11/4311

Elfenbein, J.R., Knodler, L.A., Nakayasu, E.S., Nakayasu, E.S., Brewer, H.M., Bogomolnaya, L., *et al.* (2015) Multicopy Single-Stranded DNA Directs Intestinal Colonization of Enteric Pathogens. *PLoS Genet* **11**: 1–24. https://dx.plos.org/10.1371/journal.pgen.1005472

Emond, E., Holler, B.J., Boucher, I., Vandenbergh, P.A., Vedamuthu, E.R., Kondo, J.K., and Moineau, S. (1997) Phenotypic and genetic characterization of the bacteriophage abortive infection mechanism AbiK from *Lactococcus lactis*. *Appl Environ Microbiol* **63**: 1274–1283 https://aem.asm.org/content/63/4/1274.

Farzadfard, A.F., Gharaei, N., Citorik, R.J., Lu, T.K., Farzadfard, F., Gharaei, N., *et al.* (2020) Efficient Retroelement-Mediated DNA Writing in Bacteria. *bioRxiv* 2020.02.21.958983 https://doi.org/10.1101/2020.02.21.958983.

Farzadfard, F., and Lu, T.K. (2014) Genomically encoded analog memory with precise in vivo DNA writing in living cell populations. *Science (80-)* **346**: 1256272–1256272 https://www.sciencemag.org/lookup/doi/10.1126/science.1256272.

Ferat, J.-L., and Michel, F. (1993) Group II self-splicing introns in bacteria. *Nature* **364**: 358–361 http://www.nature.com/articles/364358a0.

Ferrières, L., Hémery, G., Nham, T., Guérout, A.M., Mazel, D., Beloin, C., and Ghigo, J.M. (2010) Silent mischief: Bacteriophage Mu insertions contaminate products of

Escherichia coli random mutagenesis performed using suicidal transposon delivery plasmids mobilized by broad-host-range RP4 conjugative machinery. *J Bacteriol* **192**: 6418–6427. https://jb.asm.org/content/192/24/6418

Feyter, R. de, Wallace, C., and Lane, D. (1989) Autoregulation of the ccd operon in the F plasmid. *Mol Gen Genet MGG* **218**: 481–486 http://link.springer.com/10.1007/BF00332413.

Fineran, P.C., Blower, T.R., Foulds, I.J., Humphreys, D.P., Lilley, K.S., and Salmond, G.P.C. (2009) The phage abortive infection system, ToxIN, functions as a protein-RNA toxin-antitoxin pair. *Proc Natl Acad Sci U S A* **106**: 894–899. http://www.pnas.org/lookup/doi/10.1073/pnas.0808832106

Forde, A., and Fitzgerald, G.F. (1999) Bacteriophage defence systems in lactic acid bacteria. *Antonie van Leeuwenhoek, Int J Gen Mol Microbiol* **76**: 89–113. http://www.ncbi.nlm.nih.gov/pubmed/10532374

Fortier, L.-C., Bouchard, J.D., and Moineau, S. (2005) Expression and Site-Directed Mutagenesis of the Lactococcal Abortive Phage Infection Protein AbiK. *J Bacteriol* **187**: 3721–3730 https://jb.asm.org/content/187/11/3721.

Fraikin, N., Rousseau, C.J., Goeders, N., and Melderen, L. Van (2019) Reassessing the role of the type II MqsRA toxin-antitoxin system in stress response and biofilm formation: MqsA is transcriptionally uncoupled from mqsR. *MBio* **10**: 1–13. https://mbio.asm.org/content/10/6/e02678-19

Furuichi, T., Dhundale, A., Inouye, M., and Inouye, S. (1987a) Branched RNA covalently linked to the 5′ end of a single-stranded DNA in *Stigmatella aurantiaca*: Structure of msDNA. *Cell* **48**: 47–53. https://linkinghub.elsevier.com/retrieve/pii/0092867487903540

Furuichi, T., Inouye, S., and Inouye, M. (1987b) Biosynthesis and structure of stable branched RNA covalently linked to the 5′ end of multicopy single-stranded DNA of *Stigmatella aurantiaca*. *Cell* **48**: 55–62. https://linkinghub.elsevier.com/retrieve/pii/0092867487903552

Galardini, M., Koumoutsi, A., Herrera-Dominguez, L., Varela, J.A.C., Telzerow, A., Wagih, O., *et al.* (2017) Phenotype inference in an *Escherichia coli* strain panel. *Elife* **6**. https://elifesciences.org/articles/31035

Gao, L., Altae-Tran, H., Böhning, F., Makarova, K.S., Segel, M., Schmid-Burgk, J.L., *et al.* (2020) Diverse enzymatic activities mediate antiviral immunity in prokaryotes. *Science (80-)* **369**: 1077–1084 http://www.ncbi.nlm.nih.gov/pubmed/32855333.

Geier, G.E., and Modrich, P. (1979) Recognition sequence of the dam methylase of *Escherichia coli* K-12 and mode of cleavage of Dpn I endonuclease. *J Biol Chem* **254**: 1408–1413. http://www.ncbi.nlm.nih.gov/pubmed/368070

Gerdes, K., Rasmussen, P.B., and Molin, S. (1986) Unique type of plasmid maintenance function: Postsegregational killing of plasmid-free cells. *Proc Natl Acad Sci U S A* **83**: 3116–3120. http://www.pnas.org/cgi/doi/10.1073/pnas.83.10.3116

Goormaghtigh, F., Fraikin, N., Putrinš, M., Hallaert, T., Hauryliuk, V., Garcia-Pino, A., *et al.* (2018a) Reassessing the Role of Type II Toxin-Antitoxin Systems in Formation of *Escherichia coli* Type II Persister Cells. *MBio* **9**: 1–14

https://mbio.asm.org/content/9/3/e00640-18.

Goormaghtigh, F., Fraikin, N., Putrinš, M., Hauryliuk, V., Garcia-Pino, A., Udekwu, K., *et al.* (2018b) Reply to Holden and Errington, "Type II toxin-antitoxin systems and persister cells." *MBio* **9**: 1–2. https://mbio.asm.org/content/9/5/e01838-18

Green, M.R., and Sambrook, J. (2016) Preparation of Plasmid DNA by Alkaline Lysis with Sodium Dodecyl Sulfate: Minipreps. *Cold Spring Harb Protoc* **2016**: pdb.prot093344 http://www.cshprotocols.org/lookup/doi/10.1101/pdb.prot093344.

Green, M.R., and Sambrook, J. (2019) Isolation of DNA Fragments from Polyacrylamide Gels by the Crush and Soak Method. *Cold Spring Harb Protoc* **2019**: pdb.prot100479 http://www.cshprotocols.org/lookup/doi/10.1101/pdb.prot100479.

Guo, H., Arambula, L., Ghosh, P., and Miller, J.F. (2015) Diversity-generating Retroelements in Phage and Bacterial Genomes. *Mob DNA III* 1237–1252. http://doi.wiley.com/10.1128/9781555819217.ch53

Hall, A.M., Gollan, B., and Helaine, S. (2017) Toxin–antitoxin systems: reversible toxicity. *Curr Opin Microbiol* **36**: 102–110 http://dx.doi.org/10.1016/j.mib.2017.02.003.

Handa, N., and Kobayashi, I. (2005) Type III restriction is alleviated by bacteriophage (RecE) homologous recombination function but enhanced by bacterial (RecBCD) function. *J Bacteriol* **187**: 7362–7373 https://jb.asm.org/content/187/21/7362.

Handa, S., Jiang, Y., Tao, S., Foreman, R., Schinazi, R., Miller, J., and Ghosh, P. (2018) Template-assisted synthesis of adenine-mutagenized cDNA by a retroelement protein complex. *Template-assisted Synth adenine-mutagenized cDNA by a retroelement protein complex* 344556 http://dx.doi.org/10.1101/344556.

Harms, A., Brodersen, D.E., Mitarai, N., and Gerdes, K. (2018) Toxins, Targets, and Triggers: An Overview of Toxin-Antitoxin Biology. *Mol Cell* **70**: 768–784 http://www.forskningsdatabasen.dk/en/catalog/2395367386.

Harrison, E., and Brockhurst, M.A. (2017) Ecological and Evolutionary Benefits of Temperate Phage: What Does or Doesn't Kill You Makes You Stronger. *BioEssays* **39**. http://doi.wiley.com/10.1002/bies.201700112

Hattman, S. (1970) DNA methylation of T-even bacteriophages and of their nonglucosylated mutants: Its role in P1-directed restriction. *Virology* **42**: 359–367 https://linkinghub.elsevier.com/retrieve/pii/0042682270902795.

Hattman, S., Wilkinson, J., Swinton, D., Schlagman, S., Macdonald, P.M., and Mosig, G. (1985) Common evolutionary origin of the phage T4 dam and host *Escherichia coli* dam DNA-adenine methyltransferase genes. *J Bacteriol* **164**: 932–937 https://jb.asm.org/content/164/2/932.

Herzer, P.J., Inouye, S., and Inouye, M. (1992) Retron-Ec107 is inserted into the Escherichia coli genome by replacing a palindromic 34bp intergenic sequence. *Mol Microbiol* **6**: 345–354. http://doi.wiley.com/10.1111/j.1365-2958.1992.tb01477.x

Herzer, P.J., Inouye, S., Inouye, M., and Whittam, T.S. (1990) Phylogenetic distribution of branched RNA-linked multicopy single-stranded DNA among natural isolates of *Escherichia coli*. *J Bacteriol* **172**: 6175–6181. https://jb.asm.org/content/172/11/6175

Hill, C., Miller, L.A., and Klaenhammer, T.R. (1990) Nucleotide sequence and distribution of the pTR2030 resistance determinant (hsp) which aborts bacteriophage infection in lactococci. *Appl Environ Microbiol* **56**: 2255–2258 https://aem.asm.org/content/56/7/2255.

Holmqvist, E., Wright, P.R., Li, L., Bischler, T., Barquist, L., Reinhardt, R., *et al.* (2016) Global RNA recognition patterns of post-transcriptional regulators Hfq and CsrA revealed by UV crosslinking *in vivo*. *EMBO J* **35**: 991–1011 https://onlinelibrary.wiley.com/doi/abs/10.15252/embj.201593360.

Horos, R., Büscher, M., Kleinendorst, R., Alleaume, A.M., Tarafder, A.K., Schwarzl, T., *et al.* (2019) The Small Non-coding Vault RNA1-1 Acts as a Riboregulator of Autophagy. *Cell* **176**: 1054-1067.e12. https://linkinghub.elsevier.com/retrieve/pii/S0092867419300935

Hsu, M.Y., Inouye, M., and Inouye, S. (1990) Retron for the 67-base multicopy single-stranded DNA from *Escherichia coli*: a potential transposable element encoding both reverse transcriptase and Dam methylase functions. *Proc Natl Acad Sci* **87**: 9454–9458 http://www.pnas.org/content/87/23/9454.short.

Hsu, M.Y., Inouye, S., and Inouye, M. (1989) Structural requirements of the RNA precursor for the biosynthesis of the branched RNA-linked multicopy single-stranded DNA of *Myxococcus xanthus*. *J Biol Chem* **264**: 6214–6219. http://www.ncbi.nlm.nih.gov/pubmed/2467910

Hughes, C.S., Moggridge, S., Müller, T., Sorensen, P.H., Morin, G.B., and Krijgsveld, J. (2019) Single-pot, solid-phase-enhanced sample preparation for proteomics experiments. *Nat Protoc* **14**: 68–85 http://www.nature.com/articles/s41596-018-0082-x.

Inouye, K., Tanimoto, S., Kamimoto, M., Shimamoto, T., and Shimamoto, T. (2011) Two novel retron elements are replaced with retron-Vc95 in *Vibrio cholerae*. *Microbiol Immunol* **55**: 510–513. http://doi.wiley.com/10.1111/j.1348-0421.2011.00342.x

Inouye, M., Ke, H., Yashio, A., Yamanaka, K., Nariya, H., Shimamoto, T., and Inouye, S. (2004) Complex formation between a putative 66-residue thumb domain of bacterial reverse transcriptase RT-Ec86 and the primer recognition RNA. *J Biol Chem* **279**: 50735–50742. http://www.jbc.org/lookup/doi/10.1074/jbc.M408462200

Inouye, M., and Phadtare, S. (2008) The Cold Shock Response. *EcoSal Plus* **3** http://www.asmscience.org/content/journal/ecosalplus/10.1128/ecosalplus.5.4.2.

Inouye, S., Hsu, M.Y., Xu, A., and Inouye, M. (1999) Highly specific recognition of primer RNA structures for 2'-OH priming reaction by bacterial reverse transcriptases. *J Biol Chem* **274**: 31236–31244. http://www.jbc.org/lookup/doi/10.1074/jbc.274.44.31236

Jankevicius, G., Ariza, A., Ahel, M., and Ahel, I. (2016) The Toxin-Antitoxin System DarTG Catalyzes Reversible ADP-Ribosylation of DNA. *Mol Cell* **64**: 1109–1116 http://dx.doi.org/10.1016/j.molcel.2016.11.014.

Janssen, B.D., Garza-Sánchez, F., and Hayes, C.S. (2015) YoeB toxin is activated during thermal stress. *Microbiologyopen* **4**: 682–697. https://onlinelibrary.wiley.com/doi/10.1002/mbo3.272

Jeong, D.W., Kim, K., and Lim, D. (1997) Evidence for the Complex Formation between

Reverse Transcriptase and Multicopy Single-stranded DNA in Retron EC83. *Mol Cells* **7**: 347–351. http://www.ncbi.nlm.nih.gov/pubmed/9264021

Jimmy, S., Saha, C.K., Kurata, T., Stavropoulos, C., Oliveira, S.R.A., Koh, A., *et al.* (2020) A widespread toxin−antitoxin system exploiting growth control via alarmone signaling. *Proc Natl Acad Sci* **117**: 10500–10510 http://www.pnas.org/lookup/doi/10.1073/pnas.1916617117.

Johnson, E.P., Strom, A.R., and Helinski, D.R. (1996) Plasmid RK2 toxin protein ParE: purification and interaction with the ParD antitoxin protein. *J Bacteriol* **178**: 1420–1429 https://jb.asm.org/content/178/5/1420.

Joseph, J.W., and Kolodner, R. (1983) Exonuclease VIII of *Escherichia coli*. II. Mechanism of action. *J Biol Chem* **258**: 10418–10424 http://www.jbc.org/content/258/17/10418.abstract.

Jung, H., Liang, J., Jung, Y., and Lim, D. (2015) Characterization of cell death in *Escherichia coli* mediated by XseA, a large subunit of exonuclease VII. *J Microbiol* **53**: 820–828 http://link.springer.com/10.1007/s12275-015-5304-0.

Kai, T., Selick, H.E., and Yonesaki, T. (1996) Destabilization of bacteriophage T4 mRNAs by a mutation of gene 61.5. *Genetics* **144**: 7–14 http://www.ncbi.nlm.nih.gov/pubmed/8878669.

Kato, F., Yoshizumi, S., Yamaguchi, Y., and Inouye, M. (2019) Genome-wide screening for identification of novel toxin-antitoxin systems in *Staphylococcus aureus*. *Appl Environ Microbiol* **85** http://aem.asm.org/lookup/doi/10.1128/AEM.00915-19.

Keseler, I.M., Mackie, A., Santos-Zavaleta, A., Billington, R., Bonavides-Martínez, C., Caspi, R., *et al.* (2017) The EcoCyc database: Reflecting new knowledge about *Escherichia coli* K-12. *Nucleic Acids Res* **45**: D543–D550. https://academic.oup.com/nar/article-lookup/doi/10.1093/nar/gkw1003

Kim, K., Jeong, D., and Lim, D. (1997) A mutational study of the site-specific cleavage of EC83, a multicopy single-stranded DNA (msDNA): Nucleotides at the msDNA stem are important for its cleavage. *J Bacteriol* **179**: 6518–6521. https://jb.asm.org/content/179/20/6518

Kirchner, J., Lim, D., Witkin, E.M., Garvey, N., and Roegner-Maniscalco, V. (1992) An SOS-inducible defective retronphage (φR86) in *Escherichia coli* strain B. *Mol Microbiol* **6**: 2815–2824. http://doi.wiley.com/10.1111/j.1365-2958.1992.tb01461.x

Koga, M., Otsuka, Y., Lemire, S., and Yonesaki, T. (2011) *Escherichia coli* rnlA and rnlB compose a novel toxin-antitoxin system. *Genetics* **187**: 123–130. http://www.genetics.org/lookup/doi/10.1534/genetics.110.121798

Kojima, K.K., and Kanehisa, M. (2008) Systematic Survey for Novel Types of Prokaryotic Retroelements Based on Gene Neighborhood and Protein Architecture. *Mol Biol Evol* **25**: 1395–1404 http://www.ncbi.nlm.nih.gov/pubmed/18391066.

Kritikos, G., Banzhaf, M., Herrera-Dominguez, L., Koumoutsi, A., Wartel, M., Zietek, M., and Typas, A. (2017) A tool named Iris for versatile high-throughput phenotyping in microorganisms. *Nat Microbiol* **2**: 17014 http://www.nature.com/articles/nmicrobiol201714.

Lampson, B.C., Inouye, M., and Inouye, S. (1989a) Reverse transcriptase with concomitant ribonuclease H activity in the cell-free synthesis of branched RNA-linked msDNA of *Myxococcus xanthus*. *Cell* **56**: 701–707. https://linkinghub.elsevier.com/retrieve/pii/0092867489905928

Lampson, B.C., Inouye, M., and Inouye, S. (2005) Retrons, msDNA, and the bacterial genome. *Cytogenet Genome Res* **110**: 491–499 https://www.karger.com/Article/FullText/84982.

Lampson, B.C., Sun, J., Hsu, M.Y., Vallejo-Ramirez, J., Inouye, S., and Inouye, M. (1989b) Reverse transcriptase in a clinical strain of *Escherichia coli*: Production of branched RNA-linked msDNA. *Science (80-)* **243**: 1033–1038. https://www.sciencemag.org/lookup/doi/10.1126/science.2466332

Lampson, B.C., Viswanathan, M., Inouye, M., and Inouye, S. (1990) Reverse transcriptase from *Escherichia coli* exists as a complex with msDNA and is able to synthesize double-stranded DNA. *J Biol Chem* **265**: 8490–8496. http://www.ncbi.nlm.nih.gov/pubmed/1692831

Lehnherr, H., Maguin, E., Jafri, S., and Yarmolinsky, M.B. (1993) Plasmid addiction genes of bacteriophage P1: doc, which causes cell death on curing of prophage, and phd, which prevents host death when prophage is retained. *J Mol Biol* **233**: 414–428. https://linkinghub.elsevier.com/retrieve/pii/S0022283683715214

Lehnherr, H., and Yarmolinsky, M.B. (1995) Addiction protein phd of plasmid prophage P1 is a substrate of the ClpXP serine protease of *Escherichia coli*. *Proc Natl Acad Sci U S A* **92**: 3274–3277. http://www.pnas.org/cgi/doi/10.1073/pnas.92.8.3274

Leplae, R., Geeraerts, D., Hallez, R., Guglielmini, J., Drze, P., and Melderen, L. Van (2011) Diversity of bacterial type II toxin-antitoxin systems: A comprehensive search and functional analysis of novel families. *Nucleic Acids Res* **39**: 5513–5525. https://academic.oup.com/nar/article-lookup/doi/10.1093/nar/gkr131

LeRoux, M., Culviner, P.H., Liu, Y.J., Littlehale, M.L., and Laub, M.T. (2020) Stress Can Induce Transcription of Toxin-Antitoxin Systems without Activating Toxin. *Mol Cell* **79**: 280-292.e8 https://doi.org/10.1016/j.molcel.2020.05.028.

Lim, D. (1992) Structure and biosynthesis of unbranched multicopy single-stranded DNA by reverse transcriptase in a clinical *Escherichia coli* isolate. *Mol Microbiol* **6**: 3531–3542. http://doi.wiley.com/10.1111/j.1365-2958.1992.tb01788.x

Lim, D., and Maas, W.K. (1989) Reverse transcriptase-dependent synthesis of a covalently linked, branched DNA-RNA compound in *E. coli* B. *Cell* **56**: 891–904. https://linkinghub.elsevier.com/retrieve/pii/0092867489906934

Lima, T.M.O., and Lim, D. (1995) Isolation and characterization of host mutants defective in msDNA synthesis: Role of ribonuclease H in msDNA synthesis. *Plasmid* **33**: 235–238 https://linkinghub.elsevier.com/retrieve/pii/S0147619X85710268.

Lima, T.M.O., and Lim, D. (1997) A novel retron that produces RNA-less msDNA in Escherichia coli using reverse transcriptase. *Plasmid* **38**: 25–33 http://www.ncbi.nlm.nih.gov/pubmed/19330487.

Liu, M., Deora, R., Doulatov, S.R., Gingery, M., Eiserling, F.A., Preston, A., *et al.* (2002) Reverse transcriptase-mediated tropism switching in *Bordetella* bacteriophage.

Science **295**: 2091–4
https://www.sciencemag.org/lookup/doi/10.1126/science.1067467.

Løbner-Olesen, A., Skovgaard, O., and Marinus, M.G. (2005) Dam methylation: coordinating cellular processes. *Curr Opin Microbiol* **8**: 154–160
https://linkinghub.elsevier.com/retrieve/pii/S1369527405000202.

Łobocka, M.B., Rose, D.J., Plunkett, G., Rusin, M., Samojedny, A., Lehnherr, H., *et al.* (2004) Genome of Bacteriophage P1. *J Bacteriol* **186**: 7032–7068
https://jb.asm.org/content/186/21/7032.

Maas, W.K., Wang, C., Lima, T., Hach, A., and Lim, D. (1996) Multicopy single-stranded DNA of *Escherichia coli* enhances mutation and recombination frequencies by titrating MutS protein. *Mol Microbiol* **19**: 505–509.
https://onlinelibrary.wiley.com/doi/abs/10.1046/j.1365-2958.1996.392921.x

Maas, W.K., Wang, C., Lima, T., Zubay, G., and Lim, D. (1994) Multicopy single-stranded DNAs with mismatched base pairs are mutagenic in *Escherichia coli*. *Mol Microbiol* **14**: 437–441. http://doi.wiley.com/10.1111/j.1365-2958.1994.tb02178.x

Magnuson, R., and Yarmolinsky, M.B. (1998) Corepression of the P1 Addiction Operon by Phd and Doc. *J Bacteriol* **180**: 6342–6351 https://jb.asm.org/content/180/23/6342.

Maki, S., Takiguchi, S., Horiuchi, T., Sekimizu, K., and Miki, T. (1996) Partner Switching Mechanisms in Inactivation and Rejuvenation of *Escherichia coli* DNA Gyrase by F Plasmid Proteins LetD (CcdB) and LetA (CcdA). *J Mol Biol* **256**: 473–482
https://linkinghub.elsevier.com/retrieve/pii/S0022283696901023.

Mao, J.-R., Shimada, M., Inouye, S., and Inouye, M. (1995) Gene Regulation by Antisense DNA Produced in Vivo. *J Biol Chem* **270**: 19684–19687
http://www.jbc.org/lookup/doi/10.1074/jbc.270.34.19684.

Mao, J.R., Inouye, S., and Inouye, M. (1996) Enhancement of frame-shift mutation by the overproduction of msDNA in *Escherichia coli*. *FEMS Microbiol Lett* **144**: 109–115.
http://doi.wiley.com/10.1016/0378-1097(96)00347-3

Marimon, O., Teixeira, J.M.C., Cordeiro, T.N., Soo, V.W.C., Wood, T.L., Mayzel, M., *et al.* (2016) An oxygen-sensitive toxin–antitoxin system. *Nat Commun* **7**: 13634
http://www.nature.com/doifinder/10.1038/ncomms13634.

Marinus, M.G., and Morris, N.R. (1973) Isolation of deoxyribonucleic acid methylase mutants of *Escherichia coli* K-12. *J Bacteriol* **114**: 1143–1150.
https://jb.asm.org/content/114/3/1143

Masuda, Y., Miyakawa, K., Nishimura, Y., and Ohtsubo, E. (1993) chpA and chpB, *Escherichia coli* chromosomal homologs of the pem locus responsible for stable maintenance of plasmid R100. *J Bacteriol* **175**: 6850–6856
https://jb.asm.org/content/175/21/6850.

Mateus, A., Bobonis, J., Kurzawa, N., Stein, F., Helm, D., Hevler, J., *et al.* (2018) Thermal proteome profiling in bacteria: probing protein state in vivo . *Mol Syst Biol* **14**: 1–15
https://onlinelibrary.wiley.com/doi/abs/10.15252/msb.20188242.

Matiasovicova, J., Faldynova, M., Pravcova, M., Karpiskova, R., Kolackova, I., Damborsky, J., and Rychlik, I. (2003) Retron reverse transcriptase rrtT is ubiquitous in strains of

Salmonella enterica serovar Typhimurium. *FEMS Microbiol Lett* **223**: 281–286. https://academic.oup.com/femsle/article-lookup/doi/10.1016/S0378-1097(03)00398-7

McNeil, B.A., Semper, C., and Zimmerly, S. (2016) Group II introns: versatile ribozymes and retroelements. *Wiley Interdiscip Rev RNA* **7**: 341–355 http://doi.wiley.com/10.1002/wrna.1339.

Melderen, L. Van (2010) Toxin-antitoxin systems: Why so many, what for? *Curr Opin Microbiol* **13**: 781–785 https://linkinghub.elsevier.com/retrieve/pii/S1369527410001670.

Melderen, L. Van, and Bast, M.S. De (2009) Bacterial toxin-Antitoxin systems: More than selfish entities? *PLoS Genet* **5**. https://dx.plos.org/10.1371/journal.pgen.1000437

Melderen, L. Van, Bernard, P., and Couturier, M. (1994) Lon-dependent proteolysis of CcdA is the key control for activation of CcdB in plasmid-free segregant bacteria. *Mol Microbiol* **11**: 1151–1157. http://doi.wiley.com/10.1111/j.1365-2958.1994.tb00391.x

Melderen, L. Van, Jurenas, D., and Garcia-Pino, A. (2018) Messing up translation from the start: How AtaT inhibits translation initiation in *E. coli*. *RNA Biol* **15**: 303–307. https://www.tandfonline.com/doi/full/10.1080/15476286.2017.1391439

Melderen, L. Van, and Wood, T.K. (2017) Commentary: What is the link between stringent response, endoribonuclease encoding type II toxin-antitoxin systems and persistence? *Front Microbiol* **8**: 2016–2018. http://journal.frontiersin.org/article/10.3389/fmicb.2016.01882/full

Michel, F., Kazuhiko, U., and Haruo, O. (1989) Comparative and functional anatomy of group II catalytic introns — a review. *Gene* **82**: 5–30 https://linkinghub.elsevier.com/retrieve/pii/0378111989900267.

Millman, A., Bernheim, A., Stokar-Avihail, A., Fedorenko, T., Voichek, M., Leavitt, A., *et al.* (2020) Bacterial Retrons Function In Anti-Phage Defense. *Cell* 1–11 https://doi.org/10.1016/j.cell.2020.09.065.

Mills, D.A., Mckay, L.L., and Dunny, G.M. (1996) Splicing of a group II intron involved in the conjugative transfer of pRS01 in lactococci. *J Bacteriol* **178**: 3531–3538. https://jb.asm.org/content/178/12/3531

Mirochnitchenko, O., Inouye, S., and Inouye, M. (1994) Production of single-stranded DNA in mammalian cells by means of a bacterial retron. *J Biol Chem* **269**: 2380–2383. http://www.ncbi.nlm.nih.gov/pubmed/7507924

Miyata, S., Ohshima, A., Inouye, S., and Inouye, M. (1992) In vivo production of a stable single-stranded cDNA in *Saccharomyces cerevisiae* by means of a bacterial retron. *Proc Natl Acad Sci U S A* **89**: 5735–5739. http://www.pnas.org/cgi/doi/10.1073/pnas.89.13.5735

Moelling, K., and Broecker, F. (2015) The reverse transcriptase-RNase H: From viruses to antiviral defense. *Ann N Y Acad Sci* **1341**: 126–135. http://doi.wiley.com/10.1111/nyas.12668

Monti, M.C., Hernández-Arriaga, A.M., Kamphuis, M.B., López-Villarejo, J., Heck, A.J.R., Boelens, R., *et al.* (2007) Interactions of Kid–Kis toxin–antitoxin complexes with the parD operator-promoter region of plasmid R1 are piloted by the Kis antitoxin and

tuned by the stoichiometry of Kid–Kis oligomers. *Nucleic Acids Res* **35**: 1737–1749 https://academic.oup.com/nar/article-lookup/doi/10.1093/nar/gkm073.

Mruk, I., and Kobayashi, I. (2014) To be or not to be: regulation of restriction–modification systems and other toxin–antitoxin systems. *Nucleic Acids Res* **42**: 70–86 http://academic.oup.com/nar/article/42/1/70/2434791/To-be-or-not-to-be-regulation-of.

Muñoz, E., Villadas, P.J., and Toro, N. (2001) Ectopic transposition of a group II intron in natural bacterial populations. *Mol Microbiol* **41**: 645–652 http://doi.wiley.com/10.1046/j.1365-2958.2001.02540.x.

Murphy, J., Mahony, J., Ainsworth, S., Nauta, A., and Sinderen, D. van (2013) Bacteriophage Orphan DNA Methyltransferases: Insights from Their Bacterial Origin, Function, and Occurrence. *Appl Environ Microbiol* **79**: 7547–7555 http://aem.asm.org/lookup/doi/10.1128/AEM.02229-13.

Muthuramalingam, M., White, J., and Bourne, C. (2016) Toxin-Antitoxin Modules Are Pliable Switches Activated by Multiple Protease Pathways. *Toxins (Basel)* **8**: 214 http://www.mdpi.com/2072-6651/8/7/214.

Naorem, S.S., Han, J., Wang, S., Lee, W.R., Heng, X., Miller, J.F., and Guo, H. (2017) DGR mutagenic transposition occurs via hypermutagenic reverse transcription primed by nicked template RNA. *Proc Natl Acad Sci U S A* **114**: E10187–E10195 http://www.pnas.org/lookup/doi/10.1073/pnas.1715952114.

Nielsen, S.V., Turnbull, K.J., Roghanian, M., Bærentsen, R., Semanjski, M., Brodersen, D.E., *et al.* (2019) Serine-threonine kinases encoded by split hipA homologs inhibit tryptophanyl-tRNA synthetase. *MBio* **10**: 1–16. https://mbio.asm.org/content/10/3/e01138-19

Odegrip, R., Nilsson, A.S., and Haggård-Ljungquist, E. (2006) Identification of a Gene Encoding a Functional Reverse Transcriptase within a Highly Variable Locus in the P2-Like Coliphages. *J Bacteriol* **188**: 1643–1647 https://jb.asm.org/content/188/4/1643.

Ogura, T., and Hiraga, S. (1983) Mini-F plasmid genes that couple host cell division to plasmid proliferation. *Proc Natl Acad Sci U S A* **80**: 4784–4788. http://www.pnas.org/cgi/doi/10.1073/pnas.80.15.4784

Otsuka, Y., Koga, M., Iwamoto, A., and Yonesaki, T. (2007) A role of RnlA in the RNase LS activity from *Escherichia coli*. *Genes Genet Syst* **82**: 291–299. http://joi.jlc.jst.go.jp/JST.JSTAGE/ggs/82.291?from=CrossRef

Otsuka, Y., Muto, A., Takeuchi, R., Okada, C., Ishikawa, M., Nakamura, K., *et al.* (2015) GenoBase: Comprehensive resource database of *Escherichia coli* K-12. *Nucleic Acids Res* **43**: D606–D617. http://academic.oup.com/nar/article/43/D1/D606/2438669/GenoBase-comprehensive-resource-database-of

Otsuka, Y., and Yonesaki, T. (2012) Dmd of bacteriophage T4 functions as an antitoxin against *Escherichia coli* LsoA and RnlA toxins. *Mol Microbiol* **83**: 669–681. http://doi.wiley.com/10.1111/j.1365-2958.2012.07975.x

Overgaard, M., Borch, J., Jørgensen, M.G., and Gerdes, K. (2008) Messenger RNA

interferase RelE controls relBE transcription by conditional cooperativity. *Mol Microbiol* **69**: 841–857 http://doi.wiley.com/10.1111/j.1365-2958.2008.06313.x.

Page, R., and Peti, W. (2016) Toxin-antitoxin systems in bacterial growth arrest and persistence. *Nat Chem Biol* **12**: 208–214 http://www.nature.com/articles/nchembio.2044.

Pandey, D.P., and Gerdes, K. (2005) Toxin-antitoxin loci are highly abundant in free-living but lost from host-associated prokaryotes. *Nucleic Acids Res* **33**: 966–976. https://academic.oup.com/nar/article-lookup/doi/10.1093/nar/gki201

Pecota, D.C., and Wood, T.K. (1996) Exclusion of T4 phage by the hok/sok killer locus from plasmid R1. *J Bacteriol* **178**: 2044–2050. https://jb.asm.org/content/178/7/2044

Pedersen, K., and Gerdes, K. (1999) Multiple hok genes on the chromosome of *Escherichia coli*. *Mol Microbiol* **32**: 1090–1102 http://doi.wiley.com/10.1046/j.1365-2958.1999.01431.x.

Pedersen, K., Zavialov, A. V., Pavlov, M.Y., Elf, J., Gerdes, K., and Ehrenberg, M. (2003) The Bacterial Toxin RelE Displays Codon-Specific Cleavage of mRNAs in the Ribosomal A Site. *Cell* **112**: 131–140 https://linkinghub.elsevier.com/retrieve/pii/S0092867402012485.

Pfalz, B. (2017) Comparing bacterial gene networks based on high-throughput phenomics. http://www.ub.uni-heidelberg.de/archiv/22920.

Pilousova, L., and Rychlik, I. (2011) Retron Se72 utilizes a unique strategy of the self-priming initiation of reverse transcription. *Cell Mol Life Sci* **68**: 3607–3617. http://link.springer.com/10.1007/s00018-011-0671-0

Pinilla-Redondo, R., Shehreen, S., Marino, N.D., Fagerlund, R.D., Brown, C.M., Sørensen, S.J., *et al.* (2020) Discovery of multiple anti-CRISPRs highlights anti-defense gene clustering in mobile genetic elements. *Nat Commun* **11**: 5652 http://dx.doi.org/10.1038/s41467-020-19415-3.

Porwollik, S., Santiviago, C.A., Cheng, P., Long, F., Desai, P., Fredlund, J., *et al.* (2014) Defined single-gene and multi-gene deletion mutant collections in *Salmonella enterica* sv typhimurium. *PLoS One* **9**. https://dx.plos.org/10.1371/journal.pone.0099820

Qu, G., Piazza, C.L., Smith, D., and Belfort, M. (2018) Group II intron inhibits conjugative relaxase expression in bacteria by mRNA targeting. *Elife* **7**: 1–23. https://elifesciences.org/articles/34268

Ramage, H.R., Connolly, L.E., and Cox, J.S. (2009) Comprehensive Functional Analysis of *Mycobacterium tuberculosis* Toxin-Antitoxin Systems: Implications for Pathogenesis, Stress Responses, and Evolution. *PLoS Genet* **5**: e1000767 https://dx.plos.org/10.1371/journal.pgen.1000767.

Ramisetty, B.C.M., and Santhosh, R.S. (2017) Endoribonuclease type II toxin-antitoxin systems: Functional or selfish? *Microbiol (United Kingdom)* **163**: 931–939 http://www.microbiologyresearch.org/content/journal/micro/10.1099/mic.0.000487.v1.

Rice, S.A., Bieber, J., Chun, J.Y., Stacey, G., and Lampson, B.C. (1993) Diversity of retron elements in a population of rhizobia and other gram- negative bacteria. *J Bacteriol*

175: 4250–4254. https://jb.asm.org/content/175/13/4250

Rice, S.A., and Lampson, B.C. (1995) Phylogenetic comparison of retron elements among the myxobacteria: Evidence for vertical inheritance. *J Bacteriol* **177**: 37–45. https://jb.asm.org/content/177/1/37

Ritchie, M.E., Phipson, B., Wu, D., Hu, Y., Law, C.W., Shi, W., and Smyth, G.K. (2015) limma powers differential expression analyses for RNA-sequencing and microarray studies. *Nucleic Acids Res* **43**: e47–e47 http://academic.oup.com/nar/article/43/7/e47/2414268/limma-powers-differential-expression-analyses-for.

Rosendahl, S., Tamman, H., Brauer, A., Remm, M., and Hõrak, R. (2020) Chromosomal toxin-antitoxin systems in *Pseudomonas putida* are rather selfish than beneficial. 1–13. http://www.nature.com/articles/s41598-020-65504-0

Rousset, F., Caballero, J.C., Piastra-Facon, F., Fernández-Rodríguez, J., Clermont, O., Denamur, E., *et al.* (2020) The impact of genetic diversity on gene essentiality within the *E. coli* species. *bioRxiv* 2020.05.25.114553. https://doi.org/10.1101/2020.05.25.114553

Roy, D., Huguet, K.T., Grenier, F., and Burrus, V. (2020) IncC conjugative plasmids and SXT/R391 elements repair double-strand breaks caused by CRISPR–Cas during conjugation. *Nucleic Acids Res* **48**: 8815–8827 https://academic.oup.com/nar/article/48/16/8815/5858453.

Saka, K., Tadenuma, M., Nakade, S., Tanaka, N., Sugawara, H., Nishikawa, K., *et al.* (2005) A complete set of *Escherichia coli* open reading frames in mobile plasmids facilitating genetic studies. *DNA Res* **12**: 63–68. https://academic.oup.com/dnaresearch/article-lookup/doi/10.1093/dnares/12.1.63

Sberro, H., Leavitt, A., Kiro, R., Koh, E., Peleg, Y., Qimron, U., and Sorek, R. (2013) Discovery of Functional Toxin/Antitoxin Systems in Bacteria by Shotgun Cloning. *Mol Cell* **50**: 136–148 http://dx.doi.org/10.1016/j.molcel.2013.02.002.

Schubert, M.G., Goodman, D.B., Wannier, T.M., Kaur, D., Farzadfard, F., Lu, T.K., *et al.* (2020) High throughput functional variant screens via in-vivo production of single-stranded DNA. *bioRxiv* 2020.03.05.975441 https://www.biorxiv.org/content/10.1101/2020.03.05.975441v1.

Sharp, P. (1991) “Five easy pieces.” *Science (80-)* **254**: 663–663 https://www.sciencemag.org/lookup/doi/10.1126/science.1948046.

Shimamoto, T., Ahmed, A.M., and Shimamoto, T. (2013) A novel retron of *Vibrio parahaemolyticus* is closely related to retron-Vc95 of *Vibrio cholerae*. *J Microbiol* **51**: 323–328. http://link.springer.com/10.1007/s12275-013-2715-7

Shimamoto, T., Hsu, M.Y., Inouye, S., and Inouye, M. (1993) Reverse transcriptases from bacterial retrons require specific secondary structures at the 5’-end of the template for the cDNA priming reaction. *J Biol Chem* **268**: 2684–2692. http://www.ncbi.nlm.nih.gov/pubmed/7679101

Shimamoto, T., Shimada, M., Inouye, M., and Inouye, S. (1995) The role of ribonuclease H in multicopy single-stranded DNA synthesis in retron-Ec73 and retron-Ec107 of *Escherichia coli*. *J Bacteriol* **177**: 264–267. https://jb.asm.org/content/177/1/264

Shinedling, S., Parma, D., and Gold, L. (1987) Wild-type bacteriophage T4 is restricted by the lambda rex genes. *J Virol* **61**: 3790–4 https://www.ncbi.nlm.nih.gov/pmc/articles/PMC255994/pdf/jvirol00103-0152.pdf.

Short, F.L., Pei, X.Y., Blower, T.R., Ong, S.L., Fineran, P.C., Luisi, B.F., and Salmond, G.P.C. (2013) Selectivity and self-assembly in the control of a bacterial toxin by an antitoxic noncoding RNA pseudoknot. *Proc Natl Acad Sci U S A* **110**: E241–E249. http://www.pnas.org/cgi/doi/10.1073/pnas.1216039110

Silas, S., Mohr, G., Sidote, D.J., Markham, L.M., Sanchez-Amat, A., Bhaya, D., *et al.* (2016) Direct CRISPR spacer acquisition from RNA by a natural reverse transcriptase-Cas1 fusion protein. *Science (80-)* **351**: aad4234–aad4234 https://www.sciencemag.org/lookup/doi/10.1126/science.aad4234.

Simon, A.J., Ellington, A.D., and Finkelstein, I.J. (2019) Retrons and their applications in genome engineering. *Nucleic Acids Res* **47**: 11007–11019. https://academic.oup.com/nar/article/47/21/11007/5584520

Simon, D.M., and Zimmerly, S. (2008) A diversity of uncharacterized reverse transcriptases in bacteria. *Nucleic Acids Res* **36**: 7219–7229 https://academic.oup.com/nar/article-lookup/doi/10.1093/nar/gkn867.

Slater, S.C., Lifsics, M.R., O'Donnell, M., and Maurer, R. (1994) holE, the gene coding for the theta subunit of DNA polymerase III of *Escherichia coli*: characterization of a holE mutant and comparison with a dnaQ (epsilon-subunit) mutant. *J Bacteriol* **176**: 815–821 https://jb.asm.org/content/176/3/815.

Soma, A., Ikeuchi, Y., Kanemasa, S., Kobayashi, K., Ogasawara, N., Ote, T., *et al.* (2003) An RNA-Modifying Enzyme that Governs Both the Codon and Amino Acid Specificities of Isoleucine tRNA. *Mol Cell* **12**: 689–698 https://linkinghub.elsevier.com/retrieve/pii/S1097276503003460.

Song, S., and Wood, T.K. (2018) Post-segregational killing and phage inhibition are not mediated by cell death through toxin/antitoxin systems. *Front Microbiol* **9**: 1–6. http://journal.frontiersin.org/article/10.3389/fmicb.2018.00814/full

Song, S., and Wood, T.K. (2020) Toxin/Antitoxin System Paradigms: Toxins Bound to Antitoxins Are Not Likely Activated by Preferential Antitoxin Degradation. *Adv Biosyst* **4**: 1900290 https://onlinelibrary.wiley.com/doi/abs/10.1002/adbi.201900290.

Sternberg, N., and Coulby, J. (1990) Cleavage of the bacteriophage P1 packaging site (pac) is regulated by adenine methylation. *Proc Natl Acad Sci U S A* **87**: 8070–8074. http://www.pnas.org/cgi/doi/10.1073/pnas.87.20.8070

Studier, F.W., Daegelen, P., Lenski, R.E., Maslov, S., and Kim, J.F. (2009) Understanding the Differences between Genome Sequences of *Escherichia coli* B Strains REL606 and BL21(DE3) and Comparison of the *E. coli* B and K-12 Genomes. *J Mol Biol* **394**: 653–680 http://dx.doi.org/10.1016/j.jmb.2009.09.021.

Sun, J., Herzer, P.J., Weinstein, M.P., Lampson, B.C., Inouye, M., and Inouye, S. (1989) Extensive diversity of branched-RNA-linked multicopy single-stranded DNAs in clinical strains of *Escherichia coli*. *Proc Natl Acad Sci U S A* **86**: 7208–7212. http://www.pnas.org/cgi/doi/10.1073/pnas.86.18.7208

Szyf, M., Avraham-Haetzni, K., Reifman, A., Shlomai, J., Kaplan, F., Oppenheim, A., and

Razin, A. (1984) DNA methylation pattern is determined by the intracellular level of the methylase. *Proc Natl Acad Sci* **81**: 3278–3282 http://www.pnas.org/cgi/doi/10.1073/pnas.81.11.3278.

Talavera, A., Tamman, H., Ainelo, A., Konijnenberg, A., Hadži, S., Sobott, F., *et al.* (2019) A dual role in regulation and toxicity for the disordered N-terminus of the toxin GraT. *Nat Commun* **10**: 972 http://www.nature.com/articles/s41467-019-08865-z.

Tam, J.E., and Kline, B.C. (1989) The F plasmid ccd autorepressor is a complex of CcdA and CcdB proteins. *MGG Mol Gen Genet* **219**: 26–32. http://link.springer.com/10.1007/BF00261153

Tamman, H., Ainelo, A., Ainsaar, K., and Horak, R. (2014) A Moderate Toxin, GraT, Modulates Growth Rate and Stress Tolerance of *Pseudomonas putida*. *J Bacteriol* **196**: 157–169 https://jb.asm.org/content/196/1/157.

Tanaka, N., Meineke, B., and Shuman, S. (2011) RtcB, a Novel RNA Ligase, Can Catalyze tRNA Splicing and HAC1 mRNA Splicing in Vivo. *J Biol Chem* **286**: 30253–30257 http://www.jbc.org/lookup/doi/10.1074/jbc.C111.274597.

Temin, H.M. (1989) Retrons in bacteria. *Nature* **339**: 254–255 http://www.nature.com/articles/339254a0.

Temin, H.M., and Mizutani, S. (1970) Viral RNA-dependent DNA Polymerase: RNA-dependent DNA Polymerase in Virions of Rous Sarcoma Virus. *Nature* **226**: 1211–1213. http://www.nature.com/articles/2261211a0

Thompson, K.M., and Gottesman, S. (2014) The miaA tRNA modification enzyme is necessary for robust RpoS expression in *Escherichia coli*. *J Bacteriol* **196**: 754–761. https://jb.asm.org/content/196/4/754

Tock, M.R., and Dryden, D.T. (2005) The biology of restriction and anti-restriction. *Curr Opin Microbiol* **8**: 466–472 https://linkinghub.elsevier.com/retrieve/pii/S1369527405000779.

Toro, N., Jiménez-Zurdo, J.I., and García-Rodríguez, F.M. (2007) Bacterial group II introns: not just splicing. *FEMS Microbiol Rev* **31**: 342–358 https://academic.oup.com/femsre/article-lookup/doi/10.1111/j.1574-6976.2007.00068.x.

Toro, N., and Nisa-Martínez, R. (2014) Comprehensive phylogenetic analysis of bacterial reverse transcriptases. *PLoS One* **9**: 1–16. https://dx.plos.org/10.1371/journal.pone.0114083

Torreblanca, J., and Casadesús, J. (1996) DNA adenine methylase mutants of *Salmonella* Typhimurium and a novel dam- regulated locus. *Genetics* **144**: 15–26. http://www.ncbi.nlm.nih.gov/pubmed/8878670

Typas, A., Banzhaf, M., Berg van Saparoea, B. van den, Verheul, J., Biboy, J., Nichols, R.J., *et al.* (2010) Regulation of Peptidoglycan Synthesis by Outer-Membrane Proteins. *Cell* **143**: 1097–1109 http://dx.doi.org/10.1016/j.cell.2010.11.038.

Ude, S., Lassak, J., Starosta, A.L., Kraxenberger, T., Wilson, D.N., and Jung, K. (2013) Translation Elongation Factor EF-P Alleviates Ribosome Stalling at Polyproline Stretches. *Science (80-)* **339**: 82–85

https://www.sciencemag.org/lookup/doi/10.1126/science.1228985.

Vasu, K., and Nagaraja, V. (2013) Diverse Functions of Restriction-Modification Systems in Addition to Cellular Defense. *Microbiol Mol Biol Rev* **77**: 53–72 https://mmbr.asm.org/content/77/1/53.

Waldern, J., Schiraldi, N.J., Belfort, M., and Novikova, O. (2020) Bacterial Group II Intron Genomic Neighborhoods Reflect Survival Strategies: Hiding and Hijacking. *Mol Biol Evol* **37**: 1942–1948 https://academic.oup.com/mbe/article/37/7/1942/5781966.

Wang, C., Villion, M., Semper, C., Coros, C., Moineau, S., and Zimmerly, S. (2011) A reverse transcriptase-related protein mediates phage resistance and polymerizes untemplated DNA in vitro. *Nucleic Acids Res* **39**: 7620–7629 https://academic.oup.com/nar/article-lookup/doi/10.1093/nar/gkr397.

Wang, H., Bian, X., Xia, L., Ding, X., Müller, R., Zhang, Y., *et al.* (2014) Improved seamless mutagenesis by recombineering using ccdB for counterselection. *Nucleic Acids Res* **42**: e37–e37 https://academic.oup.com/nar/article/42/5/e37/1062706.

Wang, X., Kim, Y., Ma, Q., Hong, S.H., Pokusaeva, K., Sturino, J.M., and Wood, T.K. (2010) Cryptic prophages help bacteria cope with adverse environments. *Nat Commun* **1**: 147–149 http://dx.doi.org/10.1038/ncomms1146.

Wang, X., Lord, D.M., Cheng, H.-Y., Osbourne, D.O., Hong, S.H., Sanchez-Torres, V., *et al.* (2012) A new type V toxin-antitoxin system where mRNA for toxin GhoT is cleaved by antitoxin GhoS. *Nat Chem Biol* **8**: 855–861 http://www.nature.com/articles/nchembio.1062.

Wilbaux, M., Mine, N., Guérout, A.-M., Mazel, D., and Melderen, L. Van (2007) Functional Interactions between Coexisting Toxin-Antitoxin Systems of the ccd Family in Escherichia coli O157:H7. *J Bacteriol* **189**: 2712–2719 https://jb.asm.org/content/189/7/2712.

Wilcox, B., Osterman, I., Serebryakova, M., Lukyanov, D., Komarova, E., Gollan, B., *et al.* (2018) *Escherichia coli* ItaT is a type II toxin that inhibits translation by acetylating isoleucyl-tRNAIle. *Nucleic Acids Res* **46**: 7873–7885. https://academic.oup.com/nar/article/46/15/7873/5042027

Wu, L., Gingery, M., Abebe, M., Arambula, D., Czornyj, E., Handa, S., *et al.* (2018) Diversity-generating retroelements: natural variation, classification and evolution inferred from a large-scale genomic survey. *Nucleic Acids Res* **46**: 11–24 http://academic.oup.com/nar/article/46/1/11/4655238.

Yao, J., Zhen, X., Tang, K., Liu, T., Xu, X., Chen, Z., *et al.* (2020) Novel polyadenylylation-dependent neutralization mechanism of the HEPN/MNT toxin/antitoxin system. *Nucleic Acids Res* 1–14 https://academic.oup.com/nar/advance-article/doi/10.1093/nar/gkaa855/5921292.

Yarmolinsky, M. (1995) Programmed cell death in bacterial populations. *Science (80-)* **267**: 836–837 https://www.sciencemag.org/lookup/doi/10.1126/science.7846528.

Yee, T., Furuichi, T., Inouye, S., and Inouye, M. (1984) Multicopy single-stranded DNA isolated from a gram-negative bacterium, *Myxococcus xanthus*. *Cell* **38**: 203–209. https://linkinghub.elsevier.com/retrieve/pii/0092867484905415

Yu, X., Gao, X., Zhu, K., Yin, H., Mao, X., Wojdyla, J.A., *et al.* (2020) Characterization of a toxin-antitoxin system in *Mycobacterium tuberculosis* suggests neutralization by phosphorylation as the antitoxicity mechanism. *Commun Biol* **3**: 216 http://dx.doi.org/10.1038/s42003-020-0941-1.

Zimmerly, S., and Semper, C. (2015) Evolution of group II introns. *Mob DNA* **6**: 7 http://dx.doi.org/10.1186/s13100-015-0037-5

Zimmerly, S., and Wu, L. (2015) An Unexplored Diversity of Reverse Transcriptases in Bacteria. In *Mobile DNA III*. American Society of Microbiology, pp. 1253–1269 http://www.asmscience.org/content/book/10.1128/9781555819217.chap54.

Zuker, M. (2003) Mfold web server for nucleic acid folding and hybridization prediction. *Nucleic Acids Res* **31**: 3406–3415 https://academic.oup.com/nar/article-lookup/doi/10.1093/nar/gkg595.